



UNIVERSITY OF TM
KWAZULU-NATAL

INYUVESI
YAKWAZULU-NATALI

Allicin ameliorates some deoxynivalenol-induced cytotoxic effects in human embryonic kidney (Hek293) cells, but also elicits synergistic and potentiating adverse effects

BY

Yandisa Zintle Mamane (219095869)

BSc (Biochemistry and Microbiology, University of Zululand)

BSc Honours (Microbiology, University of Zululand)

Submitted in fulfillment of the requirement for the degree of
Master of Medical Science in the Discipline of Medical Biochemistry and Chemical Pathology
School of Laboratory Medicine and Medical Sciences
College of Health Sciences
University of KwaZulu-Natal
Durban

2020

DECLARATION

I, Yandisa Zintle Mamane, declare that:

1. This dissertation contains original work done by the author and has not been submitted to UKZN or any other tertiary institution for the purposes of obtaining an academic qualification, whether by myself or any other party. The use of work by others has been duly acknowledged in the text.
2. The research described in this study was carried out in the Department of Medical Biochemistry and Chemical Pathology, School of Laboratory Medicine and Medical Science, Faculty of Health Sciences, University of KwaZulu-Natal, Durban, under the supervision of Dr RB Khan.

Signed:

Date: 15 September 2020

ACKNOWLEDGEMENTS

My Lord and Saviour Jesus Christ

Thank you, Jesus, words are not enough. You are my everything. I am grateful, my Father.

My family

In loving memory of my bold mother, I am thankful. My grandfather, who always believed in me and taught me that I could achieve anything. My aunt who taught me that education is the key to success. My grandmothers always remind me of who I am and to run my race. My supportive father I thank you Dad. My uncles who showed me so much love and inspired me to be greater. Thankful to the friends who became family, I love you all.

Dr Rene Khan

Thank you for so much for giving me a chance, always encouraging me to do more and believing in me. Mostly, thank you for leading by example, you are the greatness I aspire to be. I am grateful to have been mentored by you as an excellent researcher and scientist.

Department of Medical Biochemistry

To my research group (Nomali, Thobeka, Ntombi, Angela, Lebo, Lloyd, and Letty), thank you for always assisting me and showing great teamwork. The entire staff of the department of Medical biochemistry, thank you for your patience, unwavering support, and assistance during this project.

University of KwaZulu-Natal College of Health Sciences and National Research Foundation

I appreciate the awarded scholarships that financially facilitated in the completion of this degree.

ABBREVIATIONS

AIF	Apoptosis-inducing factor
AF	Aflatoxins
AREs	Antioxidant response elements
APAF-1	Apoptotic-protease-activating-factor-1
ATP	Adenosine triphosphate
BAD	BCL ₂ associated agonist of cell death
Bax	BCL ₂ -associated X
BCA	Bicinchoninic acid
BCL ₂	B-cell lymphoma/leukemia-2
BH	BCL ₂ homology
BH3	BCL ₂ homology domain 3
BHT	Butylated hydroxytoluene
BID	BH3 interacting domain death agonist
BIK	BCL ₂ interacting killer
BSA	Bovine serum albumin
BUN	Blood, urea, nitrogen (BUN)
CAD	Caspase-activated DNase
CCM	Complete culture medium
cDNA	Complimentary DNA
cIAPs	Cellular inhibitor of apoptosis protein
CO ₂	Carbon dioxide
Con A	Concanavalin A
COX-2	Cyclooxygenase-2
CRE	Creatinine
CuSO ₄	Copper sulphate
DADS	Diallyl disulfide
DAS	Diallyl sulfide
DAT	Diallyl trisulfide
DD	Death domain
dH ₂ O	De-ionized water
DISC	Death inducing signalling complex

DMEM	Dulbecco's Modified Eagle's Medium
DMSO	Dimethyl sulphoxide
DNA	Deoxyribonucleic acid
DNase	Deoxyribonuclease
DON	Deoxynivalenol
DR5	Death receptor 5
EC ₅₀	Half maximal effective concentration
EDTA	Ethylenediaminetetraacetic acid
ETC	Electron transport chain
FAD ⁺	Flavin adenine dinucleotide
FADD	Fas-associated death domain
FAS	First apoptotic signal
FASL	Fatty acid synthase ligand
FB ₁	Fumonisin B ₁
FDA	Food and drug administration
GMO	Genetically modified organism
GPx	Glutathione peroxidase
GR	Glutathione reductase
GRAS	Generally regarded as safe
GSH	Glutathione
GST	Glutathione-S-transferase
H ₂ O	Water
H ₂ O ₂	Hydrogen peroxide
H ₃ PO ₄	Phosphoric acid
HCl	Hydrochloric acid
Hek293	Human embryonic kidney cells
HO-1	Heme oxygenase
HO [•]	Hydroxyl radical
HOO [•]	Perhydroxyl radical
HPBLs	Human peripheral blood lymphocytes
HSP70	Heat shock protein 70
HT29	Human colon carcinoma
HUVEC	Human umbilical vein endothelial
IARC	International agency for research on cancer

IC ₅₀	Median Inhibition Concentration
iCAD	Inhibitors of caspase DNase
IgA	Immunoglobulin A
LDH	Lactate dehydrogenase
MCF7	Human breast cancer
MDA	Malondialdehyde
mRNA	Messenger RNA
miRNA	MicroRNA
MOMP	Mitochondrial outer membrane permeability pores
MTT	Methyl tetrazolium
NaCl	Sodium chloride
NAD ⁺	Nicotinamide-adenine dinucleotide
NADPH	Nicotinamide-adenine dinucleotide phosphate
NaOH	Sodium hydroxide
NEDD	N-(1-naphthyl) ethylenediamine
Nm	Nanometer
NO	Nitric oxide
Nrf2	Nuclear factor erythroid 2-related factor 2
O ₂	Oxygen
O ₂ ⁻	Superoxide ion
OH ⁻	Hydroxy group
ONOO ⁻	Peroxynitrite
OC	Oesophageal cancer
OTA	Ochratoxins
PARP	Poly (ADP-ribose) polymerase
PBMCs	Peripheral blood mononuclear cells
PBS	Phosphate-buffered saline
PCR	Polymerase chain reaction
PI	Propidium iodide
PKR	Double-stranded RNA-associated protein kinase
Prxs	Peroxidase
PS	Phosphatidylserine
PUFs	Poly-unsaturated fatty acids
qPCR	Quantitative polymerase chain reaction

RFU	Relative fluorescent units
RLU	Relative light unit
rRNA	Ribosomal RNA
RNA	Ribonucleic acid
RNS	Reactive nitrogen species
ROS	Reactive oxygen species
RSS	Reactive sulphur species
RT	Room temperature
SAC	S-allylcysteine
SCGE	Single cell gel electrophoresis
SDS	Sodium dodecyl sulfate
SMAC	Second mitochondria-derived activator of caspases
SOD	Superoxide dismutase
SULF	Sulfanilamide
TBA	Thiobarbituric Acid
TBARS	Thiobarbituric Acid Reactive Substances
tBID	Truncated BH3 interacting-domain death agonist
TDI	Tolerable daily intake
THs	Trichothecenes
TNF	Tumor necrosis factor
TRAIL	TNF-related apoptosis-inducing ligand
TTBS	Tris-buffered saline containing 0.5% Tween20
VCl ₃	Vanadium (III) chloride
XIAP	X chromosome-linked inhibitor of apoptosis
ZEN	Zearalenone

TABLE OF CONTENTS

DECLARATION.....	i
ACKNOWLEDGEMENTS	ii
ABBREVIATIONS	iii
LIST OF FIGURES	x
LIST OF TABLES	xiii
ABSTRACT	xiv
CHAPTER 1 : INTRODUCTION.....	1
1.1 FOCUS OF STUDY	1
1.2 PROBLEM STATEMENT AND RATIONALE	3
1.3 HYPOTHESIS	3
1.4 AIM.....	4
1.5 OBJECTIVES	4
CHAPTER 2 : LITERATURE REVIEW.....	5
2.1 MYCOTOXINS.....	5
2.1.1 Mycotoxins and food.....	5
2.1.2 Mycotoxins and animals.....	6
2.1.3 Mycotoxins and humans.....	7
2.2 DON.....	7
2.2.2 Prevalence of DON.....	9
2.2.3 Mechanism of action	11
2.2.4 DON toxicity	12
2.3 MEDICINAL PLANTS.....	14
2.3.1 Garlic	15
2.3.2 Bioactive compounds in garlic	15
2.3.3 Allicin	15
2.4 OXIDATIVE STRESS	17

2.5	APOPTOSIS	19
2.6	DON-INDUCED OXIDATIVE STRESS AND APOPTOSIS	21
CHAPTER 3 : MATERIALS AND METHODS		23
3.1	MATERIALS.....	23
3.2	CELL CULTURE	23
3.3	DON AND ALLICIN PREPARATIONS AND TREATMENTS	23
3.4	THE METHYLTHIAZOL TETRAZOLIUM (MTT) ASSAY	24
3.4.1	Principle.....	24
3.4.2	Procedure	25
3.5	CELL TITER-GLO® LUMINESCENT CELL VIABILITY ASSAY	26
3.5.1	Principle.....	26
3.5.2	Procedure	26
3.6	NITRIC OXIDE SYNTHASE (NOS) ASSAY	27
3.6.1	Principle.....	27
3.6.2	Procedure	27
3.7	THIOBARBITURIC ACID REACTIVE SUBSTANCES (TBARS) ASSAY	28
3.7.1	Principle.....	28
3.7.2	Procedure	28
3.8	GLUTATHIONE ASSAY	29
3.8.1	Principle.....	29
3.8.2	Procedure	29
3.9	ANNEXIN V AND NECROSIS ASSAY	30
3.9.1	Principle.....	30
3.9.2	Procedure	30
3.10	CASPASES.....	31
3.10.1	Principle.....	31
3.11	LACTATE DEHYDROGENASE (LDH) ASSAY	33
3.11.1	Principle.....	33

3.11.2	Procedure	34
3.12	WESTERN BLOTTING.....	34
3.12.1	Principle.....	34
3.12.2	Procedure	34
3.13	DNA FRAGMENTATION ASSAY	36
3.13.1	Principle.....	36
3.13.2	Procedure	36
3.14	STATISTICAL ANALYSIS	37
CHAPTER 4 : RESULTS		38
4.1	CELL VIABILITY	38
4.2	ATP ASSAY	38
4.3	NOS ASSAY	39
4.4	TBARS ASSAY	40
4.5	GSH ASSAY	41
4.6	OXIDATIVE STRESS MARKER PROTEINS	42
4.7	ANNEXIN V	45
4.8	CASPASES.....	46
4.9	LDH ASSAY	47
4.10	APOPTOSIS PROTEINS	47
4.11	DNA FRAGMENTATION	49
CHAPTER 5 : DISCUSSION		50
CHAPTER 6 : CONCLUSION AND FUTURE RECOMMENDATIONS		55
APPENDICES		69
Appendix A	: Ethics exemption letter.....	69
Appendix B	: Turnitin report	70
Appendix C	: Allicin cell viability data.....	73
Appendix D	: Nitrates standard curve.....	74
Appendix E	: Protein standard curve	75

LIST OF FIGURES

Figure 2.1: The contamination of cereal crops by mycotoxin-producing fungi showing the commonly occurring mycotoxins (adapted from (Liu <i>et al.</i> , 2016)).	6
Figure 2.2: Classification of trichothecene structures. EPT core structure; R groups may be OH, H, O-Acyl, or dissimilarities in the macrolide chain (McCormick <i>et al.</i> , 2011).	8
Figure 2.3: The chemical structure of DON, a type B-trichothecene sesquiterpenoid polar organic compound (Singh <i>et al.</i> , 2015).	9
Figure 2.4: DON provides an example of pleiotropy at various degrees of density, and over the different biotic macromolecules. The crosstalk of the molecular modifications at genomic, proteomic, transcriptomic, and metabolomic levels can result in a series of physiological and cellular effects (Dellafiora and Dall'Asta, 2017).	12
Figure 2.5: Allicin biosynthesis. The non-proteinogenic amino acid alliin is converted by the alliinase enzyme activation to dehydroalanine and allyl sulfenic acid. Two molecules of allyl sulfenic acid condensed spontaneously to a single allicin molecule (Gruhlke <i>et al.</i> , 2016).	16
Figure 2.6: The superoxide anion (O_2^-) is produced as a by-product of oxidative metabolism in the mitochondria, but also by cytoplasmic enzymes. Oxidative stress may be averted by antioxidants such as glutathione, glutathione peroxidase, and catalase, which function to convert free radicals to water. However, the Fenton reaction produces the potent hydroxyl radical (HO^\cdot) that is implicated in macromolecule damage. Reactive nitrogen species (RNS) such as peroxynitrite ($ONOO^-$) produced when superoxide reacts with nitric oxide may also cause damage to cellular macromolecules (Kaushal <i>et al.</i> , 2019).	17
Figure 2.7: Major pathways governing oxidative stress, ROS production by mitochondria, main ROS production sites ETC complexes I and III. Cumulative mtDNA damage and progressive ETC dysfunction are caused by increased ROS production. Nrf2 localization can be increased by hydrogen sulfide, antioxidant gene expression by modulation, and HO-1 signaling pathway activation (Koutakis <i>et al.</i> , 2018).	19
Figure 2.8: Programmed cell death signaling pathways. The binding to cell death ligands induces the death receptor apoptosis pathway, TNF, FASL, or TRAIL, to cell death receptors TNFR, FAS, or DR5, respectively. Caspase 8 activated cell death is a result of death receptor activation (Marquez <i>et al.</i> , 2013).	21
Figure 2.9: DON proposed mode of action for oxidative stress. ROS production increased, may induce oxidative damage which leads to toxicity and apoptosis (Mishra <i>et al.</i> , 2014).	22

Figure 3.1: The MTT assay is based on the conversion of the yellow MTT to an insoluble purple formazan product that is solubilized with DMSO (Ali-Boucetta <i>et al.</i> , 2011).....	25
Figure 3.2: The ATP assay catalyzed through the luciferase reaction to generate a light signal (Coussens <i>et al.</i> , 2018).	26
Figure 3.3: The Griess Reaction. A two-step diazotization reaction, NO ₂ ⁻ reacts with SULF to produce a diazonium cation which couples to NEDD to form a red-violet chromophoric diazo product (Bryan and Grisham, 2007).....	27
Figure 3.4: The representation of TBARS reaction between MDA and TBA/BHT used as a lipid peroxidation indicator of oxidative stress (Bio-technie, 2014).	28
Figure 3.5: The luminescent representation for the quantification and detection of GSH in cells, luciferin derivative, is converted into luciferin in the presence of GST (Promega).	29
Figure 3.6: The Annexin V assay used for apoptotic cell detection. Annexin V binds to externalized PS on an early apoptotic cell and can be detected using flow cytometry or luminometry (GmbH, 2019)..	30
Figure 3.7: The aminoluciferin released by caspase cleavage of Z-DEVD is a substrate for luciferase. In the presence of ATP, oxygen, and magnesium, this reaction produces a light signal which is directly proportional to caspase activity (Promega).	32
Figure 3.8: Representation of a damaged cell releasing LDH, that is spectrophotometrically detected as a formazan product (Forest <i>et al.</i> , 2015).	33
Figure 3.9: The detection and characterization of proteins is a rapid and sensitive called Western blotting (protein blotting or immunoblotting) procedure (Bhandari, 2017).	34
Figure 3.10: DNA extraction principle (Ali, 2019).....	36
Figure 4.1: The non-linear regression (curve fit) for the percentage cell viability of Hek293 cells treated with varying concentrations of allicin.	38
Figure 4.2: DON and allicin ATP levels in Hek293 cell treatments; DON reduced ATP production in the treated cells.....	39
Figure 4.3: RNS production in Hek293 cell treatments was increased for all treatments relative to the control (* $p = 0.0310$, ** $p = 0.0011$). Of particular significance is the increased RNS in DON+A treated cells when compared to the individual treatments (••• $p < 0.0001$, # $p = 0.0332$ compared to DON and allicin, respectively). Students <i>t</i> -test with Welch's correction.	40
Figure 4.4: DON and allicin MDA levels in treated Hek293 cells were decreased for all treatments (*** $p < 0.0001$, *** $p = 0.0003$, and $p = 0.0001$ respectively). The DON+A treatment increased MDA towards control levels compared to the individual DON (••• $p < 0.0001$) and allicin (# $p = 0.0109$) treatment; Students <i>t</i> -test with Welch's correction.	41

Figure 4.5: The decreased GSH concentration in all treatments compared to the control, with severe depletion in the combination treatment ($*p = 0.0342$; Students *t*-test with Welch's correction)..... 42

Figure 4.6: Expression of oxidative stress associated proteins on untreated and treated cells; (A) SOD2 was significantly decreased by DON ($***p < 0.0001$) and upregulated by allicin ($***p < 0.0001$); DON+A was similar to the control. (B) Catalase was significantly decreased by DON ($***p < 0.0001$) and upregulated by allicin ($***p < 0.0001$); DON+A returned catalase to control levels ($***p = 0.0006$). (C) GPx1 protein expression was upregulated by all treatments, particularly allicin ($***p = 0.0001$). (D) Nrf2 protein expression was significantly decreased by DON ($***p < 0.0001$) and slightly downregulated by allicin ($***p = 0.0021$); DON+A returned catalase towards control levels ($***p < 0.0001$). (E) Hsp70 was significantly upregulated by allicin and DON+A ($***p < 0.0001$). Unpaired student *t*-test with Welch's correction..... 44

Figure 4.7.1: The annexin V graph representing apoptotic cells in Hek293 cells. Apoptosis was reduced in DON, and DON+A treated cells ($*p = 0.0488$, Students *t*-test with Welch's correction). 45

Figure 4.7.2: The levels of necrosis for all Hek293 treated cells were not significantly different from the control. 45

Figure 4.8: Caspase activity following Hek293 cell exposure to DON, allicin and DON+A treatments. Initiator caspase 9 (A), as well as executioner caspase 3/7 (B) were downregulated for all Hek293 cell treatments. The combined treatment for caspase 9 ($\#p = 0.0397$) and caspase 3/7 ($\#p = 0.0067$) were significantly different from the allicin-only treatment, Students *t*-test with Welch's correction..... 46
..... 48

Figure 4.10: Expression of apoptosis-associated proteins in untreated and treated Hek293 cells. (A) PARP-1 was significantly upregulated by allicin ($***p = 0.0048$) and DON+A ($***p = 0.0004$) (B) p53 protein expression was upregulated by all treatments ($***p < 0.0001$). (C) Bax was downregulated by DON ($p = 0.1071$); and upregulated by allicin ($p < 0.0001$) and in the DON+A treatment ($p = 0.0026$). Unpaired student *t*-test with Welch's correction..... 48

Figure 4.11: A 2% agarose gel electrophoresis depicting DNA fragmentation in DON-treated Hek293 cells. 49

Figure 6.1: Schematic overview of the biochemical effects of DON, allicin and DON+A in human embryonic kidney (Hek293) cells (Prepared by author). 56

LIST OF TABLES

Table 2.1: The mean and maximum concentration of DON occurrence, in SA commercial maize and wheat samples collected after harvest in four consecutive production seasons (Meyer <i>et al.</i> , 2019a) . .	10
Table 2.2: Distribution of DON concentrated range in commercial SA post-harvest yellow and white maize (South Africa Foodstuffs, 2016).	10

ABSTRACT

Introduction: Deoxynivalenol (DON), a type B trichothecene produced by plant pathogenic fungi, especially *Fusarium graminearum* and *F. culmorum*, is a highly toxic mycotoxin found throughout South Africa. DON is consumed unintentionally through maize derived products and is rapidly becoming a potential health risk to humans and animals. It is a known immunosuppressant that induces apoptosis and oxidative stress and may cause liver lesions and kidney problems. Recently, dietary therapeutics have demonstrated a role against mycotoxin-induced cytotoxicity. Garlic (*Allium sativum*) is part of the Alliaceae family. The garlic bulb is used for medicine and as food consumption. The aqueous extract has recently demonstrated the potential to protect against mycotoxin-induced cell death and decrease reactive oxygen species (ROS).

Aim: This study investigated the induction of apoptosis and oxidative stress by DON in Hek293 cells, and the ability of allicin to ameliorate these effects.

Methods: Hek293 cells were treated with a range of allicin concentrations (0-150mM) over 24hrs. An EC₅₀ of 1.7mM was obtained from the MTT assay and used in all subsequent assays. Hek293 cells were treated with 5μM DON, 1.7mM allicin (A), or a combination (DON+A) for 24hrs; untreated cells served as the control. Lipid peroxidation [malondialdehyde (MDA) and lactate dehydrogenase (LDH) assays] were used to indirectly quantify reactive oxygen species (ROS) and oxidative stress; reactive nitrogen species (RNS) were quantified using the nitrates assay. Apoptotic induction was determined by the detection of phosphatidylserine (annexin V) and DNA fragmentation. Necrotic cells were distinguished by propidium iodide uptake. Luminometric quantification of ATP, reduced glutathione (GSH), and caspase 9, 3/7, were used to verify these events. In addition, antioxidant enzymes protein expression of superoxide dismutase (SOD2), catalase and glutathione peroxidase (GPx1); as well as nuclear factor erythroid 2-related factor 2 (Nrf2) and heat shock protein (Hsp70), and apoptotic markers associated protein expression of p53, Bax, and poly (ADP-ribose) polymerase (PARP) were detected by western blotting.

Results: DON-induced ROS production was suggested by the depletion of antioxidants including SOD2 ($p < 0.0001$), catalase ($p < 0.0001$) and GSH ($p = 0.0886$). Decreased lipid peroxidation indicated by the decreased MDA concentration ($p < 0.0001$) and reduced LDH ($p = 0.0342$) imply that the Hek293 cells were spared from the membrane-damaging effect of oxidative stress. A reduction in Hsp70 ($p = 0.0056$) and Nrf2 ($p < 0.0001$), and upregulation of GPx1 ($p = 0.0362$) protein expression was noted. In addition, increased nitrate concentration in all treatments compared to the control ($p < 0.0001$) suggested a shift to RNS production. Notably, allicin maintained Nrf2 protein expression similar to the control. The decrease in MDA concentration ($p = 0.0109$) by allicin was concurrent with depleted GSH ($p = 0.0504$)

and increased SOD2, catalase and GPx1 ($p < 0.0001$), and suggests allicin induced an oxidative stress response. Allicin also protected DON-treated cells from oxidative stress by upregulating Hsp70 ($p < 0.0001$), catalase ($p = 0.0006$) and GPx1 ($p = 0.0018$), with concurrent decreased GSH ($p = 0.0342$) and ATP ($p = 0.2028$) concentration, which were also decreased by DON. In addition, allicin increased MDA ($p < 0.0001$) and LDH ($p = 0.1267$) towards control levels in the combined treatment. Apoptosis was reduced in the DON ($p = 0.4631$) and DON+A ($p < 0.0488$) treated cells in comparison to the control, necrosis was not evident in any treatment. The slight induction of p53 ($p = 0.0008$) and PARP-1 ($p = 0.4036$) by DON implies an attempt at DNA repair, but the Hek293 cells experienced reduced levels of apoptosis. Indeed, Bax expression was slightly reduced ($p = 0.1071$), caspases 9 ($p = 0.0705$) and 3/7 ($p = 0.4431$) activities were diminished, phosphatidylserine was not externalized, and PARP-1 was not cleaved. A non-fragmented DNA profile in allicin-treated and DON+A-treated Hek293 cells may be explained by increased expression of DNA repair proteins, PARP-1 ($p = 0.0048$ and $p = 0.0004$ respectively) and p53 ($p < 0.0001$). The upregulation of p53 is associated with an increase in Bax expression ($p < 0.0001$ and $p = 0.0026$ respectively). However, caspases 9 ($p = 0.0596$) and 3/7 ($p = 0.0311$) were not activated and apoptosis did not occur.

Conclusion: DON treatment induced oxidative stress but not apoptosis in Hek293 cells at the concentration tested. In addition, its mechanism of toxicity in Hek293 cells appears to be more related to nitrosative stress and induction of DNA damage. Oxidative stress and not apoptosis is the possible mechanism of allicin-induced effects in Hek293 cells. Although allicin ameliorated some of the effects of DON in Hek293 cells, it also elicited synergistically or potentiating adverse effects that require further investigation.

Keywords: deoxynivalenol, allicin, oxidative stress, apoptosis, Hek293 cells

CHAPTER 1 : INTRODUCTION

1.1 FOCUS OF STUDY

Natural contaminants produced by a range of fungal species are mycotoxins. Mycotoxins commonly occur in food and livestock feed pose a health threat to animals and humans. The threat is instigated through direct contamination of agricultural commodities or by mycotoxins and their metabolites into animal products following consumption of contaminated feed (Milicevic *et al.*, 2015). The most significant agro-economic classes of mycotoxins are aflatoxins (AF), ochratoxins (OTA), zearalenone (ZEN), trichothecenes, and fumonisins (F) produced by species of *Fusarium*, *Penicillium*, and *Aspergillus* fungal species (Richard, 2007). *Fusarium* species are the primary mycotoxin producers, and the frequently occurring *Fusarium* toxins include deoxynivalenol (DON) and ZEN. DON and ZEN were reported to be present in 17,316 samples of feed and feed raw materials worldwide, in 55% and 36% of samples, respectively (Streit *et al.*, 2013).

DON (12,13-epoxy-3 α ,7 α ,15-trihydroxytrichothec-9-en-8-on) is a type B trichothecene produced by some plant pathogenic fungi, especially *F. graminearum* and *F. culmorum* (Herrera *et al.*, 2019). It is frequently found in wheat, maize, rye, rice, oats, and barley infected with *Fusarium* head blight (FHB) (Huang *et al.*, 2019). Structurally, DON contains 3 free hydroxy groups (-OH), making it an organic polar compound that is water-soluble and polar solvents such as aqueous methanol and ethyl acetate; its toxicity is associated with its polarity (Sobrova *et al.*, 2010). DON is not associated with carcinogenesis and has been classified by the International Agency for Research on Cancer (IARC) as a group 3 carcinogen (Pestka, 2010b). However, DON at low dose ingestion chronic causes reduced growth, anorexia, and declined nutritional efficiency, while high doses cause acute effects such as vomiting, rectal bleeding, and diarrhea. DON has chronic toxic effects on the reproduction, growth, and immune system (Milicevic *et al.*, 2015). In addition, DON is a known immunosuppressant and may cause liver lesions and kidney problems (Pestka, 2003, Sun *et al.*, 2014). DON exposure causes kidney damage in animals; creatinine and blood urea nitrogen (critical markers of kidney function) are associated with renal injury induced by DON (Chen *et al.*, 2008, Hou *et al.*, 2013a, Liang *et al.*, 2015). More recently, *in vivo* results indicated that DON could induce kidney dysfunction, oxidative stress, and apoptosis in female mice (Liang *et al.*, 2015).

The mechanism of DON-induced toxicity is inhibition of translation, which may be partial or complete dependent on the dose and exposure duration. There is considerable *in vitro* evidence that at certain concentrations of DON induces gene expression, but exposure prolonged to high concentrations results

in cell death, usually by apoptosis (Pestka, 2008, Kang *et al.*, 2019, Lee *et al.*, 2019). Programmed cell death is apoptosis, a mediation precisely controlled by the deletion of “unwanted” cells. It leads to the swift phagocytic clearance of intact cells; tissues are protected against the noxious effect of cell contents (Elmore, 2007, Guerrero-Netro *et al.*, 2017, Gu *et al.*, 2019). Apoptosis occurs via the extrinsic and/or intrinsic signalling pathways. The extrinsic pathway is activated through the binding of death receptors to ligands to transmit apoptotic signals and activate initiator caspase 8, while the intrinsic pathway is triggered by numerous mitochondrial stimuli such as DNA damage, oxidative stress, and growth factor deprivation (Elmore, 2007, Mukhopadhyay *et al.*, 2014). The tumour suppressor p53 initiates transcription of pro-apoptotic Puma and Noxa to sequester the anti-apoptotic members of the BCl₂ family, including BCl₂. This allows Bax, a pro-apoptotic BCl₂ protein, to dimerize and cause mitochondrial outer membrane permeability. The subsequent release of cytochrome c and apoptosome formation causes the activation of initiator caspase 9 (Aupanun *et al.*, 2019b). Execution of apoptosis is accomplished when initiator caspases cleave and activate caspase 3/7 to direct the dismantling of the cell; active caspase 3/7 results in externalization of phosphatidylserine (PS), activation of caspase-activated DNase (CAD), and cleavage of poly (ADP-ribose) polymerase (PARP) (Bensassi *et al.*, 2012). Morphological features that result are fragmentation of internucleosomal DNA, membrane blebbing, and formation of apoptotic bodies (Elmore, 2007, Zhang *et al.*, 2017a, Habrowska-Gorczyńska *et al.*, 2019).

Oxidative stress occurs when the concentration of reactive oxygen species (ROS) exceeds the antioxidant capacity to detoxify them (da Silva *et al.*, 2018). Oxidative stress is initiated by ROS, such as the superoxide anion (O₂⁻), perhydroxyl radical (HOO[·]) and hydroxyl radical (HO[·]), and by reactive nitrogen species (RNS), including nitric oxide (NO) and peroxynitrite (Liguori *et al.*, 2018). ROS and RNS initiate the process of lipid peroxidation in the lipid membrane causing damage to phospholipids, also DNA damage and protein by generating a chain reaction (Braca *et al.*, 2002). Antioxidants are required to reverse these detrimental processes and detoxify ROS. Primary antioxidant enzymes responsible for protection from ROS are superoxide dismutase (SOD2), catalase and glutathione peroxidase (GPx1). SOD2 catalyzes the dismutation of the free radical O₂⁻ to less reactive hydrogen peroxide (H₂O₂), which is detoxified to water by catalase and/or GPx1. GPx1 uses reduced glutathione (GSH) in the detoxification of H₂O₂; in the process, GSH is oxidized (GSSG) and requires reduction by glutathione reductase (GR) (da Silva *et al.*, 2018). The master regulator, nuclear factor erythroid 2-related factor 2 (Nrf2) functions to upregulate the expression of an array of enzymes and antioxidants involved in the cell protection of against oxidative stress (Yu *et al.*, 2017b).

The toxic effects of mycotoxins have resulted in much research on how to reduce these detrimental effects, including better agricultural practice and monitoring of levels in food and feed. Recently, dietary therapeutics have demonstrated a role against mycotoxin-induced cytotoxicity. *Allium sativum* aqueous extract showed this potential when it was found to reduce cell death, ROS production, and DNA damage in Vero cells caused by ZEN (Abid-Essefi *et al.*, 2009). *Allium sativum* (garlic) belongs to the Alliaceae family. The garlic bulb is consumed as food or medicine. Garlic has several uses; it contains antibacterial, antiprotozoal, antifungal, antiviral, and properties; it benefits the cardiovascular and immune systems (Bayan *et al.*, 2014). Garlic is rich in sulphur-containing compounds, including allicin, which is associated with the beneficial effects of garlic (Oosthuizen *et al.*, 2018). Therefore, the effects of allicin against DON-induced cytotoxicity will be evaluated in Hek293 cells.

1.2 PROBLEM STATEMENT AND RATIONALE

The global contamination of foods and feeds through mycotoxins is a substantial problem because they exert harmful effects on humans, animals, and crops and are responsible for causing illnesses and significant economic losses. DON is one of the most common food contaminating mycotoxins. DON's effects include feed refusal, emetic effects, and generalized gastrointestinal toxicity. DON is a potent immunotoxin, hepatotoxin, and nephrotoxin that can induce a wide variety of health problems in both humans and animals. Indeed, although kidney damage is a known feature of DON exposure, there are inadequate studies that have investigated the effects of DON in human kidney cells.

Given the severe effects associated with mycotoxins, research into ways of reducing these effects is ongoing. Efforts have been made to improve farming practice in order to limit the production of mycotoxins. Likewise, exposure may be reduced by setting minimal levels in food. Recently, phytochemical research has revealed their protective effects on mycotoxin-induced toxicity. Aqueous extracts of *Allium sativum* were effective in reducing ZEN toxicity in Vero cells. Allicin is the bioactive phytochemical in *Allium sativum*. While recent research demonstrates the potential for medicinal plants such as *Allium sativum* to ameliorate mycotoxin-induced effects, the mechanisms of these as they relate to DON are unknown. Thus, the specific protective mechanisms of allicin in DON-induced kidney toxicity at the cellular and molecular level needs to be elucidated.

1.3 HYPOTHESIS

Allicin will alleviate the cytotoxic effects associated with apoptosis and oxidative stress induced by deoxynivalenol in Hek293 cells.

1.4 AIM

This study aims to determine the cellular and molecular mechanisms of deoxynivalenol-induced cytotoxicity in human embryonic kidney (Hek293) cells and the possible ameliorative effects of allicin.

1.5 OBJECTIVES

This study will

- determine the EC₅₀ of allicin in Hek293 cells using the methylthiazol tetrazolium (MTT) assay
- assess oxidative stress induced by DON and the ameliorative effect of allicin as follows:
 - Free radical production will be indirectly quantified by measuring malondialdehyde, a marker of lipid peroxidation, using the thiobarbituric reactive substances (TBARS) assay
 - NO, an intermediate in the production of RNS, will be indirectly measured using the s nitric oxide synthase (NOS) assay, which quantifies nitrate and nitrites
 - GSH will be assayed by luminometric quantification
 - Protein expression of antioxidant enzymes SOD2, catalase, and GPx1, as well as Nrf2 and Hsp70 will be quantified using western blotting
- determine the effects of DON and allicin and a combination of DON and allicin exposure on apoptosis induction by
 - quantifying PS externalization as an early marker of apoptosis
 - assessing caspase activity using luminometry
 - using western blotting to determine protein expression of p53, Bax, and PARP-1

CHAPTER 2 : LITERATURE REVIEW

2.1 MYCOTOXINS

Mycotoxins are toxic secondary metabolites produced under opportune environmental conditions by filamentous fungi mainly of the *Fusarium*, *Aspergillus*, and *Penicillium* genera (Bennett and Klich, 2003, Bertero *et al.*, 2018). Species such as *F. verticillioides* and *F. graminearum* each have the ability to synthesize more than one metabolite. Mycotoxins are characterized by their minimal molecular weight, have caused a wide range of diseases, death in humans and certain animals. *Fusarium* producing mycotoxins are naturally occurring contaminants in produces, food, and feed (Ferrigo *et al.*, 2016). They have any biochemical consequence in the growth and development of the host fungus, often produced as an adaptive response to a change in the availability of nutrients or other environmental conditions (Zain, 2011). Mycotoxins are extremely toxic compounds usually produced for purposes of self-defense or to dissolve cellular membranes as part of their fungal pathogenicity (Bertero *et al.*, 2018). The chemical structures of mycotoxins vary considerably, which accounts for the differences in toxic effects (Peraica *et al.*, 1999, Yiannikouris and Jouany, 2002).

2.1.1 Mycotoxins and food

The global impact induced by mycotoxins in the contamination of foods and feeds a major problem (Zain, 2011, Spanic *et al.*, 2019, Stanciu *et al.*, 2019). The most common food contaminating mycotoxins, including aflatoxin, fumonisins, trichothecenes, and ochratoxins (Figure 2.1), are common contaminants of grain products like maize (Figure 2.1). While direct contamination of agricultural commodities (Figure 2.1) may lead to human exposure, “carry-over” of mycotoxins and their by-off products into animal tissues, eggs, and milk destined for human consumption may occur when animals are exposed to contaminated feed (Milicevic *et al.*, 2015). Mycotoxins are a known threat in the health of humans and animals through illnesses, disability, or death (Peraica *et al.*, 1999, Zain, 2011, Njobeh *et al.*, 2012, Chilaka *et al.*, 2017, Al-Jaal *et al.*, 2019, Amarasinghe *et al.*, 2019). The often unrecognized diseases that result are known as mycotoxicosis (Peraica *et al.*, 1999, Zain, 2011). Mycotoxicosis is common in areas where there are inferior methods of food handling, and improper storage of food is carried out. It also frequently occurs in countries such as South Africa (SA) where malnutrition is a problem and where maize and cereal grains form part of a staple diet for many people (Bennett and Klich, 2003, Misihairabgwi *et al.*, 2017).

The high occurrence of mycotoxins in foods may cause varied effects ranging from severe to chronic toxicity (mutagenic, teratogenic, carcinogenic), immunotoxicity, growth hindrance, and much higher

dosages can affect with development and reproduction (Pestka, 2010c, Warth *et al.*, 2013). Toxicities include modified (altered) neuroendocrine responses that precede from pathophysiological events, pro-inflammatory gene expression through upregulation, disruption of gastrointestinal tract permeability manifestations in humans, animals, and interference with growth hormone signalling (Richard, 2007, Foroud *et al.*, 2019). Mycotoxins impact on the economy includes the loss of human and animal life, reduced livestock production, healthcare increments, and veterinary care costs, as well as financial loss due to discarding of contaminated foods and feedstuffs (Hussein and Brasel, 2001, Misihairabgwi *et al.*, 2017, Sefater *et al.*, 2019).

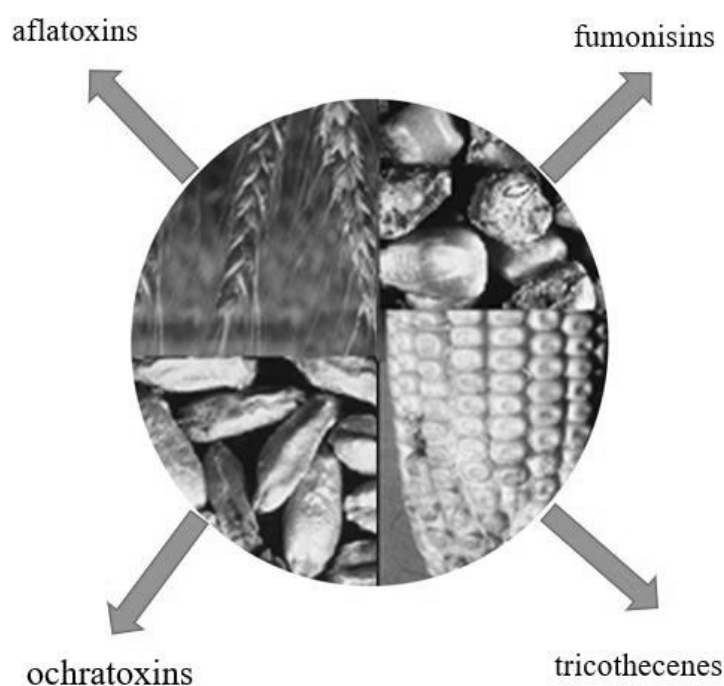


Figure 2.1: The contamination of cereal crops by mycotoxin-producing fungi showing the commonly occurring mycotoxins (adapted from (Liu *et al.*, 2016)).

2.1.2 Mycotoxins and animals

Mycotoxin contamination of feed causes numerous toxicities in diverse animal species. This may be attributed to the varied range of feed components used and the molecular differences amid and within species (Hussein and Brasel, 2001, Aupanun *et al.*, 2019a). Early studies on the effects of acute aflatoxicosis indicated several toxicities in different animal species (Bertero *et al.*, 2018). In monogastrics, variable responses have been publicized with all mycotoxins. For example, pigs have been shown to be very sensitive to T-2 toxin, DON, and ZEN (Deng *et al.*, 2015, Alizadeh *et al.*, 2016). T-2 and DON adversely affected poultry; however, has resistance to oestrogenic effects caused by ZEN (Cheeke, 1998, Reddy *et al.*, 2018, Hooft *et al.*, 2019).

2.1.3 Mycotoxins and humans

Humans may be exposed to mycotoxins through ingesting contaminated foods along with the carry-over of mycotoxins and toxic metabolites in animal products such as milk, meat, and eggs (Yiannikouris and Jouany, 2002, Zain, 2011). However, inhalation of spore-borne toxins and skin-contact by mold-infested substrates and are also important sources of exposure (Wild and Gong, 2010). Acute and chronic manifestations are associated with toxicity. For example, aflatoxin causes aflatoxicosis, which in its acute stage ends in death; chronic aflatoxicosis causes cancer and immune suppression. The primary target organ is the liver; the feeding aflatoxin B₁ to nonhuman primates, fish, rodents, and poultry causes liver damage (Zain, 2011, Al-Jaal *et al.*, 2019). Alimentary toxic aleukia is a human disease associated with T-2 and diacetoxyscirpenol. Inflammation of the skin, vomiting, and damage to hematopoietic tissues are the symptoms associated with this disease. The severe phase is accompanied by necrosis in the oral cavity, mouth, vaginal and nose bleeding, and disorders in central nervous system (Bennett and Klich, 2003, Chilaka *et al.*, 2017, Al-Jaal *et al.*, 2019).

2.2 DON

DON is a trichothecene synthesized by *Fusarium* species. Trichothecenes (THs) are *Fusarium* derived - *Fusarium graminearum* species complex (Fg complex), *F. culmorum*, *F. cerealis*, *F. pseudograminearum*, *F. sporotrichioides*, *F. langsethiae*, *F. sibiricum*, and *F. poae* produce toxins with a high potency that are commonly associated with *Fusarium* head blight in cereal grains (Zinedine *et al.*, 2007). Trichothecenes are a family of over 200 toxins with a common tricyclic 12,13-epoxytrichothec-9 ene (EPT) core structure (Figure 2.2) (Valenta, 2004, McCormick *et al.*, 2011). They have been classified into four groups (Types A, B, C, and D) based on the substitution pattern of EPT (Figure 2.2) (Y, 1977, Ueno, 1984). Types A, B, and C can be differentiated based on the substitution at the C-8 position. Type A trichothecenes include compounds that have a hydroxyl group at C-8 (e.g., neosolaniol), an ester function at C-8 (e.g., T-2 toxin), or no oxygen substitution at C-8 (e.g., trichodermin, 4,15-diacetoxyscirpenol, and harzianum A). Type B trichothecenes have a keto (carbonyl) function at C-8 (e.g., nivalenol, deoxynivalenol, and trichothecene) and a C-7 hydroxyl group, but this structural feature is not present in other genera. Crotocin is an example of a Type C trichothecenes with a C-7/C-8 epoxide (e.g.,). In contrast, type D trichothecenes have an additional ring linking the C-4 and C-15 position (e.g., roridin A, verrucarins A, satratoxin H) (Altomare *et al.*, 1995, Garvey *et al.*, 2008, Gottschalk *et al.*, 2009).

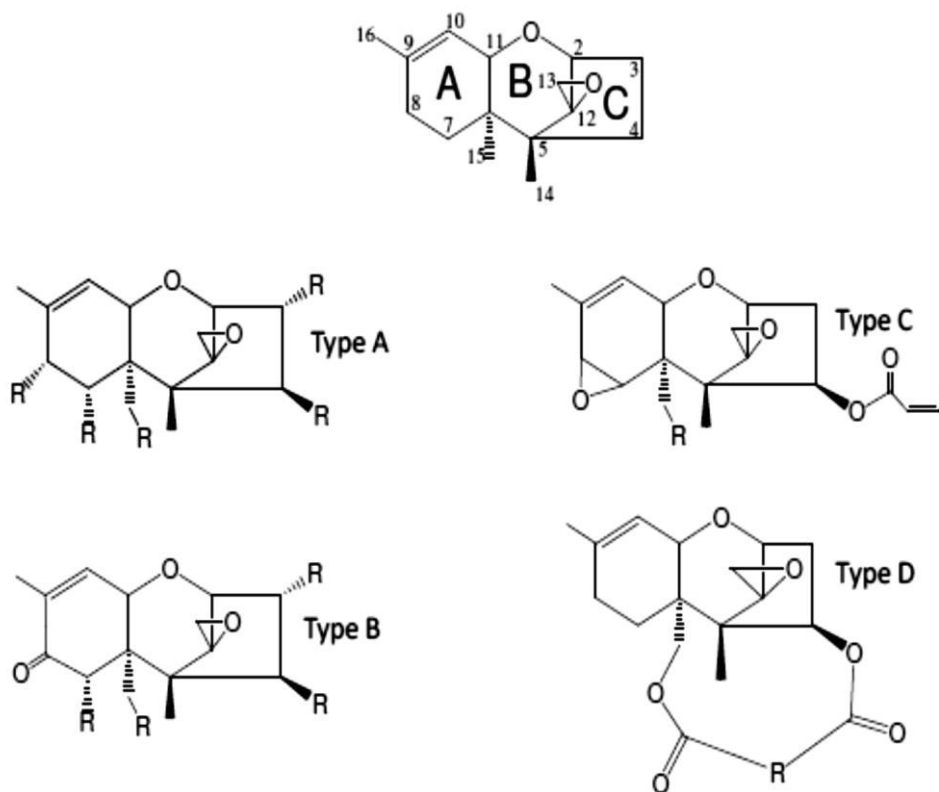


Figure 2.2: Classification of trichothecene structures. EPT core structure; R groups may be OH, H, O-Acyl, or dissimilarities in the macrolide chain (McCormick *et al.*, 2011).

Those of significance are types A and commonly occurring type B THs. Type A common THs are T-2 and HT-2 toxin, while DON and its acetylated byproducts 3-ADON and 15-ADON are type B THs. South Africa has insufficient data on TH toxins (Chilaka *et al.*, 2017, Misihairabgwi *et al.*, 2017, Meyer *et al.*, 2019b).

2.2.1 DON chemistry

Toxigenic *Fusarium* species that are common pathogens of cereal crops in moderate climates produced deoxynivalenol (Kokkonen *et al.*, 2010, Cambaza *et al.*, 2019). DON chemically (Figure 2.3) is a polar organic sesquiterpenoid compound, a type B trichothecene since it contains a carbonyl group in C-8, a conjugated double bond between C9 and C10, and an epoxide moiety at position C12-C13 (Woelflingseder *et al.*, 2018). DON is highly hydrosoluble, unchanging at cooking temperatures (120°C), milling processes, and storage conditions (Bretz *et al.*, 2006, Hazel *et al.*, 2009).

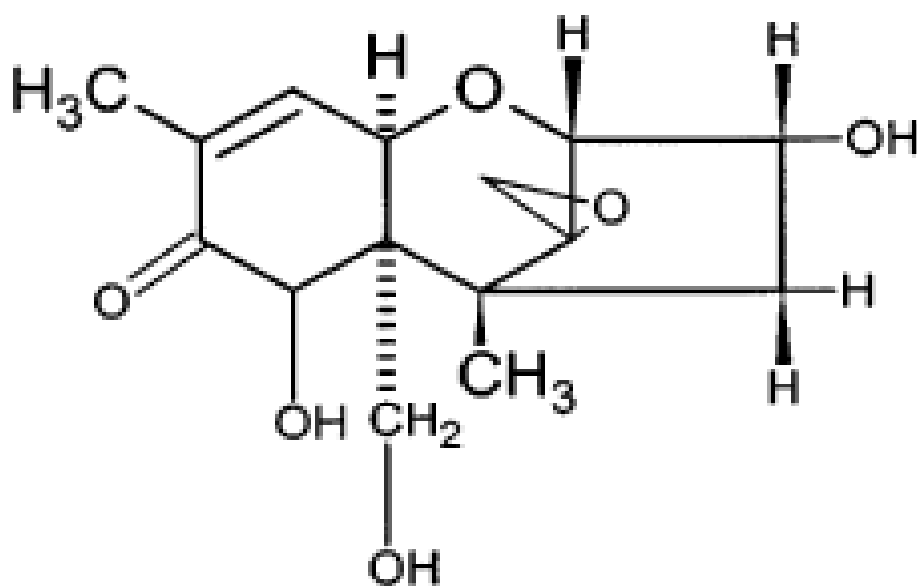


Figure 2.3: The chemical structure of DON, a type B-trichothecene sesquiterpenoid polar organic compound (Singh *et al.*, 2015).

2.2.2 Prevalence of DON

DON is one of the most predominant food-associated mycotoxin naturally present in food supplies, particularly grains such as maize, rice, oats and wheat (Hoofst *et al.*, 2019, Meyer *et al.*, 2019b). It has been approximated that 25% of the world's crop production may be infected with this mycotoxin (Maresca, 2013, Pinton and Oswald, 2014, Viljoen *et al.*, 2017, Amarasinghe *et al.*, 2019). A European survey revealed that 61%, 89%, and 47% of maize, barley, wheat, and samples respectively are DON contaminated (Schothorst *et al.*, 2005). The DON incidence has been constantly reported in South African crop-based harvests (Table 2.1 and 2.2). For this particular reason, the mycotoxin is of great interest in the country (Njobeh *et al.*, 2012, Chilaka *et al.*, 2017, Viljoen *et al.*, 2017, Meyer *et al.*, 2019b).

DON contamination of South African wheat and maize is usually low (Table 2.1 and 2.2), with the incidence rate highest at 17.5% (7/40), as observed in the season of 2017–2018 (Meyer *et al.*, 2019a). The mean concentrations ranged between 202 and 397 $\mu\text{g}/\text{kg}$, and the maximum concentration (593 $\mu\text{g}/\text{kg}$) was discovered in a wheat sample taken from the production of 2015–2016. The DON contaminated samples came from different regions of production (Meyer *et al.*, 2019a). The regulation of this mycotoxin in poultry feed is done by the Department of Agriculture, Forestry, and Fisheries (DAFFs) South Africa, limiting the level to 4000 $\mu\text{g}/\text{kg}$ in South African feedstuffs (Moghadamnia *et al.*, 2019). Njobeh *et al.* (2012) found chicken feeds containing DON with mean levels of 620 ± 386 $\mu\text{g}/\text{kg}$ at a maximum level of 1980 $\mu\text{g}/\text{kg}$, while Changwa *et al.* (2018) stated DON incidence of 99%,

but at comparatively lesser levels of DON with a maximum rate at 81.6 µg/kg in dairy feeds (max: 154 µg/kg) (Njobeh *et al.*, 2012, Changwa *et al.*, 2018). South Africa has regulated DON levels in maize, barley, and wheat, for human consumption, with 2000 µg/kg the maximum permissible concentration in grain proposed for further processing (Beukes *et al.*, 2017).

Table 2.1: The mean and maximum concentration of DON occurrence in SA commercial maize and wheat samples collected after harvest in four consecutive production seasons (Meyer *et al.*, 2019a).

Produce season	Quantity DON of samples	Mean, DON concentration ¹ , µg/kg	Maximum, DON, concentration ² , µg/kg
2014 - 2015	5/40	229	361
2015 - 2016	5/40	397	593
2016 - 2017	4/40	289	501
2017 - 2018	7/40	202	570
¹ Mean values based on samples positivity. ² Maximum values found in individual samples			

Table 2.2: Distribution of DON concentrated range in commercial SA post-harvest yellow and white maize (South Africa Foodstuffs, 2016).

Percentage of DON samples								
Concentration range of DON (µg/kg)	White maize				Yellow maize			
	2013-2014	2014-2015	2015-2016	2016-2017	2013-2014	2014-2015	2015-2016	2016-2017
No. DON (<LOQ=100)	26.1	55.4	74.4	46.4	34.6	63.2	82.0	80.7
100<500	55.8	31.0	21.2	28.5	55.1	34.1	17.0	13.5
500<1000	10.3	7.7	3.8	7.3	8.1	2.7	1.0	3.5
>1000-2000	6.7	4.2	0.6	8.9	1.6	0.0	0.0	2.3
2000 ¹	1.2	1.8	0.0	8.9	0.5	0.0	0.0	0.0
¹ 2000 µg/kg is the South African regulated maximum acceptable DON level in unrefined maize aimed for human consumption								

2.2.3 Mechanism of action

Investigative studies of DON effects in cultured cells have provided an exclusive insight into this toxin's possible mechanisms of action (Figure 2.4). There is substantial evidence that suggests low to medium concentrations of DON partly inhibit protein synthesis *in vitro* and *in vivo*, and that extended exposure to high concentrations of DON may entirely prevent translation (Figure 2.4) (Azcona-Olivera *et al.*, 1995, Katika *et al.*, 2012, Dellafiora and Dall'Asta, 2017, Graziani *et al.*, 2019). The epoxide moiety at C12-C13 position is crucial for the inhibition of eukaryotic protein biosynthesis (Woelflingseder *et al.*, 2018). Deoxynivalenol is also known to induce gene expression selectively. In addition, the toxin initiates cell death by apoptosis (Pestka *et al.*, 2008, , Kang *et al.*, 2019, , Lee *et al.*, 2019).

The acknowledged mechanism for inhibition by DON translation involves interference with peptidyl transferase function on the ribosome with consequential impairment of initiation and elongation processes of protein synthesis (Shifrin and Anderson, 1999, Maresca, 2013). However, *in vitro*, findings suggest that at least three additional mechanisms may be involved in translation arrest:

1. DON can induce the instigation of a ribosome-linked kinase, in mononuclear phagocytes known as double-stranded RNA-associated protein kinase (PKR) (Zhou *et al.*, 2003, Pinton and Oswald, 2014). When activated, PKR can phosphorylate eukaryotic initiation factor 2 α (eIF2 α), thereby impeding translation.
2. DON can endorse the breakdown of 28s rRNA, which might impede ribosome function and translation (Li and Pestka, 2008, McCormick *et al.*, 2011).
3. DON may be able to upregulate many microRNAs (miRNAs), a species associated with selective gene downregulation (He and Pestka, 2010). Many DON-induced miRNAs have sequences that complement ribosomal protein mRNAs. Thus, it can be speculated that DON-exposed cells employ miRNA-downregulation of ribosome synthesis to economize and redistribute the resources needed for survival (Pestka, 2010a, Xue *et al.*, 2019).

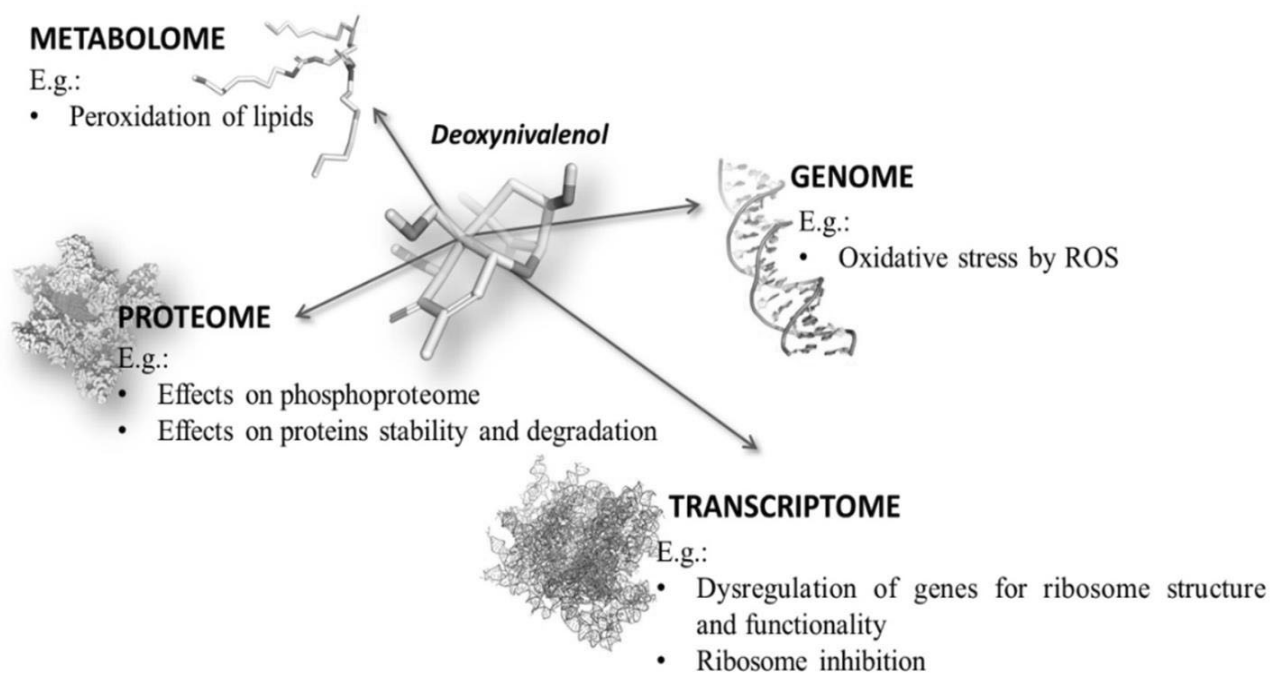


Figure 2.4: DON provides an example of pleiotropy at various degrees of density, and over the different biotic macromolecules. The crosstalk of the molecular modifications at genomic, proteomic, transcriptomic, and metabolomic levels can result in a series of physiological and cellular effects (Dellafiora and Dall’Asta, 2017).

DON has been demonstrated to inhibit both DNA and RNA synthesis. Scheduled inhibition of DNA synthesis in several types of cells as well as in mice and rats, though to a minor degree than protein synthesis (Wannemacher and Wiener, 2000). The mechanism of inhibition is not precise. The RNA synthesis inhibition is thought to be a secondary effect of the inhibition of protein synthesis (Rotter *et al.*, 1996). Furthermore, Moon and Pestka (2002) demonstrated that DON induces cyclooxygenase-2 (COX-2) macrophage expression. This rate-limiting enzyme is known to be super-induced by protein synthesis inhibitors and energizes the oxygenation of arachidonic acid to prostaglandin endoperoxides (Moon and Pestka, 2002). The resulting metabolites are then altered enzymatically into prostaglandins and thromboxane A₂, which play both pathologic and physiologic capacities in a varied range of inflammatory processes (SCF, 2002).

2.2.4 DON toxicity

DON digestion has been shown to harm functions of the immune, reproductive, nervous, and colonic systems. It has been shown that interim and sub-chronic contact to DON could lead to anorexia in mice, resultant in reduced body weight. Equally, an overdose can cause a shock-induced death (Sobrova *et al.*, 2010). Additionally, DON-induced toxicity has been shown to raise genotoxicity and oxidative stress in

animal primary cell culture (Yang *et al.*, 2014, Singh *et al.*, 2015) along with hindering protein synthesis and DNA (Hassan *et al.*, 2015, Yu *et al.*, 2017a). Subsequent to acute exposure, bloody diarrhea and vomiting have been observed (Pestka, 2010b). DON has had a negative impact on the health of humans and animals.

2.2.4.1 Toxic effects in animals

Various studies have researched the effects DON may induce in animals such as mice, chicken, and pigs (Savard *et al.*, 2014, Chen *et al.*, 2017, Li *et al.*, 2019). Researchers have found that pigs are most vulnerable to DON (Deng *et al.*, 2015). The main overt effects at low dietary concentrations or subchronic exposure in various animal species have been demonstrated to reduce feedstuff intake (anorexia), different levels in blood parameters, and weight gain, including serum immunoglobulins. Over the years, numerous studies have demonstrated the DON effects on immunoglobulin A (IgA), which indicates the possibility of suppression of the humoral and cellular immune system, resulting in increased susceptibility to various infectious diseases. Postnatal mortality and embryotoxic effects have also been observed in mice at maternally toxic doses of 75 µg/30 g (Scientific Committee on Food, 1999, Sobrova *et al.*, 2010). At higher dietary concentrations, the main effects of DON include vomiting (in pigs), tardy gastric discharging (in rats and mice), weight loss, feed refusal, and diarrhea (Sobrova *et al.*, 2010).

Symptoms of DON intoxication might include reduced weight gain, a reduction in food consumption, neuroendocrine fluctuations, and alteration of intestinal and immune functions (Payros *et al.*, 2016). As the organ central in metabolism, the kidney is a vital research issue on mycotoxin toxicity (O'Brien and Dietrich, 2005). Kidney impairment is a known feature of exposure to DON in animals (Liang *et al.*, 2015). However, few known studies have investigated the effects of DON on kidneys, with importance on kidney index and histopathological changes (Forsell *et al.*, 1986, Borutova *et al.*, 2008). Hence, studies intended to determine the DON effects of kidney toxicity in female mice. Creatinine (CRE) and blood urea nitrogen (BUN) are formed through protein and creatinine metabolism, respectively, and primarily used to assess glomerular filtration; these constraints are the two most vital indicators that imitate the degree of renal damage (El-Sawi *et al.*, 2001, Vander *et al.*, 2001). The concentration of CRE and BUN was essentially affected by the DON administration. This outcome indicated severe impairment in kidney function. The DON toxicity to kidney functioning restrictions presented sub-additive effects. Similarly, former studies showed that renal damage is DON induced (Chen *et al.*, 2008, Hou *et al.*, 2013b). Zhen and co-workers reported *in vivo* findings that indicated that DON causes kidney dysfunction, apoptosis, and oxidative stress in female mice (Liang *et al.*, 2015).

2.2.4.2 Toxic effects in humans

Occurrences of toxicosis related with consumption of mould contaminated corn and wheat are connected to the presence of *F. graminearum* and have been conveyed in Japan (red mould disease), India (DON toxicosis), and China (fusariotoxigenosis) (Bhat *et al.*, 1989, Li *et al.*, 1999, Wijnands and Van Leusden, 2000). Acute toxic manifestations in humans include vomiting and respiratory tract irritation. DON demonstrated dose-dependent (100–5000 ng/ml) immunotoxicity in human peripheral blood mononuclear cells (PBMCs) by inhibition of concanavalin A (Con A) and induced -PHA lymphocyte blast transformation (T lymphocyte proliferation). In addition, DON has inhibited natural killer cell activity antibody-dependent cell-mediated cytotoxicity of monocyte-free PBMCs (Berek *et al.*, 2001, Gimeno, 2004, Lima, 2010). Further evidence for immunotoxicity in PBMCs was evident when DON stimulated cytokine production and impaired apoptosis within the immune system (Pestka, 2008). Observation in cell proliferation decreases, as well as cellular defense activity impairments, including a variation of cytokine production and natural killer cell activity. Though it is not clear how these *in vitro* studies interpret to an intact human system, modulation of immune function through the ingesting of DON-contaminated food products has the potential to increase vulnerability to disease (Pestka and Smolinski, 2005).

Humans are primarily exposed to DON through cereal-derived food. The European tolerable daily intake (TDI) of 1 µg/kg body weight per day for DON was established; however, it can be DON exposure to young children occurs at levels close to or greater than the TDI (EFSA, 2013, Payros *et al.*, 2017b). There is no evidence for carcinogenic properties of DON, and it was classified into group 3 by the International Agency for Research on Cancer (IARC) (Payros *et al.*, 2017b).

In 2003, Sundstol-Eriksen and Pettersson investigated the intestinal metabolism of DON and the ability of the human gastrointestinal organisms to change trichothecenes 3-acetyldeoxynivalenol and nivalenol. They found that no de-epoxidized metabolites were detected, in dissimilarity to what has been stated for other species such as rats, mice, and pigs. The results suggested that the humans in their study may have lacked the microflora for an essential detoxification step for DON (Sundstol Eriksen and Pettersson, 2003).

2.3 MEDICINAL PLANTS

Medicinal plants provide an important source of nutrition and a plethora of phytochemicals recommended for their therapeutic value, which can be used in drug development and synthesis. Some

medicinal plants such as garlic, ginger, green tea, and walnuts form part of the diet. The metabolites produced by plants are an auspicious alternate against the treatment of mycotoxin toxicity. Plants are recognized to have antimicrobial activity for plant defense, including alkaloids, tannins, flavonoids, glycosides, isoflavonoids, phenylpropanes, coumarins, terpenes, and organic acids. Currently, plants have attracted growing interest due to their relatively safe status; several of them are considered 'Generally Regarded As Safe' (GRAS) by the US Food and Drug Administration (FDA) (Cabral *et al.*, 2013, Xue *et al.*, 2019).

2.3.1 Garlic

Allium species are one of the world's oldest cultured plants due to their long-life storage. *Allium sativum*, known as garlic, belongs to the family of Alliaceae. Garlic is originally indigenous to Central Asia and the north-eastern parts of Iran and is also cultivated generally around the world (Kew.org., 2016). The plant forms a bulb that is ingested as food and medicine. Pollination of hermaphrodite flowers is by bees and other insects. The plant favours well-drained acidic soils, with medium-light to perform at its prime (Oosthuizen *et al.*, 2018). The garlic bulb is mostly prepared raw or by cooking for flavouring and has all edible parts. Garlic has been reported to contain antiviral, antifungal, antibacterial, and antiprotozoal properties and advantageous cardiovascular and immune system effects (Harris *et al.*, 2001). Polysulfide oils are the active oils in garlic, which contribute to biological properties (Oosthuizen *et al.*, 2018, Salehia *et al.*, 2019).

2.3.2 Bioactive compounds in garlic

There are numerous sulfur-comprising compounds in garlic such as alliin, diallyl trisulfide, diallyl disulfide, S-allylcysteine, diallyl sulfide, ajoene, and allyl mercaptan. Crushed garlic activates the alliinase enzyme, and alliin produces allicin (Figure 2.5) (Bayan *et al.*, 2014). Allicin (allyl 2-propenethiosulfinate or diallyl thiosulfinate) is the key bioactive compound present in the fluid garlic extract or raw garlic homogenate (Gruhlke *et al.*, 2016). Additionally, to allicin, fresh garlic extract comprises of active chemical elements, with amino acids, sulfur compounds, minerals, and enzymes (Salehia *et al.*, 2019).

2.3.3 Allicin

2.3.3.1 Biosynthesis of allicin and its products

Allicin (diallylthiosulfinate), garlic produced, is formed from the non-proteinogenic amino acid alliin (allylcysteine sulfoxide). A two-step reaction forms allicin, where alliinase is used to convert alliin to

acid dehydroalanine and allylsulfenic. In step two, allylsulfenic acid of two molecules condenses spontaneously to form one molecule of allicin (Figure 2.5) (Borlinghaus *et al.*, 2014, Oosthuizen *et al.*, 2018). Allicin reactivity is due to the thiol-groups; nevertheless, under certain conditions, it reacts with itself, forming more compounds that can be bioactive, such as ajoene, polysulfanes, and vinyl-dithiins (Jacob and Anwar, 2008, Gruhlke *et al.*, 2016).

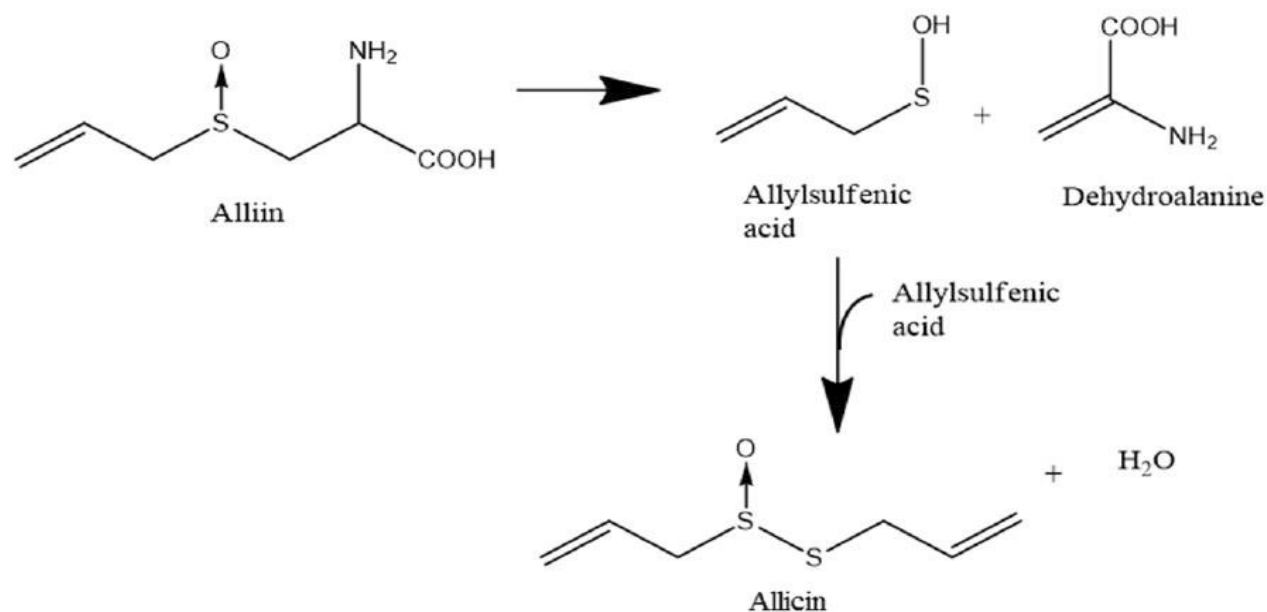


Figure 2.5: Allicin biosynthesis. The non-proteinogenic amino acid alliin is converted by the alliinase enzyme activation to dehydroalanine and allyl sulfenic acid. Two molecules of allyl sulfenic acid condensed spontaneously to a single allicin molecule (Gruhlke *et al.*, 2016).

2.3.3.2 Effects of allicin

In 1960, it was initially stated that tumour cells were killed through the incubation of an allicin solution (Dipaolo and Carruthers, 1960). Thus, anti-cancer activity is among the many health benefits conferred by allicin. Allicin mediates its anti-cancer effects via apoptosis and inhibition of cancer cell proliferation in different cell lines (Siegers *et al.*, 1999, Hirsch *et al.*, 2000, Bat-Chen *et al.*, 2010). Both caspase-dependent (Oommen *et al.*, 2004, Bat-Chen *et al.*, 2010) and caspase-independent (Park *et al.*, 2005) apoptosis has been induced by allicin in different cell lines. Modulation of tubulin, which subsequently interferes with mitotic spindle formation and cell division, is postulated to be the mechanism by which allicin mediates the inhibition of cell proliferation (Prager-Khoutorsky *et al.*, 2007). All living cells comprise of ubiquitous thiol groups. Allicin's membrane-permeability (Miron *et al.*, 2000) allows cells to easily enter and react with cellular thiols such as glutathione (GSH) (Rabinkov *et al.*, 2000) or cysteine

residues in proteins (Wallock-Richards *et al.*, 2014). Under physiological conditions, allicin oxidizes these essential biomolecules; it, therefore, fulfills the definition of a reactive sulphur species (RSS) (Gruhlke and Slusarenko, 2012). Allicin has free radical scavenging effects by inhibiting superoxide production in the presence of ox stress; allicin also induces phase II detoxification and upregulates Nrf2, thus fulfilling replenishing essential antioxidants, superoxide dismutase 2 (SOD2) and GSH (Gruhlke *et al.*, 2016, Salehia *et al.*, 2019).

2.4 OXIDATIVE STRESS

Free radicals are generated as a result of physiological reactions, e.g., cellular respiration, may be produced by cells in homeostasis. The overproduction of free radicals can be promoted by a variety of exogenous factors and leads to oxidative stress (Young and Woodside, 2001). Cells undergo oxidative stress when the reactive oxygen species (ROS) production such as the peroxy radical (HOO^\cdot), hydroxyl radical (HO^\cdot), superoxide anion ($\text{O}_2^{\cdot-}$), and reactive nitrogen species (RNS), inclusive of nitric oxide (NO), and peroxynitrite (ONOO^-), surpasses the capacity of antioxidants in a cell (Figure 2.6) (Valko *et al.*, 2007, Kaushal *et al.*, 2019). Oxidative stress can also occur due to changes in intracellular antioxidants (Halliwell and Whiteman, 2004).

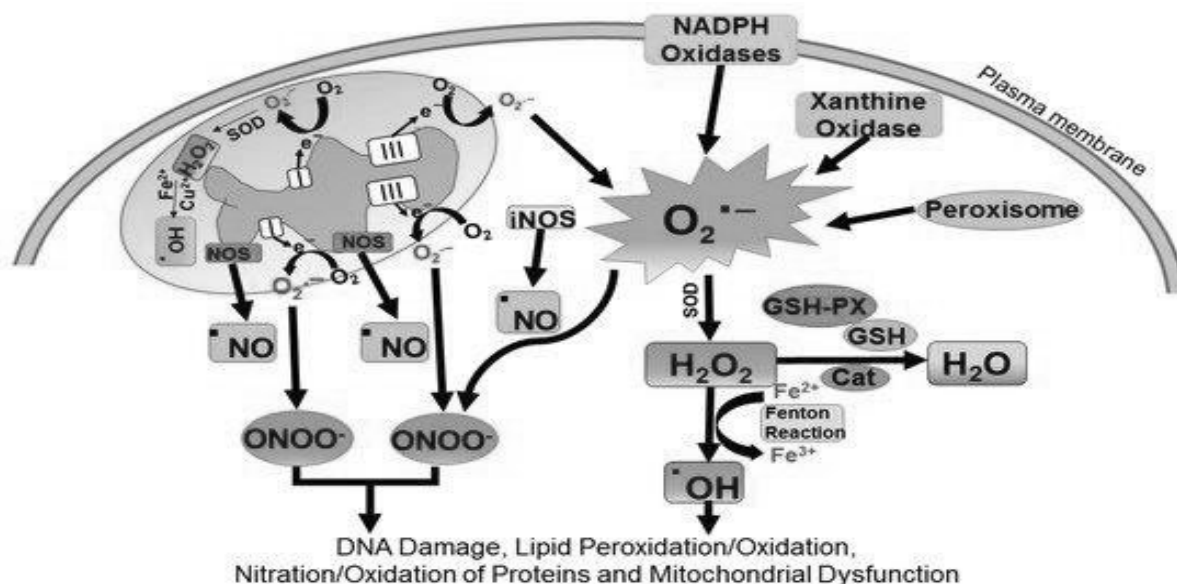


Figure 2.6: The superoxide anion ($\text{O}_2^{\cdot-}$) is produced as a by-product of oxidative metabolism in the mitochondria, but also by cytoplasmic enzymes. Oxidative stress may be averted by antioxidants such as glutathione, glutathione peroxidase, and catalase, which function to convert free radicals to water. However, the Fenton reaction produces the potent hydroxyl radical (HO^\cdot) that is implicated in macromolecule damage. Reactive nitrogen species (RNS) such as peroxynitrite (ONOO^-) produced when superoxide reacts with nitric oxide may also cause damage to cellular macromolecules (Kaushal *et al.*, 2019).

Several intracellular mechanisms that promote oxidative damage to DNA, lipids, and proteins are altered by increased ROS production (Figure 2.6). DNA damage includes oxo-guanine formation as abasic sites, DNA strand breaks, and oxidized DNA bases. It leads to the instability of the genome (Krokan *et al.*, 1997, Achanta and Huang, 2004, da Silva *et al.*, 2018). Protein targets of ROS are certain amino acids (lysine, arginine, proline, threonine) and carbonylation (Barreiro, 2016, Liguori *et al.*, 2018). Polyunsaturated fatty acids (PUFAs) are essential targets of ROS, resulting in lipid peroxidation that is facilitated by peroxy radicals and hydroxyl. When PUFAs undergo lipid oxidation, several diverse reactive aldehydes are produced, including malondialdehyde (MDA) (Liguori *et al.*, 2018).

ROS-induced damage has caused cells to develop primary and secondary enzymatic systems (Valko *et al.*, 2007). Primary antioxidant enzymes (SOD, catalase, glutathione reductase (GR), and GPx1) combine toxic compounds with GSH or prompt the breakdown of free radicals (Figure 2.6). These enzymes have diverse mechanisms of action. O_2^- is broken into water (H_2O) and oxygen (O_2) by SOD, catalase catalyzes hydrogen peroxide decomposition (H_2O_2) into H_2O and O_2 (Figure 2.6). GPx1 reduces H_2O_2 to H_2O ; GSH is regenerated by GR (Figure 2.6) (Droge, 2002, Kaushal *et al.*, 2019). In contrast, a secondary detoxification enzyme, glutathione S-transferase (GST), binds ROS to GSH (Hayes and Strange, 1995) by detoxifying lipid peroxides (Pickett and Lu, 1989). In the physiological control of ROS generation, mechanisms such as GSH and cysteine are involved (Droge, 2002). Several antioxidant enzymes interact with GSH to moderate the action of GR, GPx1, and GST (reduction in enzymatic activity is caused by a decline in GSH content and is indicative of oxidative stress) (da Silva *et al.*, 2018).

Expression of enzymes with antioxidant activity have a control mechanism. Nuclear factor erythroid 2-related factor 2 (Nrf2) activate antioxidant response elements (AREs), which regulate the control mechanism (Jin *et al.*, 2014). A vital signalling pathway associated with antioxidant activity is Nrf2-ARE (Figure 2.7). Oxidative stress subjected cells induce Nrf2 translocation to the nucleus, thus activating genes encoding antioxidant enzymes and detoxifying enzymes of phase II (e.g., SOD) via binding ARE. Nrf2 is associated with high antioxidant induction; during ROS activation of this pathway, ROS also activates a cell death- signalling pathway causing a limited response (Valko *et al.*, 2007, Jin *et al.*, 2014).

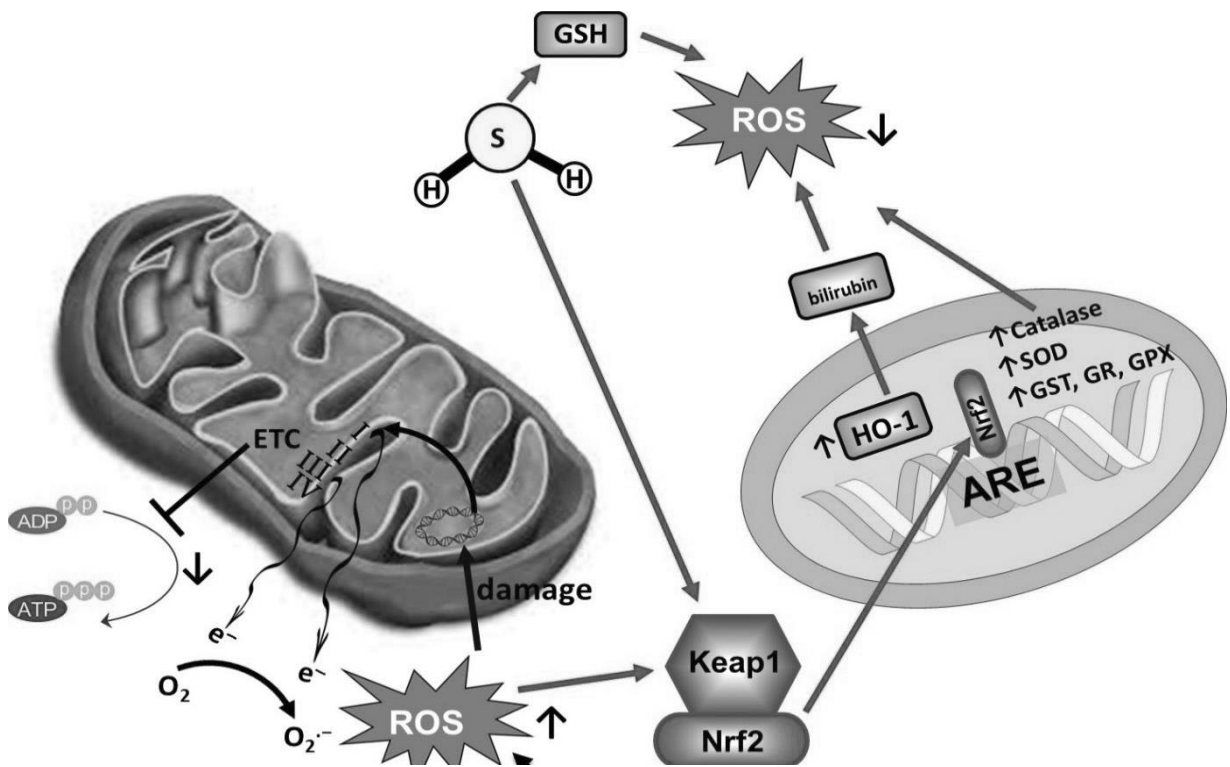


Figure 2.7: Major pathways governing oxidative stress, ROS production by mitochondria, main ROS production sites ETC complexes I and III. Cumulative mtDNA damage and progressive ETC dysfunction are caused by increased ROS production. Nrf2 localization can be increased by hydrogen sulfide, antioxidant gene expression by modulation, and HO-1 signaling pathway activation (Koutakis *et al.*, 2018).

2.5 APOPTOSIS

Apoptosis (programmed cell death) is responsible for the deletion of cells in normal tissues as well as in some pathological states (Kerr *et al.*, 1994, Elmore, 2007, Dutordoir and Bates, 2016). A multiplex cascade that relates the initial stimuli to cell death, and involves an organized set of actions comprising of multiple activations of caspases, is an energy-dependent apoptotic cell death (Elmore, 2007, Marquez *et al.*, 2013). Two signaling apoptosis pathways (intrinsic and extrinsic) culminate in the execution of cell death (Figure 2.8) (Mukhopadhyay *et al.*, 2014). Tumorigenesis is increased cell survival during chemo/radiotherapy, due to the dramatic dysregulation of both the apoptosis signalling pathways (Kang *et al.*, 2019).

The binding to cell death ligands induces the extrinsic (death receptor) apoptosis pathway, tumor necrosis factor (TNF), Fatty acid synthase ligand (FASL) or TNF-related apoptosis-inducing ligand (TRAIL), to cell death receptors TNFR, FAS, or Death receptor-5 (DR5), respectively (Bensassi *et al.*, 2012). The first apoptotic signal (FAS) and TNF- related apoptosis-inducing ligand (TRAIL) engage with one of the

death receptors to attract death domain molecules, Fas-associated death domain (FADD) proteins (Koff *et al.*, 2015). FAS attracts death domain proteins caspase 8 to promote the formation of the death-inducing complex (DISC) (Figure 2.8) (Dutordoir and Bates, 2016). The activation of caspase 8 leads to the amplification of the death signal through the activation of caspases 3 and 7 (Zhang *et al.*, 2018). Interdependence between the apoptosis pathways occurs through caspase 8 cleavage and the BH3 interacting domain death agonist (BID) activation (Figure 2.8) (Sun *et al.*, 2015).

The intrinsic (mitochondrial or B cell CLL/lymphoma-2 (BCL₂) apoptosis pathway activation can be by chemo/radiotherapies or cellular stresses BCL₂ homology (BH) has pro and anti-apoptotic members (Edmonds, 2010). The pro-apoptotic proteins are BAD, BIK, BID, and BAX; they intercalate and dimerize to form mitochondrial outer membrane permeability pores (MOMP) (Koff *et al.*, 2015). The activation functional of the family proteins pro-apoptotic BCL₂, induces cytochrome c, the second mitochondria-derived activator of caspases (SMAC), and endonuclease G release into the cytosol (Figure 2.8) (Marquez *et al.*, 2013). Apoptosome complex formation is induced by cytochrome c, which compromises of pro-caspase 9, cytochrome c, and apoptotic protease-activating factor-1 (APAF-1), leads to caspase 3 and 7 downstream activation (Figure 2.8). SMAC can promote apoptosis by X chromosome-linked inhibitor of apoptosis protein (XIAP), which causes caspase 9 consequent release and downstream apoptosis activation. Cellular inhibitor of apoptosis protein (cIAPs) can inhibit SMAC interaction by blocking (Zhang *et al.*, 2018).

The inhibitor of caspase-activated DNase (iCAD) is then released from the mitochondria and translocates to the nucleus; after cleavage of the inhibitor by caspase 3/7, CAD leads to oligonucleosomal DNA fragmentation and chromatin condensation advancement (Li *et al.*, 2014). Endonuclease G and Apoptosis-inducing factor (AIF) translocates to the nucleus and causes DNA condensation of peripheral nuclear chromatin and cleavage of nuclear chromatin to produce oligonucleosomal DNA fragments ~50–300kb in length; AIF and endo G are caspase-independent (Yuan and Kroemer, 2010). Caspase 3/7 can cleave and inactivate poly (ADP-ribose) polymerase (PARP), which causes externalization of phosphatidylserine and microtubule effects that result in the formation of apoptotic bodies (Bensassi *et al.*, 2012).

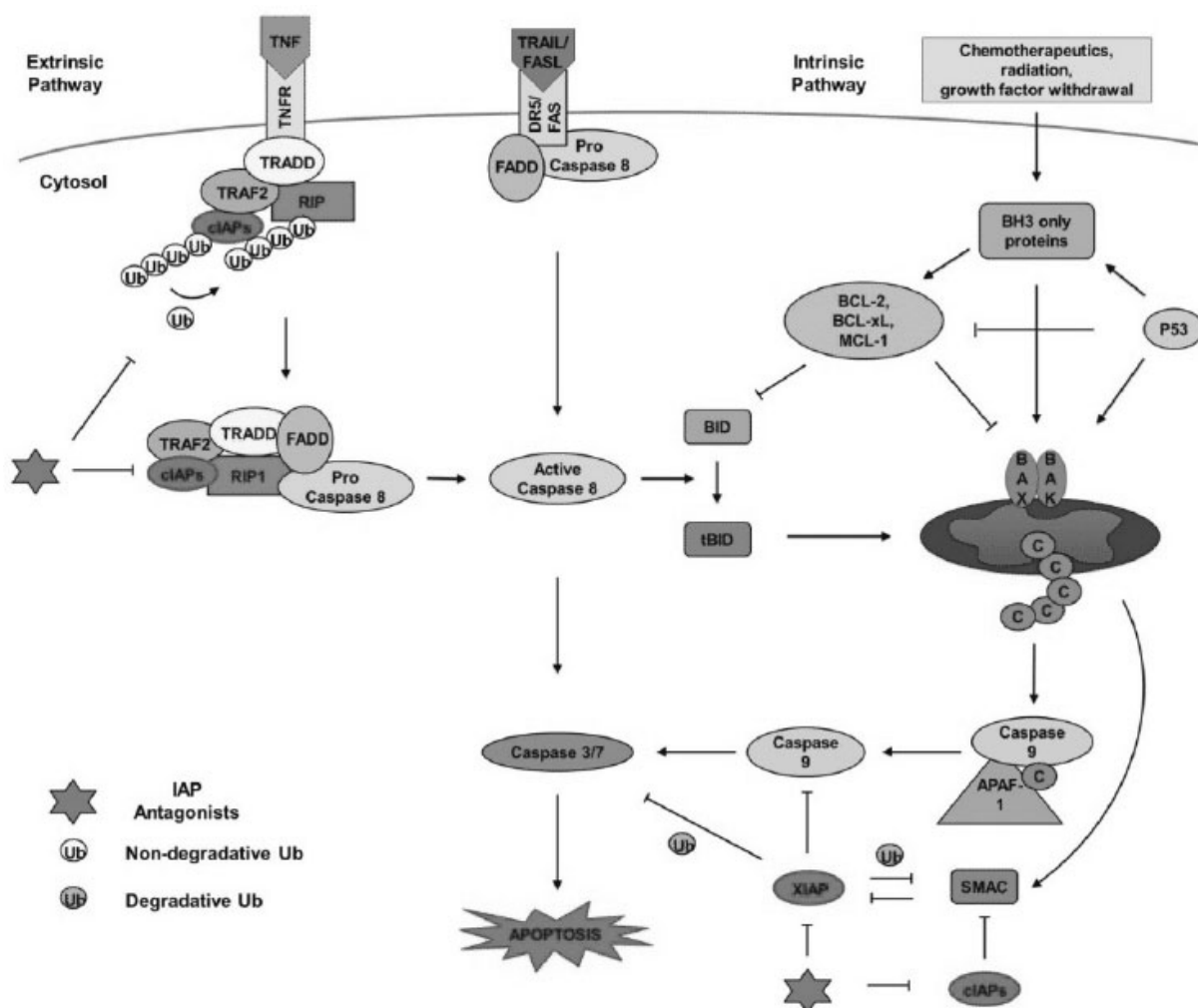


Figure 2.8: Programmed cell death signaling pathways. The binding to cell death ligands induces the death receptor apoptosis pathway, TNF, FASL, or TRAIL, to cell death receptors TNFR, FAS, or DR5, respectively. Caspase 8 activated cell death is a result of death receptor activation (Marquez *et al.*, 2013).

2.6 DON-INDUCED OXIDATIVE STRESS AND APOPTOSIS

Cell culture studies have reported DON-dependent production of ROS (Ji *et al.*, 1998, Ikwegbue *et al.*, 2017). Oxidative cellular stress was reported in rat liver clone-9 cells where DON (0.1 g/ml) was able to induce ROS generation, which was further linked with hepatotoxicity (Sahu *et al.*, 2008). Costa *et al.* (2009) conducted a study that revealed DON caused ROS levels in U937 cells to increase significantly, thereby causing cell damage. Although GPx1 activity was able to be enhanced by DON, cell death still occurred (Costa *et al.*, 2009). An additional study showed that ROS production in human ovarian cancer (A2780) cells were induced by DON, and flavan-3-ols protected the cells (Braicu *et al.*, 2009). Increased ROS observed resulted in damage to vital cellular macromolecules such as lipids, DNA, and

proteins leading to cell death by necrosis or apoptosis mechanisms or cell transformation (Figure 2.9) (Mishra *et al.*, 2014). Upregulation of the antioxidant defense system and other protective systems is due to cells response to oxidative stress; however, failure to detoxify ROS causes mitochondrial toxicity and cell death. In addition, if the DNA repair mechanisms fail, tumorigenesis may occur (Mishra *et al.*, 2014, Yu *et al.*, 2018, Habrowska-Gorczyńska *et al.*, 2019).

Extended exposure to DON in high concentrations (i.e., completely inhibit translation) typically causes apoptotic cell death (Pestka, 2008, Knutsen *et al.*, 2017). DON exposure to human peripheral blood lymphocytes (HPBLs) was monitored for apoptosis (Sun *et al.*, 2002). DON was found to significantly increase apoptosis in HPBLs. Increasing DON concentrations caused apoptosis rates to rise, ranging from 50 to 2000 ng/ml. An additional study conducted by Yang and co-investigators (2000) assessed the DON effect on apoptosis in a human monocyte line. The study revealed that DON exerted no significant effects on both the treated and control cells (Yang *et al.*, 2000, Liang *et al.*, 2015, Kang *et al.*, 2019).

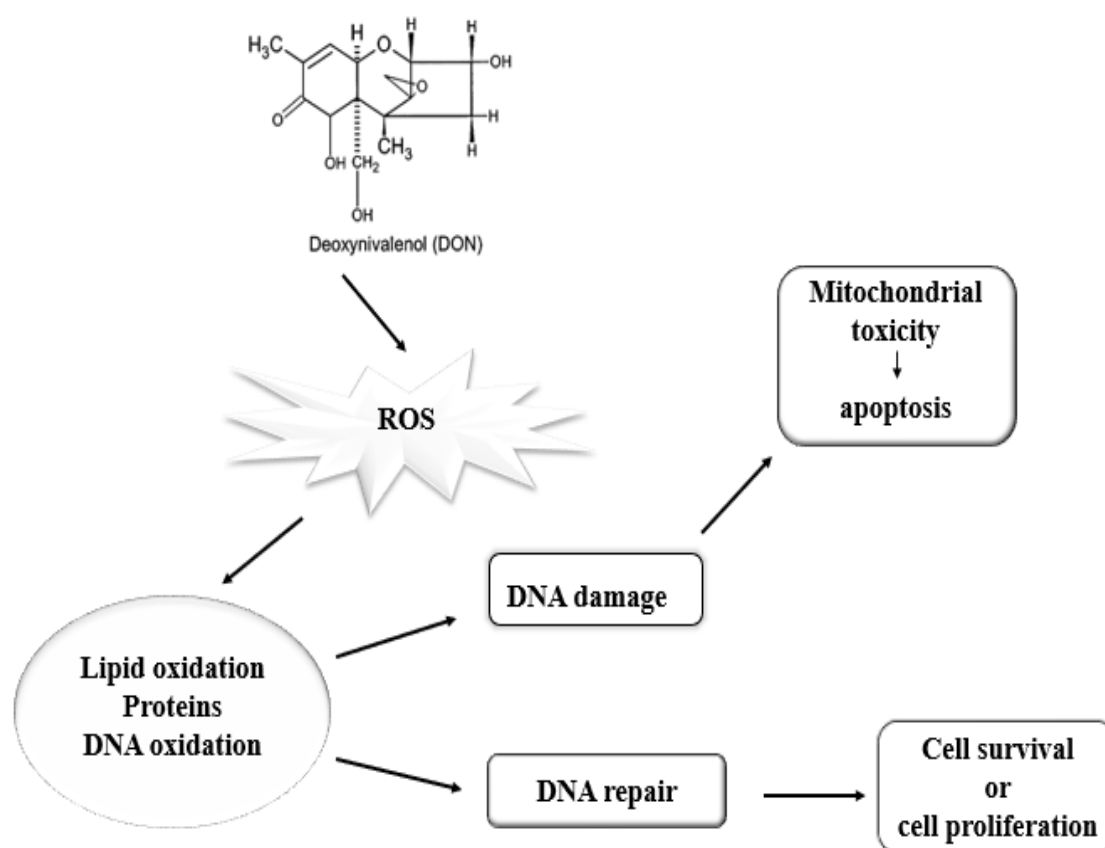


Figure 2.9: DON proposed mode of action for oxidative stress. ROS production increased, may induce oxidative damage which leads to toxicity and apoptosis (Mishra *et al.*, 2014).

CHAPTER 3 : MATERIALS AND METHODS

3.1 MATERIALS

The human embryonic kidney (Hek293) cells were purchased from Highveld Biological (Johannesburg, South Africa (SA)). Reagents for cell culture were acquired from Whitehead Scientific (Johannesburg, SA). Western blotting reagents were procured from Bio-Rad (Hercules, California, United States). The Promega CellTiter-Glo®, Caspase-Glo® 3/7, 8, and 9 luminometry assays, and Cell Signaling Technology (CST) antibodies were procured from Anatech (Johannesburg, SA). Sigma Aldrich (St Louis, Missouri, United States) products purchased from Capital Laboratories (Johannesburg, SA) were phosphate-buffered saline (PBS) tablets, methylthiazol tetrazolium (MTT) salts, malondialdehyde (MDA), DON (#118M4011V), bicinchoninic acid (BCA) reagents and bovine serum albumin (BSA). Protease/phosphatase inhibitors were acquired from Roche Diagnostics (Johannesburg, South Africa). Additional reagents were obtained from Merck (Darmstadt, Germany).

3.2 CELL CULTURE

The Hek293 cell line was initially produced in 1973 from normal fetal human embryonic kidney cells (Simmons, 2019). Hek293 cells grow rapidly, easily maintainable, and high reproducibility. This cell line is effective at protein production (Simmons, 2019). The Hek293 cell line is also sensitive to DON (Dinu *et al.*, 2011, Le *et al.*, 2018). Therefore, Hek293 cells are the ideal toxicity model to use.

The Hek293 cell line was reconstituted by transferring a vial of cryopreserved cells into a sterile 25 cm² cell culture flask containing 10 ml of complete culture medium (CCM) comprising of Dulbecco's Modified Eagle's Medium (DMEM) supplemented with 10% foetal calf serum, 25 mM HEPES, 1% L-glutamine and 1% penicillin-streptomycin-fungizone. The flask was incubated for 4 hours (4hrs) at 37°C in a 5% CO₂-supplemented incubator, after which the CCM was discarded and replaced with 5 ml of fresh CCM. Maintenance of cells was until 90% confluency was attained. Media from the confluent flasks was discarded, then the cells were dislodged by gentle agitation and resuspended in 2 ml CCM. The cells were counted (150 µl of CCM, 50 µl of trypan blue, 50 µl of cell suspension in an Eppendorf tube, and 10µl of this mixture were pipetted onto a haemocytometer) for sub-culturing or storage.

3.3 DON AND ALLICIN PREPARATIONS AND TREATMENTS

Dinu and co-investigators (2011) determined that DON cytotoxicity was exerted on Hek293 cells in both a time-dependent and dose manner. The DON concentration of 5 µM utilized in this study was

extrapolated from Dinu *et al.* (2011) and was prepared from a stock solution of 100 μM DON (Dinu *et al.*, 2011). Alli-biotic is a capsule containing 100% pure and stabilized allicin, the infection-fighting ingredient in garlic (Robyn, 2019). The ingredients contained in each alli-biotic capsule is stabilized allisure allicin extract (280 mg per capsule) and non-GMO maltodextrin. Non-GMO organic maltodextrin Yucu root is a starch drying agent that was used to prevent clumping. Clumping is a normal occurrence for real, whole, natural food powders. A 164 mM stock solution of allicin was prepared in 10 ml of CCM. These stocks were stored at 4°C and diluted for the subsequent assays.

Hek293 cells were seeded into appropriate cell culture vessels as required for individual assays. After allowing 24hrs for attachment of cells, the cells were treated in triplicate for 24hrs as follows: control untreated cells (C), 5 μM DON (DON), 1.7 mM allicin (A), and combined 5 μM DON and 1.7 mM allicin treatment (DON+A).

3.4 THE METHYLTHIAZOL TETRAZOLIUM (MTT) ASSAY

3.4.1 Principle

The 3-(4,5-Dimethylthiazol-2-yl)-2,5-Diphenyltetrazolium Bromide (MTT) assay was used in measuring cell viability, proliferation, and cytotoxicity in Hek293 cells following exposure to allicin. The yellow MTT salt crosses the membranes of living cells and is reduced by NAD(P)H-dependent mitochondrial dehydrogenases resulting in the formation of an intracellular purple formazan (requires solubilization) product and reducing equivalents $\text{NAD}^+/\text{NADP}^+/\text{FAD}^+$ (Figure 3.1) (Ali-Boucetta *et al.*, 2011). The produced formazan amount is directly proportional to the number of viable cells (Riss *et al.*, 2011).

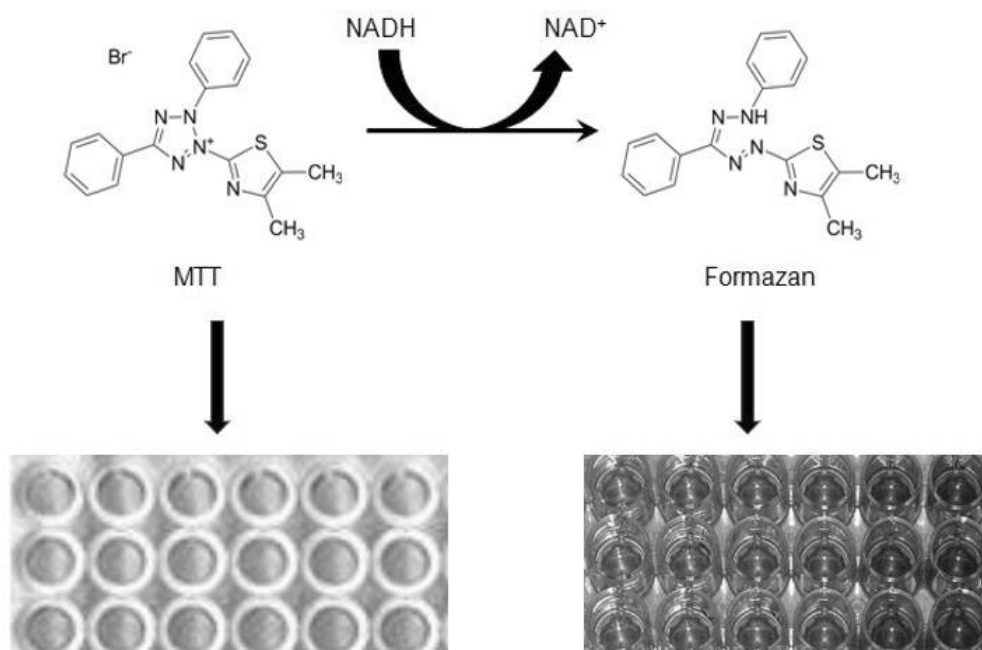


Figure 3.1: The MTT assay is based on the conversion of the yellow MTT to an insoluble purple formazan product that is solubilized with DMSO (Ali-Boucetta *et al.*, 2011).

3.4.2 Procedure

The Hek293 cells were sub-cultured into a 96-well microtitre plate at a density of 20,000 cells/well (200 μ l CCM) in triplicates and allowed to attach overnight. The cells were incubated with a range of allicin concentrations (0-150 mM, 300 μ l) at 37°C for 24hrs, the treatment media was removed, and cells were incubated with 120 μ l MTT salt solution (4 mg dissolved in 800 μ l of PBS and 4 ml of CCM) at 37°C. After 4hrs of incubation, the MTT salt was discarded and replaced with 100 μ l of DMSO for the solubilization of formazan crystals, and further incubated for an hour at 37°C. The optical density (OD) of the samples was read at 570 nm and 690 nm using the Bio-Tek μ Quant spectrophotometer (USA). The cell viability and the concentration-dependent response curve were plotted using GraphPad Prism v5.0 software. The MTT assay generates a half maximum inhibitory concentration (IC₅₀) that refers to a concentration that inhibits a population's biochemical functioning by 50%. The IC₅₀ was used as the treatment dose in subsequent assays.

$$\% \text{ Cell viability} = \frac{\text{mean absorbance of treated cells}}{\text{mean absorbance of control cells}} \times 100$$

3.5 CELL TITER-GLO® LUMINESCENT CELL VIABILITY ASSAY

3.5.1 Principle

ATP is the universal energy transducer in mammalian cells produced during cellular respiration. Intracellular levels of ATP are a useful indicator of mitochondrial function and respiratory capacity (Nunnari, 2014). The assay uses bioluminescence to determine intracellular ATP levels to indicate the number of viable cells within a culture. During this reaction, cellular ATP is used in the luciferase reaction to generate a light signal (Figure 3.6). The intensity of light produced by this reaction is directly proportional to the concentration of intracellular ATP (Coussens *et al.*, 2018).

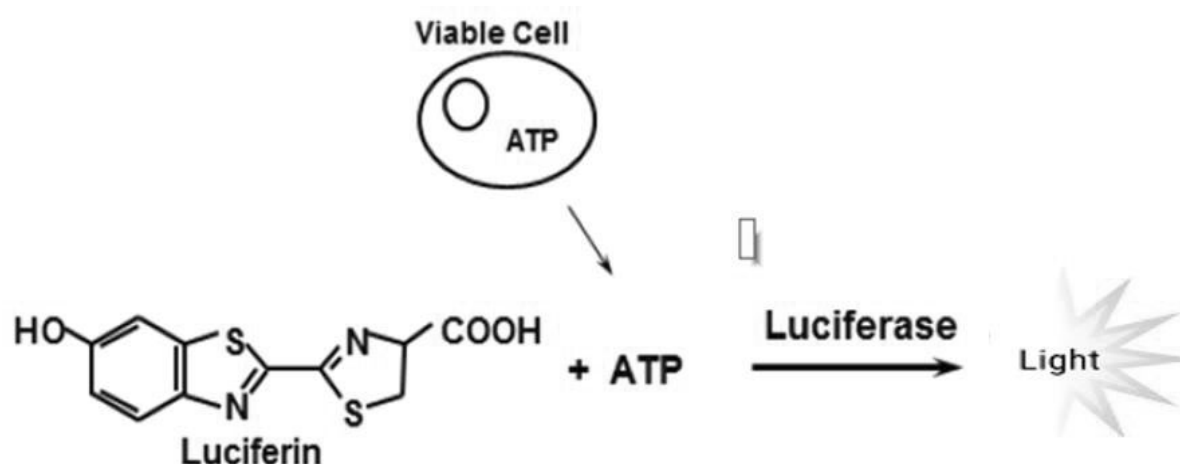


Figure 3.2: The ATP assay catalyzed through the luciferase reaction to generate a light signal (Coussens *et al.*, 2018).

3.5.2 Procedure

The ATP concentration in treated Hek293 cells was detected with the Promega CellTiter-Glo® Assay (#G755). Hek293 cells (20000 cells/200 μ l CCM/well) were sub-cultured in a white, opaque luminometer 96 well plate for 24hrs at 37°C. Cells were treated in triplicates with 300 μ l of different treatments as follows: control untreated cells (C), 5 μ M DON (DON), 1.7 mM allicin (A) and combined 5 μ M DON and 1.7 mM allicin treatment (DON+A) and incubated for 24hrs at 37°C. Treatment media was discarded, cells were washed once with 300 μ l of PBS, and 50 μ l of PBS was added to each well. Thereafter, 25 μ l the reagent for ATP was added into each well and incubated at RT in the dark for 30min. The luminescence was detected using a Modulus™ microplate luminometer (Turner Biosystems, Sunnyvale, USA) as RLU.

3.6 NITRIC OXIDE SYNTHASE (NOS) ASSAY

3.6.1 Principle

RNS are formed when NO reacts with superoxide to produce peroxynitrite. It is therefore important to evaluate the production of NO to determine if nitrosative stress is present. The assay indirectly quantifies NO and thus gives a measure of the RNS present. The NOS assay is a traditional method used to measure the conversion of L-[3H] arginine to L-[3H] citrulline (Figure 3.8). However, because NO is oxidized to nitrates and nitrites in biological samples, it is these end-products that are quantified in this two-step reaction assay used to measure oxidative stress. The Griess reaction is used as follows: vanadium (III) chloride (VCl_3), sulphanilamide (SULF), and N-1-Naphthyl ethylenediamine dihydrochloride (NEDD) are each added in quick succession to facilitate reduction, inhibition of enzymatic reactions involving para-aminobenzoic acid and colour change (detected at 540nm) respectively (Figure 3.8) (Beda and Nedospasov, 2005).

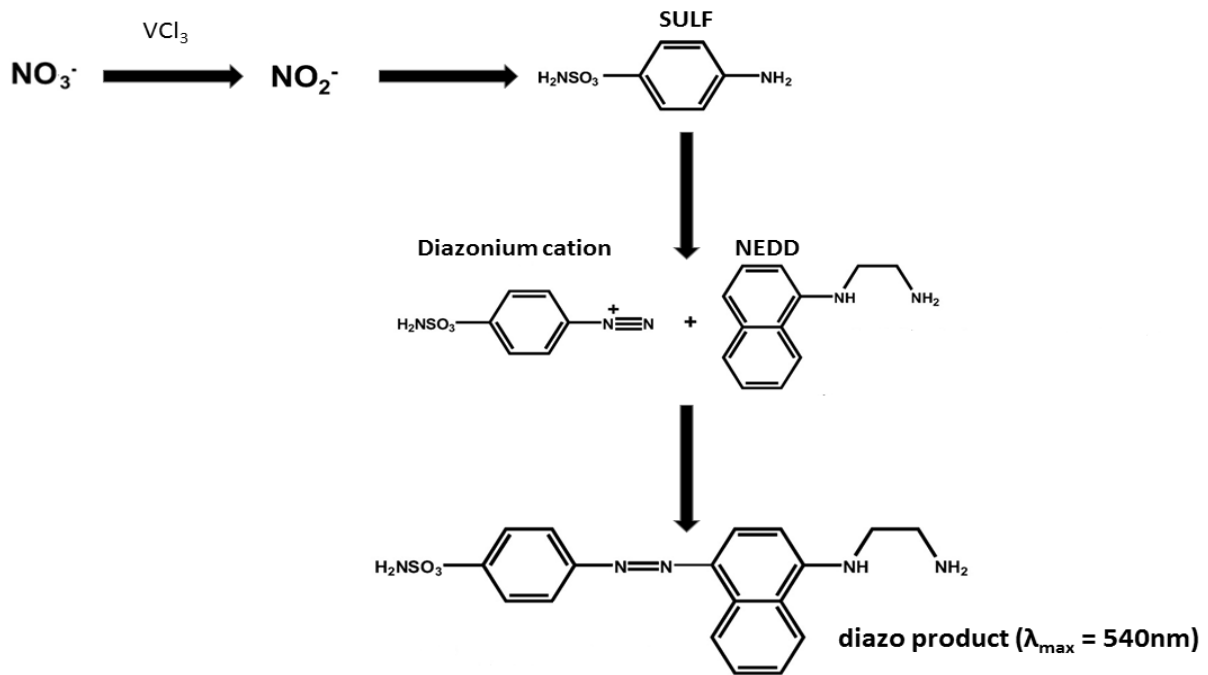


Figure 3.3: The Griess Reaction. A two-step diazotization reaction, NO_2^- reacts with SULF to produce a diazonium cation which couples to NEDD to form a red-violet chromophoric diazo product (Bryan and Grisham, 2007).

3.6.2 Procedure

Sodium nitrate standards were prepared (0–200 μM), and 50 μl of each standard, in addition to the relevant treatments, were plated into a 96 well plate in triplicate. Subsequently, 50 μl VCl_3 (8 mg/ml in 1 M HCl) was added into all the wells (samples and standards), the addition of 25 μl SULF (20 mg/ml

in 5% HCl), and 50 μ l NEDD (1 mg/ml in dH₂O). The incubation of the plate was at 37°C for 45min. After incubation, the absorbance was read using a Bio-Tek μ Quant plate reader (USA) at a wavelength of 540 nm/690 nm. A standard curve was then plotted using the standards, and the RNS concentrations of the samples were extrapolated from the graph.

3.7 THIOBARBITURIC ACID REACTIVE SUBSTANCES (TBARS) ASSAY

3.7.1 Principle

Oxidative stress detection has mainly relied on malondialdehyde (MDA) quantification, which are formed by the degradation of the initial products of free radical attack on membrane lipids. In the reaction between 2-thiobarbituric acid (TBA) and MDA, low pH and high temperature facilitate the reaction. The addition of butylated hydroxytoluene (BHT) protects the intact lipids from the artificial peroxidation of the assay (Stepić *et al.*, 2012). The reaction of MDA with TBA produces a coloured product that can be detected at 532 nm (Figure 3.7).

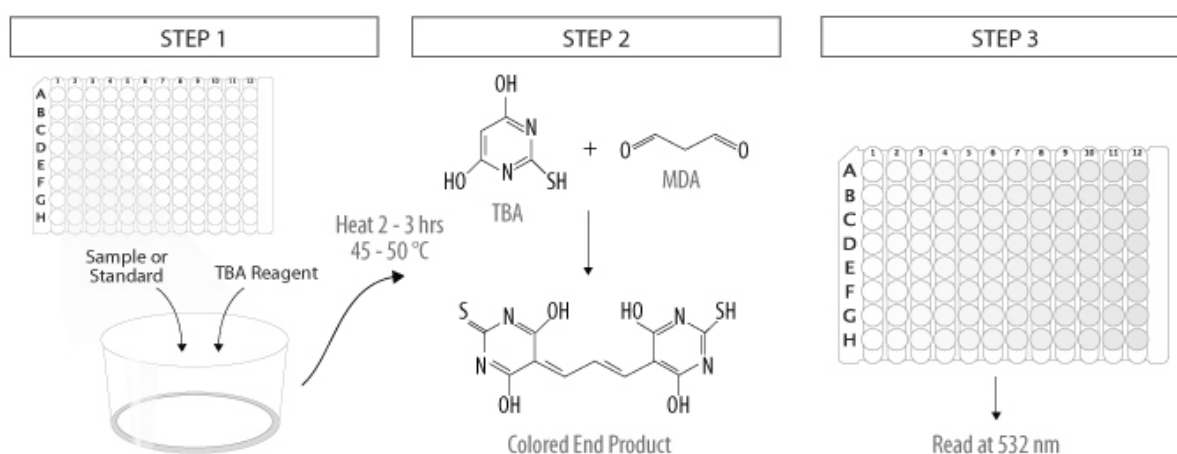


Figure 3.4: The representation of TBARS reaction between MDA and TBA/BHT used as a lipid peroxidation indicator of oxidative stress (Bio-technie, 2014).

3.7.2 Procedure

The homogenized treated cell suspension (100000 cells/200 μ l CCM) was added to individual test tubes, the negative control contained 200 μ l of CCM, and the positive control consisted of 199 μ l CCM and 1 μ l MDA. Subsequently, 200 μ l phosphoric acid (2% H₃PO₄), 200 μ l of 7% H₃PO₄, and 400 μ l of TBA/BHT (NaOH 0.1 g, TBA 0.5 g, BHT (20 mM) 250 μ l dissolved in 40 ml dH₂O then top to 50 ml) were added to each tube except to the negative control (it received 400 μ l 3 mM HCl). The test tube solutions were each briefly vortexed. The sample pH was reduced to 1.5 by adding 200 μ l of 1 M HCl. The solutions were then heated in a boiling water bath at 100°C for 15min. Following cooling at RT, 1500 μ l of butanol was added to each test tube for adduct extraction. The test tubes were vortexed for 30 seconds.

The test tubes were allowed to stand until the two phases became distinct. Thereafter, 200 μl /well from each test tube supernatant was plated into a 96-well plate in triplicate. Absorbance was measured at 532 nm/600 nm. Absorbance was converted to MDA concentration using the equation: $\frac{\text{sample absorbance}}{156 \text{ mM}^{-1}} \times 1000$.

3.8 GLUTATHIONE ASSAY

3.8.1 Principle

The GSH-Glo™ Assay is luminescent-based used for the identification and quantification of GSH in cells. Changes in GSH levels is vital in the assessment of toxicological responses and is an indicator of oxidative stress, possibly leading to apoptosis or cell death (Li *et al.*, 2014, Woelflingseder *et al.*, 2018). In the presence of GSH, luciferin is formed through a luciferin derivative conversion (Figure 3.5). A GST enzyme catalyzes the reaction. The formed luciferin is detected in a coupled reaction using Ultra-Glo™ Recombinant Luciferase that produces a glow type luminescence that is proportional to the GSH amount present in cells (Promega).

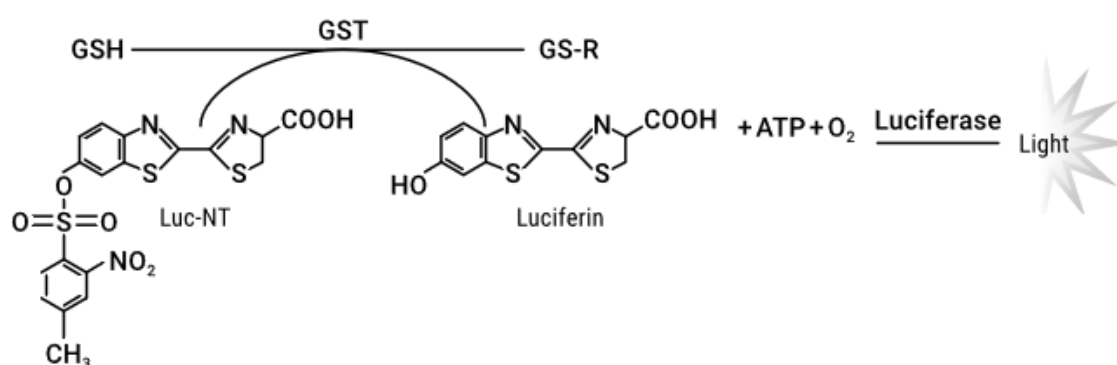


Figure 3.5: The luminescent representation for the quantification and detection of GSH in cells, luciferin derivative, is converted into luciferin in the presence of GST (Promega).

3.8.2 Procedure

The Hek293 cells (20000 cells in 200 μl CCM per well) were sub-cultured in a white luminometer 96-well plate for 24hrs at (37°C). Treated cells were in triplicates with 300 μl of different treatments: control untreated cells (C), 5 μM DON (DON), 1.7 mM allicin (A), and combined 5 μM DON and 1.7 mM allicin treatment (DON+A). After 24hrs at 37°C, the treatment media was discarded, the plate was washed once using 300 μl of PBS, and 50 μl of GSH reagent (#65862) was added to each well. Thereafter, incubation of the plate was for 30min (RT). The luciferase reagent (25 μl , #V687) was added and incubated for 15min. The luminescence was determined using a Modulus™ microplate luminometer (Turner Bio-systems, Sunnyvale, USA) as RLU.

3.9 ANNEXIN V AND NECROSIS ASSAY

3.9.1 Principle

Apoptosis, in its early event, is the flipping of phosphatidylserine (PS) from the inside surface to the outside surface of the plasma membrane. Labelled Annexin V can be used to detect apoptotic cells because it binds specifically to the exposed charged head groups of PS in a Ca^{2+} dependent process (Figure 3.3). Propidium iodide (PI) is used in combination with labelled Annexin V. The cell membrane integrity excludes PI in viable and apoptotic cells, while necrotic cells are permeable to PI (Figure 3.3). Hence, dual parameter luminometry allows for the discernment between viable, necrotic, and apoptotic cells (GmbH, 2019).

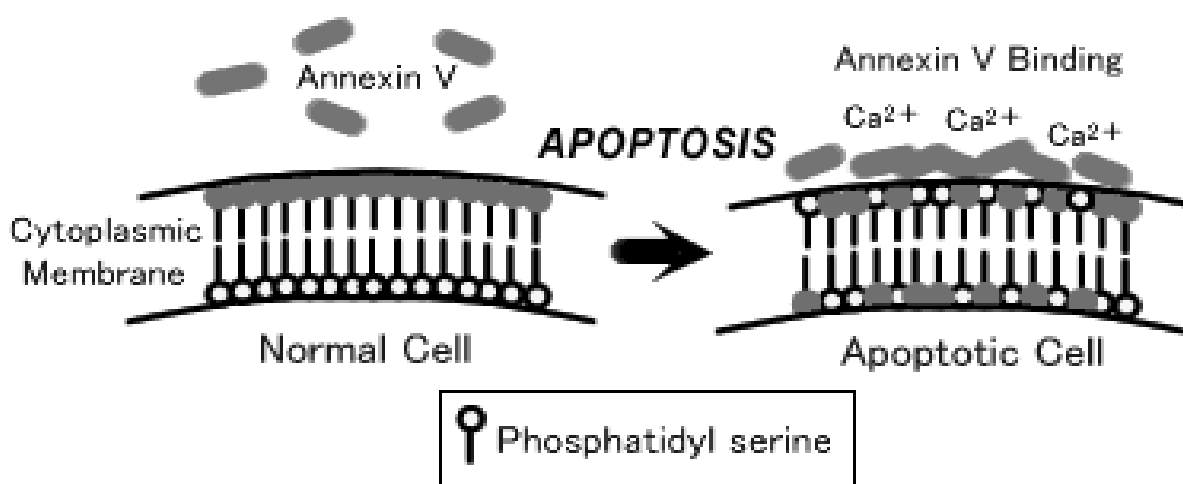


Figure 3.6: The Annexin V assay used for apoptotic cell detection. Annexin V binds to externalized PS on an early apoptotic cell and can be detected using flow cytometry or luminometry (GmbH, 2019).

3.9.2 Procedure

Hek293 cell suspension was seeded into a white, opaque 96-well luminometer plate at a density of 20000/cells/well (200 μl) in triplicate for each treatment for 24hrs at 37°C. Cells were treated using 300 μl of the different treatments as follows: control untreated cells (C), 5 μM DON (DON), 1.7 mM allicin (A) and combined 5 μM DON and 1.7 mM allicin treatment (DON+A) thereafter, incubated for 24hrs at 37°C. The treatment media was retained for the LDH assay, and cells were washed once with 300 μl of PBS. Cells were then replenished with 50 μl of PBS.

The RealTime-Glo™ Annexin-V Apoptosis and Necrosis Assay (JA1011, Promega, USA) was used to determine an apoptotic marker PS, in treated cells. The 2X Detection Reagent components were thawed at RT; the 2X Detection Reagent was prepared by a 500-fold dilution with 0.1 M PBS (pH 7.4) in a 1 ml Eppendorf tube. The Annexin-V NanoBiT™ substrate (1 μl) was added into 1ml Eppendorf tube containing 500 μL of 0.1 M PBS (pH 7.4) and vortexed immediately, 1 μL of calcium chloride (CaCl_2),

1µl Necrosis Detection Reagent were added and mixed well, followed by adding 1µl of Annexin-V SmBiT and Annexin-V LgBiT (1µl) thereafter mixed by inversion and stored on ice until use.

The 2X Detection Reagents (25µl/well) were added to each well, and incubation was for 30min at RT. The Annexin-V apoptosis luminescence signal was measured using the Modulus™ microplate luminometer (Turner Biosystems, Sunnyvale, California, USA) and reported as RLU, while the necrosis fluorescence signal was measured with the excitation of 490 nm and collected with the emission of 510-730 nm using GloMax® Multi Detection System (Promega Corporation, USA) and reported as relative fluorescent units (RFU).

3.10 CASPASES

3.10.1 Principle

Cysteine proteases are from a family of caspases that have a focal role in initiating and execution of programmed cell death. In all types of cells, caspase expression is observed and are primarily produced as dormant zymogens; activation occurs through apoptotic signalling (McIlwain *et al.*, 2013, Coussens *et al.*, 2018). A luminogenic substrate conjugated aminoluciferin cleavage by the caspase is involved. Aminoluciferin serves as the luciferase substrate; when released, a reaction occurs with luciferase in the presence of ATP and molecular oxygen to generate a luminescent signal (Figure 3.2). The luminescent signal is directly proportional to the caspase activity level of the sample (Brunelle and Zhang, 2010, Coussens *et al.*, 2018). The activity of the initiator caspase 9 and executioner caspases 3/7 were quantified using the CellTiter Caspase-Glo assay.

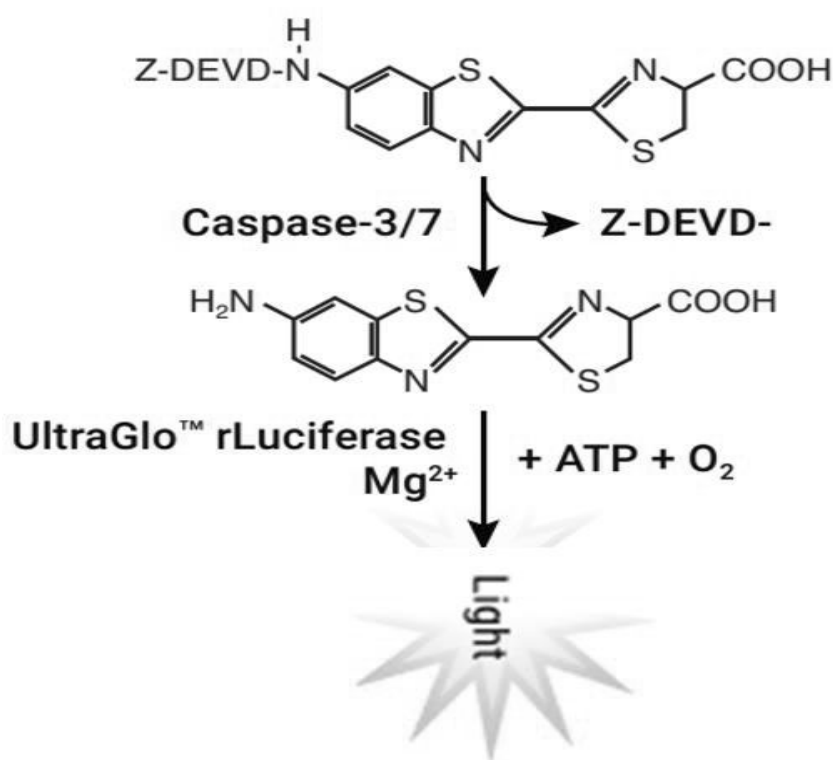


Figure 3.7: The aminoluciferin released by caspase cleavage of Z-DEVD is a substrate for luciferase. In the presence of ATP, oxygen, and magnesium, this reaction produces a light signal which is directly proportional to caspase activity (Promega).

3.10.2 Procedure

Activities of caspases 3/7 and 9 were detected using the Promega Caspase-Glo® assay (#G811A and #G816A, respectively). A white, opaque 96-well luminometer plate was used to sub-culture a Hek293 cell suspension at a density of 20000/cells/well (200 μ l) in triplicate for each caspase treatment for 24hrs at 37°C. Treated cells with 300 μ l of the different treatments as follows: control untreated cells (C), 5 μ M DON (DON), 1.7 mM allicin (A) and combined 5 μ M DON and 1.7 mM allicin treatment (DON+A) and incubated for 24hrs at 37°C. The treatment media was discarded, and cells were washed once with 300 μ l of PBS. Cells were then replenished with 50 μ l of PBS. Thereafter, 25 μ l of the caspases 3/7 and 9 reagents were added into their respective wells and incubated at room temperature (RT) in a dark place for 30min. The luminescence was detected using a Modulus™ microplate luminometer (Turner Biosystems, Sunnyvale, USA) as relative light units (RLU).

3.11 LACTATE DEHYDROGENASE (LDH) ASSAY

3.11.1 Principle

Mammalian cells contain lactate dehydrogenase (LDH), a present stable cytosolic enzyme (Chan *et al.*, 2013). Through anaerobic glycolysis, lactate is subjected to an oxidation reaction catalyzed by cytosolic LDH and co-enzyme nicotinamide-adenine dinucleotide (NAD^+) to form pyruvate and NADH. The re-oxidation of NAD^+ is essential and ensures the NAD^+ concentration is adequately high to sustain the glycolytic flux. LDH is released from the cell membrane into the extracellular medium due to cell damage caused by stress, intercellular signals, or injuries (Figure 3.4). Measuring extracellular LDH levels functions as a biochemical marker for cytotoxicity and cell death (Fiume *et al.*, 2014). The enzymatic reaction, where NAD^+ is reduced to NADH/H^+ by the oxidation of lactate to pyruvate, is the LDH two-step process. Diaphorase catalyst or phenazine methosulphate (PMS) transfers H/H^+ from NADH/H^+ to a tetrazolium salt, which yields a formazan product (Chan *et al.*, 2013).

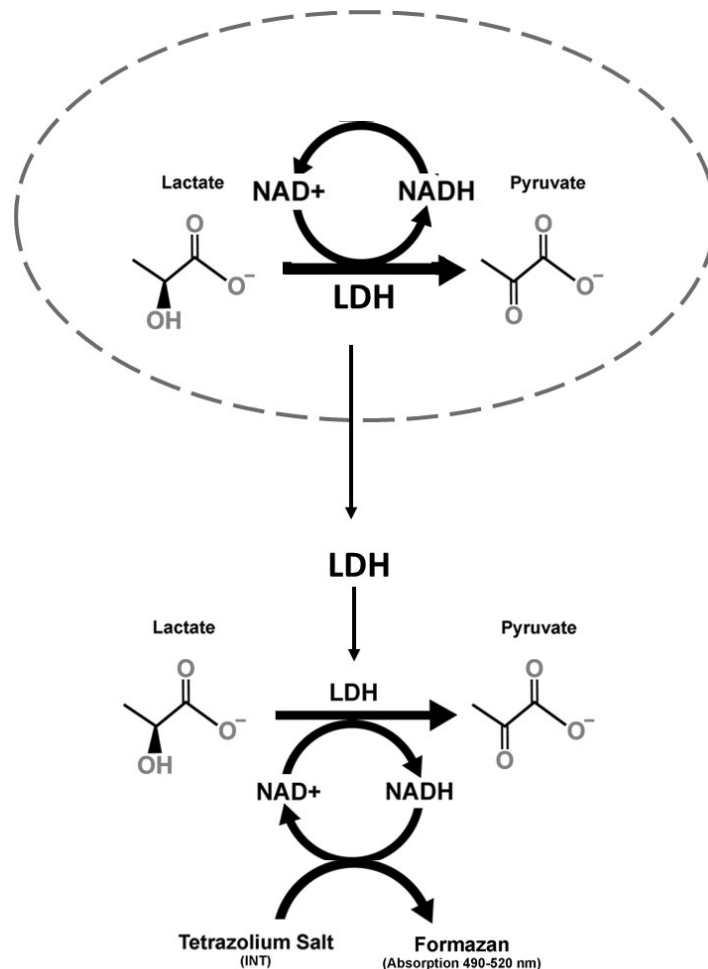


Figure 3.8: Representation of a damaged cell releasing LDH, that is spectrophotometrically detected as a formazan product (Forest *et al.*, 2015).

3.11.2 Procedure

The LDH cytotoxicity detection kit was used measured to LDH activity (11644793001) (Roche, Mannheim, Germany). The treatment medium retained from the Annexin assay (50 μ l) were transferred, in triplicate, into a 96-well microtitre plate. A substrate mixture (25 μ l) catalyst containing (diaphorase/NAD⁺) and dye solution (INT/sodium lactate) was added into each well and permitted to react (30min, RT). A stop solution of 25 μ l was added to each well after incubation. A formazan product was formed, and optical density was measured at 490/600nm and 490/690nm with an ELISA plate reader (BioTek μ Quant, USA). The data obtained was represented as mean optical density.

3.12 WESTERN BLOTTING

3.12.1 Principle

The detection and characterization of proteins is a rapid and sensitive assay called Western blotting (protein blotting or immunoblotting). Proteins are separated in a polyacrylamide gel according to their molecular weight based on the immunochromatography principle (Figure 3.9). Proteins separate then are electro-transferred onto nitrocellulose or polyvinylidene membrane and detected using a specific primary antibody, secondary antibody, and detection substrate (Bhandari, 2017).

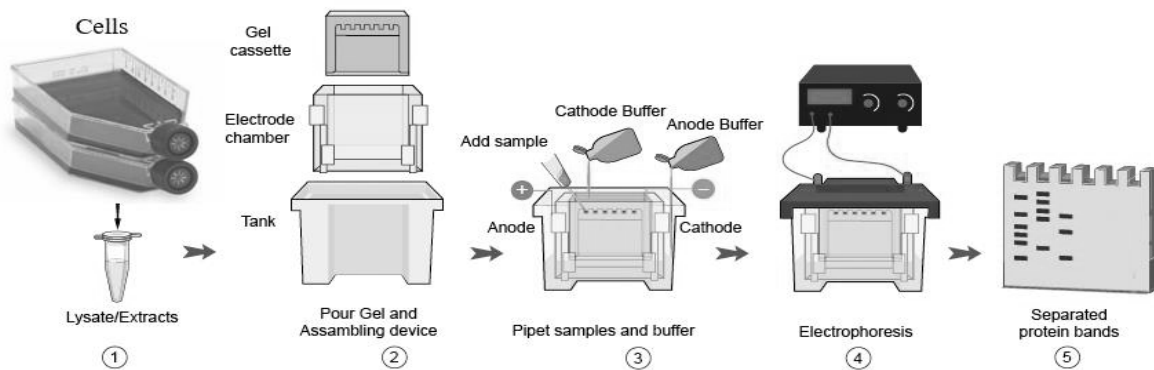


Figure 3.9: The detection and characterization of proteins is a rapid and sensitive called Western blotting (protein blotting or immunoblotting) procedure (Bhandari, 2017).

3.12.2 Procedure

3.12.2.1 Protein isolation and standardization

Isolated crude protein from treated cells using the CytobusterTM reagent containing protease and phosphatase inhibitors (300 μ l). Flasks were placed on ice for 15min, and cells were scraped off the flasks and transferred to 1.5 ml Eppendorf tubes, which were also placed on ice for a further 15min. The

cells were centrifuged at 2000 x g for 5min (4°C) to remove cellular debris. The crude protein obtained was quantified using the bichinchoninic acid (BCA) assay.

Bovine serum albumin (BSA) standards (0 – 1 mg/ml) were prepared to determine the concentration of protein samples. The standards and samples were pipetted (25 µl) in triplicate into a 96-well microtiter plate. The BCA reagent (198 µl BCA+4 µl CuSO₄) was added in each well (200 µl) and incubated at 37°C for 30min. Absorbance was detected using a Bio-Tek µQuant spectrophotometer (USA) at 562 nm. A standard curve was constructed, and concentrations of proteins were derived from this curve. Proteins were standardized to 1 mg/ml, then Laemmli buffer (dH₂O, 0.5 M Tris-HCl (pH 6.8), glycerol, 10% SDS, β-mercaptoethanol, 1% bromophenol blue) was added to each sample (1:4, total volume 250 µl), and the protein was heated at 100°C (5min).

3.12.2.2 Protein separation and electrotransfer

Denatured, standardized proteins (25 µl) were loaded onto an SDS-polyacrylamide gel (10% resolving gel and 4% stacking gel) for protein separation (1.5hrs at 150 V, Bio-Rad compact power supply, Hercules, California, USA) using running buffer (1.5 M Tris, 14.4 g glycine, 10% SDS, dH₂O), after which transfer onto nitrocellulose membranes was achieved with transfer buffer (1.5 M Tris, 14.4 g glycine, 200 ml methanol, dH₂O) using the Transblot® Turbo™ Transfer system (Bio-Rad, Hercules, California, USA).

3.12.2.3 Immunoprobings

Membranes were blocked with 5% BSA in Tween 20 Tris-buffered saline (TTBS, 25 mM Tris (pH 7.5), 150 mM NaCl, 0.05% Tween 20) for 2hrs, and incubation with primary antibodies (GPx1 [#3286], SOD2 [#12721], Nrf2 [#8242], p53 [#48818], Bax [#5023], PARP [#9542], Catalase [#12980], and Hsp70 [#46477]) in 5% BSA/TTBS (1:1000 dilution in 5% BSA/TTBS) overnight. The primary antibodies were removed, and membranes were washed 5X with TTBS (10min each), then incubation in matched secondary antibody (anti-rabbit IgG [#7074] or anti-mouse IgG [#7076]) as required, in 5% BSA/TTBS (1:2500 dilution) for 2hrs. After incubation, TTBS was used to wash membranes (5X, 10min each). Clarity Western ECL Substrate (Bio-Rad) [#170-560] (200 µl) was added to the membranes and images were captured using a Bio-Rad Molecular Imager® Chemidoc™ XRS and BioRad imaging system (Hercules, California, USA). The membranes were then quenched with 5% H₂O₂, rinsed thrice (10min, TTBS), blocked in 5% BSA (2hrs; RT) and probed with β-actin [#026M4820V] (Sigma, St Louis, Missouri, USA) in a 1:5 000 dilution with 5% BSA (30min) for protein normalization and loading

control. The band density was measured for the respective protein, data was expressed as fold change (FC).

3.13 DNA FRAGMENTATION ASSAY

3.13.1 Principle

During cell lysis, the cell membrane is disturbed chemically or physically to attain a lysate with all the cell components (e.g., DNA). In the cell lysis process, different reagents and chemicals are used to disintegrate different cell components, e.g., detergents and surfactants break down lipids, proteases break down proteins, and RNase breaks down RNA. A concentrated salt solution is used to treat lysate to cause the clumping together of the broken components and allow the DNA to float in the solution freely. To separate the clumped debris from DNA, the solution (containing lysate, detergents, surfactants, broken proteins, lipids, and RNA) was centrifuged. The precipitation process of DNA is done by adding ice-cold alcohol plus salt for ionic strength increment. The DNA pellet obtained by centrifugation of this solution is suspended either in a slightly alkaline solution such as (Tris-EDTA) TE buffer or ultra-pure water (dissolved gases and organic particles removed) for subsequent DNA experimentation, PCR, or electrophoresis (Figure 3.10) (Ali, 2019).

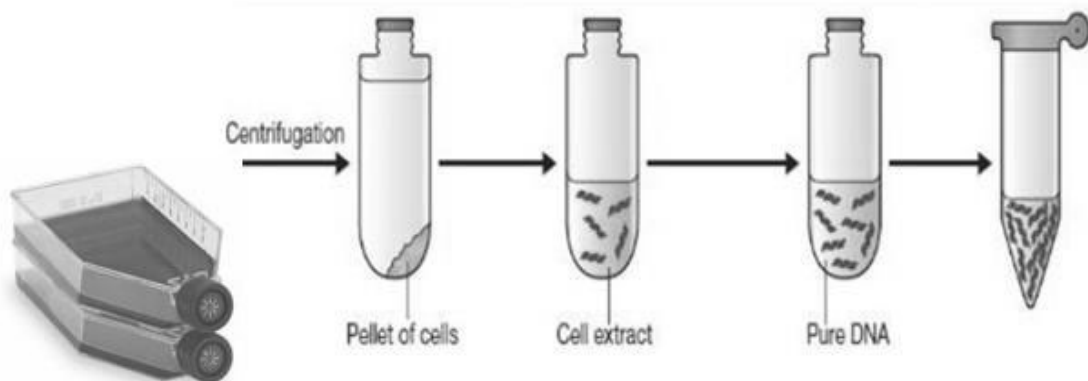


Figure 3.10: DNA extraction principle (Ali, 2019).

3.13.2 Procedure

The treated cells were lysed overnight in 600 μ l of DNA lysis buffer (0.5 M EDTA, Tris-Cl, 0.1% SDS, dH₂O). Thereafter, 600 μ l of potassium acetate was added to the cell lysate; tubes were vortexed, and invert mixed for 8min. The solution was vortexed again and centrifuged at RT, 13000 rpm for 5min. The clear supernatant was decanted into two labelled Eppendorf tubes, to which 600 μ l of isopropanol was added. The tubes were invert mixed for 5min. Thereafter, centrifugation at 13000 rpm for 5min yielded pellets in each tube. The pellets were combined, and 300 μ l of 70% ethanol was added to the final pellet.

This solution was vigorously vortexed, then centrifuged at 13000 rpm for 5min (RT). The appearance of the pellet was noted to be a clean white pellet when the ethanol was decanted. The tubes were inverted on an absorbent towel and allowed to dry for 1hr. Thereafter, 40 μ l of DNA hydration solution (1X TE solution (10 mM EDTA, 100 Tris-Cl, dH₂O)) was added to the pellet. The solution was vortexed and heated at 65°C for 15min. The solution was then allowed to cool for 15min and stored at -80°C.

The DNA was thawed and quantified using the Thermo Scientific™ Nanodrop 2000 (Thermo Fisher Scientific; Johannesburg, South Africa) to determine the quality and quantity of the isolated DNA. The absorbance ratio of 260 nm/280 nm was used to determine the purity of samples (~2). DNA samples were standardized to a concentration of 70 ng/ μ l with 1X TE buffer and stored at -80°C. The 1.8% and 2% agarose gels [#8012] were prepared to run gel electrophoresis. The gel setting apparatus was assembled: gel cassette, blocks, iron bars, and comb. In a 250 ml volumetric flask, 1.8 g/2 g of agarose powder was added and 100 ml of 1X TBE buffer (Tris, Boric acid, 0.5 M EDTA, and dH₂O) respectively. The solution was gently swirled and covered with foil. The solution was heated in the microwave and monitored so that it didn't boil. The flask was removed from the microwave and swirled until the solution was clear. Once the solution was cool, 2 μ l of gel red [41003] was added to the solution and swirled. The gel solution was then poured into the cassette, ensuring that no bubbles were present.

Once the gel was set, the combs were removed, and the gel was placed in the electrophoresis tank. Adequate 1X TBE buffer was poured into the tank to cover the gel. The samples were prepared for loading (25 μ l of sample + 25 μ l of 1X DNA loading dye [#R0611]); 10 μ l of the sample was loaded into each well. The DNA ladder [10787-018] (10 μ l) was also loaded. The gel electrophoresis proceeded at 120 V, and the migration of the dye was monitored until it had moved halfway through the gel. The gel was viewed using the Bio-Rad ChemiDoc System using Trans UV illumination, and an image was captured with the gel electrophoresis imager using the Bio-Rad ChemiDoc System (Hercules, California, USA).

3.14 STATISTICAL ANALYSIS

The data were evaluated using GraphPad Prism V5.0 Software (La Jolla California USA). The data attained was presented as averages and equivalent standard deviations for 3 replicates; experiments were repeated to ensure validity. The data were evaluated using a one-way analysis of variance (ANOVA), post hoc (Tukey's) analysis or an unpaired Student *t*-test with Welch's correction and was considered significant if the $p \leq 0.5$.

CHAPTER 4 : RESULTS

4.1 CELL VIABILITY

The dose-response of allicin was assessed using the MTT assay and generated the EC_{50} for use in this study. Allicin induced a non-consistent increase in cell viability to higher than 100% from 0 – 150mM (Figure 4.1). The highest cell viability (159%) was reached at a concentration of log 100mM (2) (Figure 4.1). An EC_{50} of 1.7mM was calculated. This concentration was used in conjunction with DON to determine the effect of allicin in DON-treated cells.

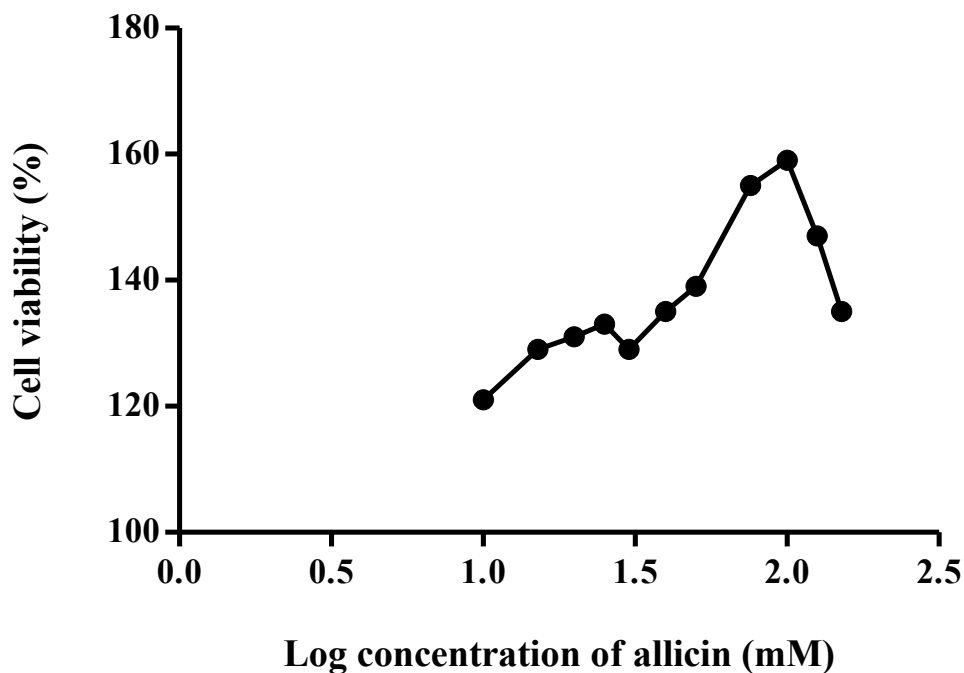


Figure 4.1: The non-linear regression (curve fit) for the percentage cell viability of Hek293 cells treated with varying concentrations of allicin.

4.2 ATP ASSAY

The ATP concentration in Hek293 cells was assessed using luminometry. There was an insignificant decrease in ATP levels for all the treatments ($p = 0.0482$), except allicin, which was slightly increased (Figure 4.2). DON treated induced a 25% decrease in ATP concentration ($1.41 \times 10^6 \pm 1.5 \times 10^6$ RLU, $p = 0.4546$) from $1.86 \times 10^7 \pm 3.6 \times 10^6$ RLU in the control. Despite the presence of allicin, ATP levels were decreased further to $7.6 \times 10^6 \pm 4.1 \times 10^5$ RLU in the combined DON+A treatment when compared to the control ($p = 0.2028$) and DON individual treatment ($p = 0.1499$).

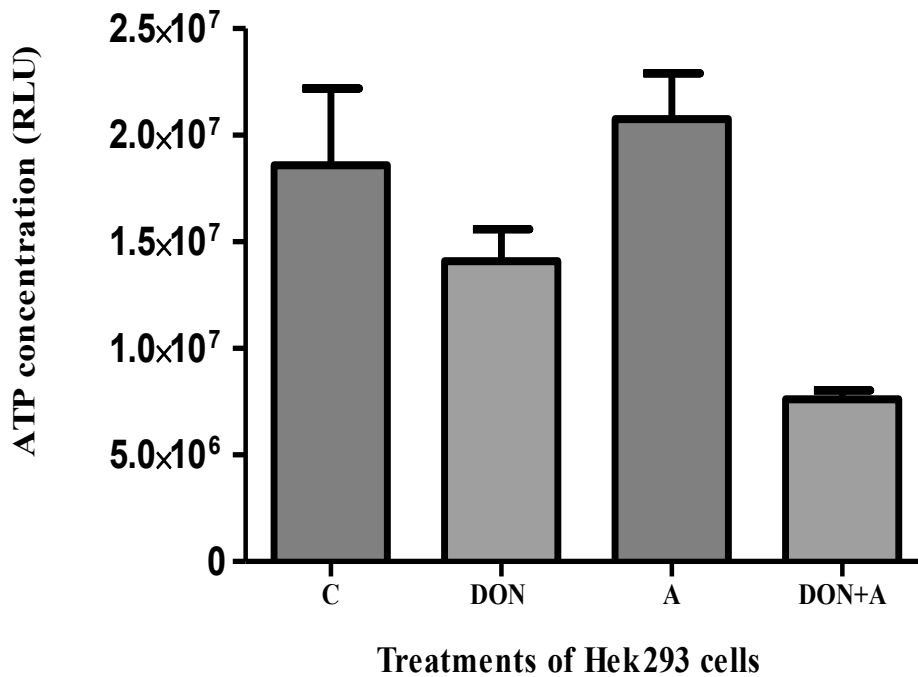
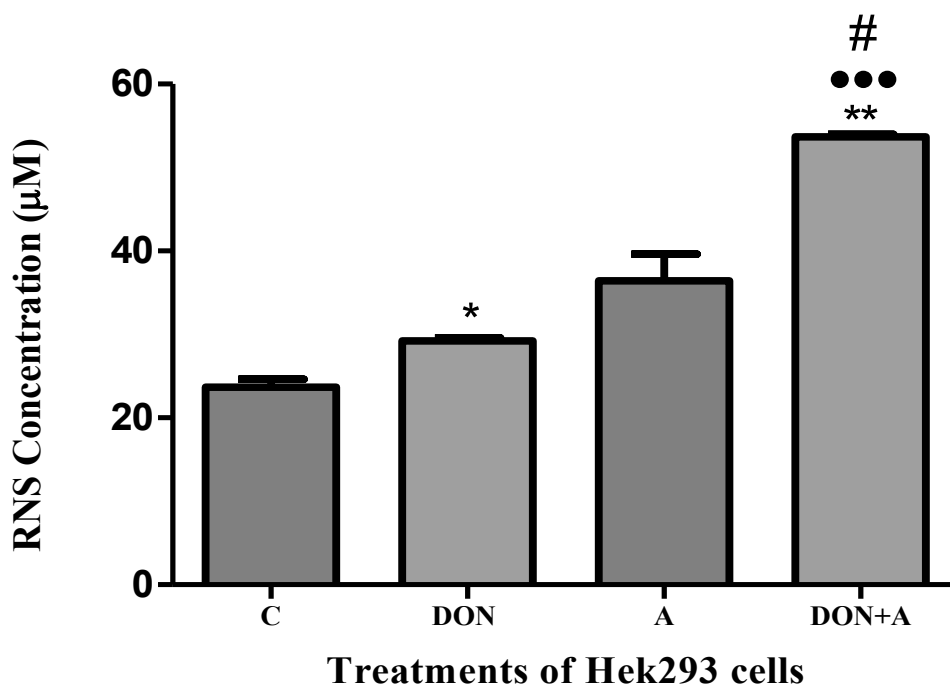


Figure 4.2: DON and allicin ATP levels in Hek293 cell treatments; DON reduced ATP production in the treated cells.

4.3 NOS ASSAY

RNS production was assessed using the NOS assay (Figure 4.3). The treatments all increased NO and thus RNS concentration compared from $23.7 \pm 0.9528\mu\text{M}$ in the control ($p < 0.0001$, ANOVA with Tukey's Multiple Comparisons Test). Both DON and allicin individual treatments induced an increase of 23% ($29.2 \pm 0.3\mu\text{M}$, $p = 0.0310$) and 54% ($36.4 \pm 3.2\mu\text{M}$, $p = 0.0622$) in RNS formation respectively; however, the combined treatment (DON+A) demonstrated a synergistic 84% increase ($53.7 \pm 0.3\mu\text{M}$) when compared to DON-treated cells ($p < 0.0001$) and 48% in comparison to allicin-treated cells ($p = 0.0332$).

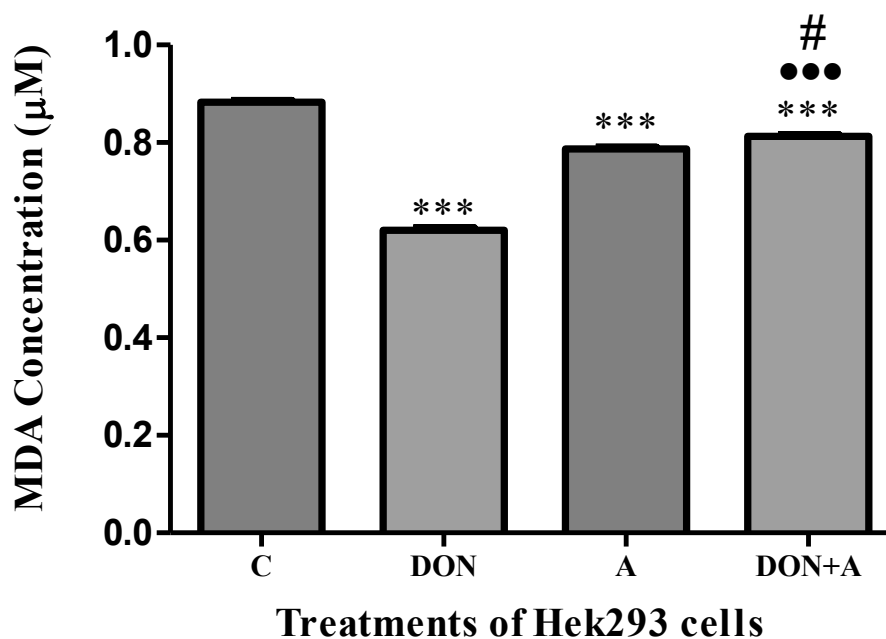


Symbol	*	•	#
Compared to	control	DON	A

Figure 4.3: RNS production in Hek293 cell treatments was increased for all treatments relative to the control (* $p = 0.0310$, ** $p = 0.0011$). Of particular significance is the increased RNS in DON+A treated cells when compared to the individual treatments (••• $p < 0.0001$, # $p = 0.0332$ compared to DON and alliin, respectively). Students t -test with Welch's correction.

4.4 TBARS ASSAY

ROS induced lipid peroxidation was assessed by MDA concentration quantification in treated Hek293 cells (Figure 4.4). All the treatments significantly decreased MDA concentration from $0.88 \pm 0.003\mu\text{M}$ in the control ($p < 0.0001$). However, alliin in the combination of DON + alliin treatment increased MDA toward control levels ($0.81 \pm 0.003\mu\text{M}$, $p = 0.0001$), and was increased relative to the individual DON ($0.62 \pm 0.006\mu\text{M}$, $p < 0.0001$) and alliin ($0.79\mu \pm 0.003\text{M}$, $p = 0.0109$) treatments (Figure 4.4).

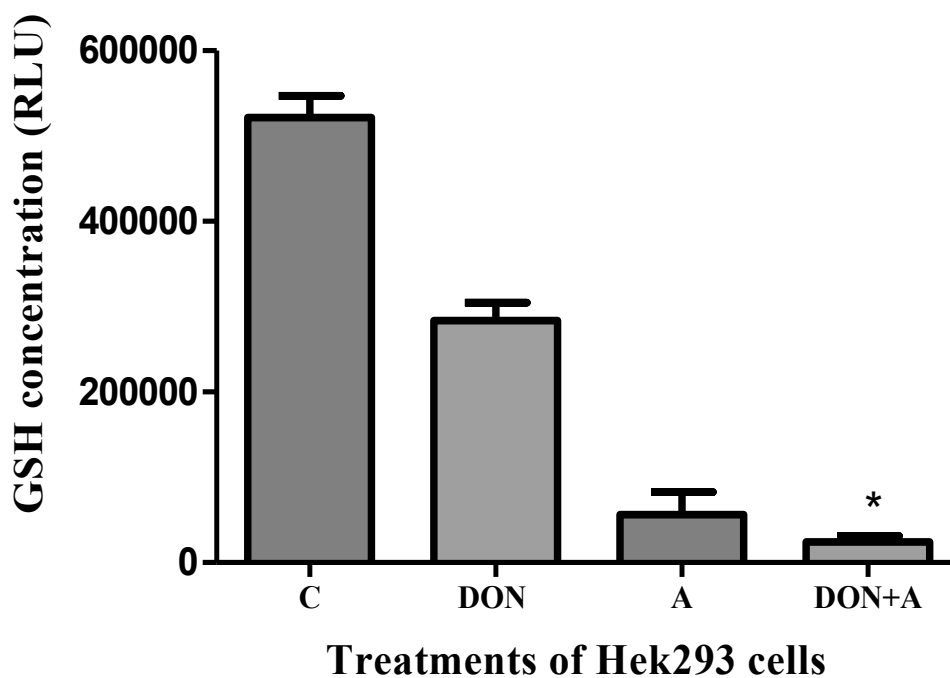


Symbol	*	•	#
Compared to	control	DON	A

Figure 4.4: DON and allicin MDA levels in treated Hek293 cells were decreased for all treatments ($***p < 0.0001$, $***p = 0.0003$, and $p = 0.0001$ respectively). The DON+A treatment increased MDA towards control levels compared to the individual DON ($••• p < 0.0001$) and allicin ($\#p = 0.0109$) treatment; Students *t*-test with Welch's correction.

4.5 GSH ASSAY

The GSH concentration was measured as a marker for intracellular antioxidant capacity. There was a severe depletion of GSH levels for all treatments in comparison to the control (521696 ± 25770 RLU), especially the combination treatment (Figure 4.5; $p = 0.0002$). The GSH concentration decreased by more than 40% to 283718 ± 21110 RLU in DON treated cells ($p = 0.0886$) but was less depleted than allicin (56254 ± 26440 RLU, $p = 0.0504$). The presence of allicin in the combined treatment caused further reduction in GSH concentration (24150 ± 7187 RLU) compared to the individual treatment ($p = 0.0546$, $p = 0.4498$ respectively) and control ($p = 0.0342$).



Symbol	*	•	#
Compared to	control	DON	A

Figure 4.5: The decreased GSH concentration in all treatments compared to the control, with severe depletion in the combination treatment (* $p = 0.0342$; Students t -test with Welch's correction).

4.6 OXIDATIVE STRESS MARKER PROTEINS

Western blotting was used to determine the expression of proteins that mediate oxidative stress, including SOD2, CAT, GPx1, Nrf2, and Hsp70 (Figure 4.6). SOD2 (Figure 4.6A) was significantly downregulated by 35% for DON treated Hek293 cells ($p < 0.0001$) compared to the control (1.4 ± 0.005 RBD), but an increase of 35% was noted for the individual allicin treatment (1.9 ± 0.005 RBD, $p < 0.0001$). This resulted in a SOD2 expression that was restored to control levels compared to DON in the DON+A treatment (1.4 ± 0.013 RBD, $p = 0.1457$). Similarly, catalase protein expression (Figure 4.6B) was significantly decreased by 40% from control levels (1.4 ± 0.006 RBD) for the individual DON treatment ($p < 0.0001$); however, catalase was significantly increased by 70% for the allicin treatment (2.4 ± 0.005 RBD, $p < 0.0001$). The combination of allicin and DON resulted in a synergistic increase in catalase expression to 1.7 ± 0.010 RBD compared to the control ($p = 0.0006$). Gpx1 was upregulated in all treatments relative to control (Figure 4.6C); both allicin (2.1 ± 0.063 RBD, $p < 0.0001$) and DON (0.5 ± 0.009 RBD, $p < 0.0001$) individual protein expression was significantly increased from control

concentration (0.2 ± 0.003 RBD). The combination of DON+A upregulated the expression of GPx1 by 150% (0.7 ± 0.046 RBD, $p = 0.0018$) in Hek293 cells compared to the control. Nrf2 was downregulated in all Hek293 treated cells (Figure 4.6D). It was noted that allicin caused less than 10% reduction in Nrf2 protein expression and was similar to the control level (1.1 ± 0.008 RBD, $p = 0.0021$). DON reduced Nrf2 expression by 58% to 0.5 ± 0.004 RBD ($p < 0.0001$), and in the combination treatment (DON+A) allicin was able to upregulate Nrf2 compared to the DON only treatment ($p < 0.0001$). Hsp70 expression (Figure 4.6E) was induced in a similar pattern to SOD2 protein expression. The DON treatment downregulated HSP70 to 1.2 ± 0.012 RBD (8%, $p = 0.0056$), while allicin treatment upregulated Hsp70 by 85% relative to the control ($p < 0.0001$) and combined treatment induced Hsp70 expression to (1.7 ± 0.012 RBD) (DON+A, $p < 0.0001$).

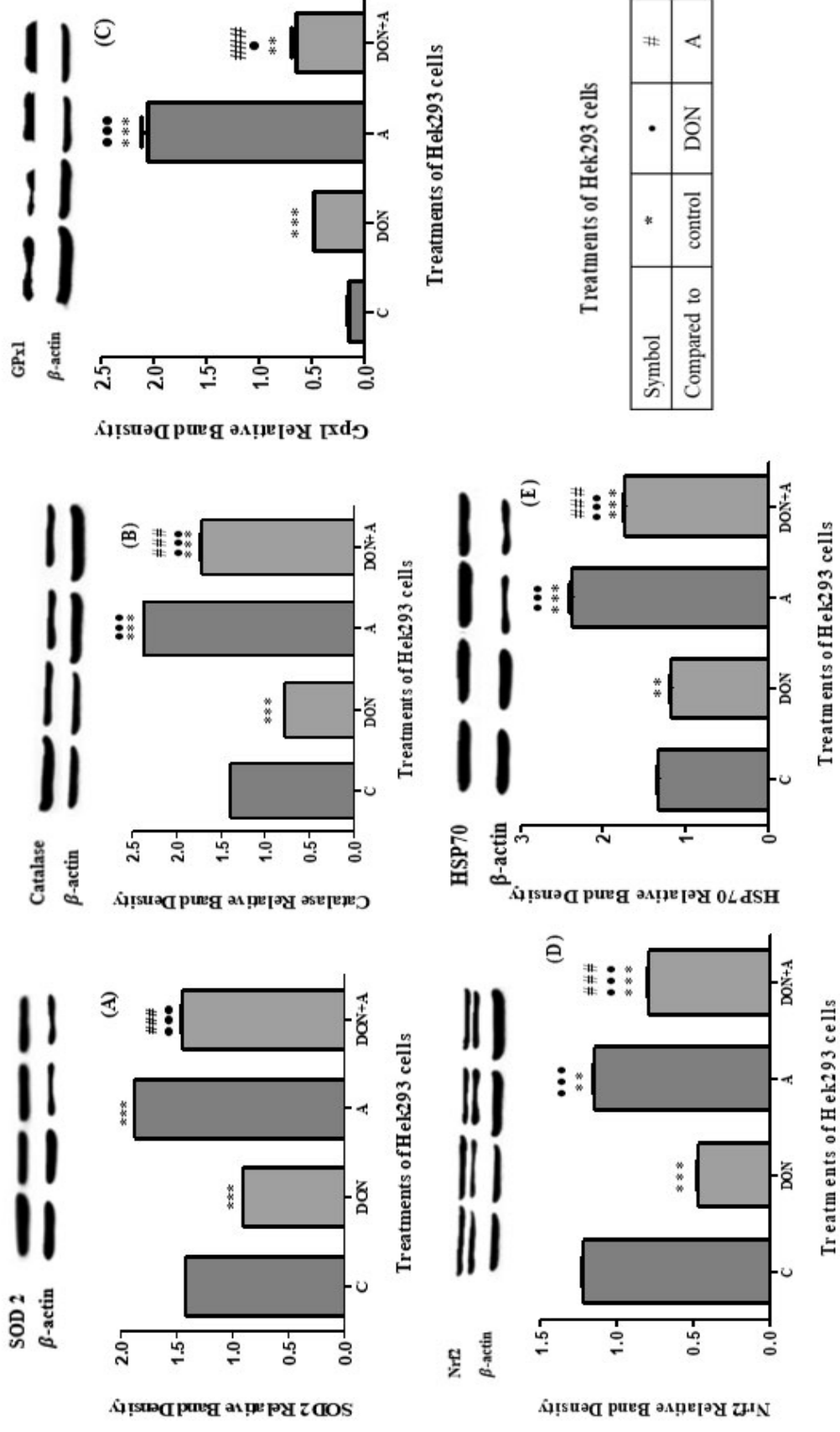


Figure 4.6: Expression of oxidative stress associated proteins on untreated and treated cells; (A) SOD2 was significantly decreased by DON ($***p < 0.0001$) and upregulated by allucin ($***p < 0.0001$); DON+A was similar to the control. (B) Catalase was significantly decreased by DON ($***p < 0.0001$) and upregulated by allucin ($***p < 0.0001$); DON+A returned catalase to control levels ($***p = 0.0006$). (C) GPx1 protein expression was upregulated by all treatments, particularly allucin ($***p = 0.0001$); DON+A returned catalase to control levels ($***p < 0.0001$). (D) Nrf2 protein expression was significantly decreased by DON ($***p < 0.0001$) and slightly downregulated by allucin ($***p = 0.0021$); DON+A returned catalase towards control levels ($***p < 0.0001$). (E) Hsp70 was significantly upregulated by allucin and DON+A ($***p < 0.0001$). Unpaired student *t*-test with Welch's correction.

4.7 ANNEXIN V

The annexin V assay was used to quantify apoptotic cells. The externalization of phosphatidylserine was decreased slightly by DON ($p = 0.4631$), remained similar to the control in allicin-treated cells, and was decreased in DON+A-treated ($p = 0.0488$) Hek293 cells were no significant increases for the individual treatments, and the combined allicin treatment (Figure 4.7.1). The levels of necrosis were similar to the control in all the treatments (Figure 4.7.2).

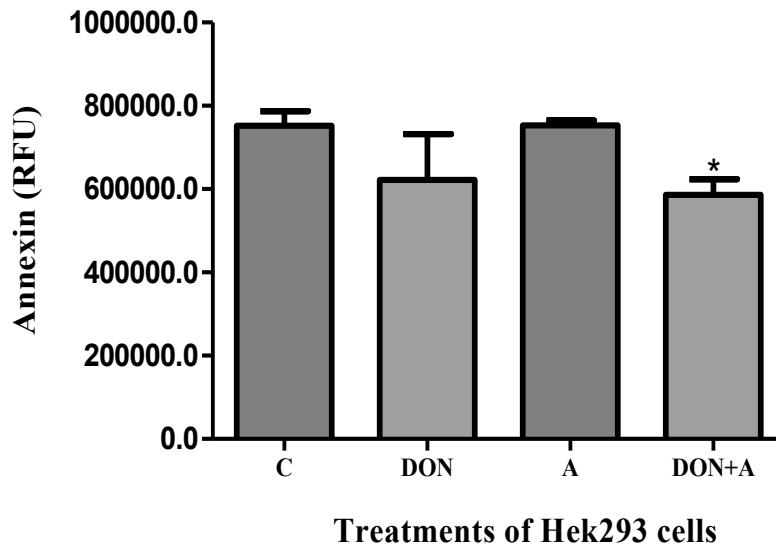


Figure 4.7.1: The annexin V graph representing apoptotic cells in Hek293 cells. Apoptosis was reduced in DON, and DON+A treated cells (* $p = 0.0488$, Students t -test with Welch's correction).

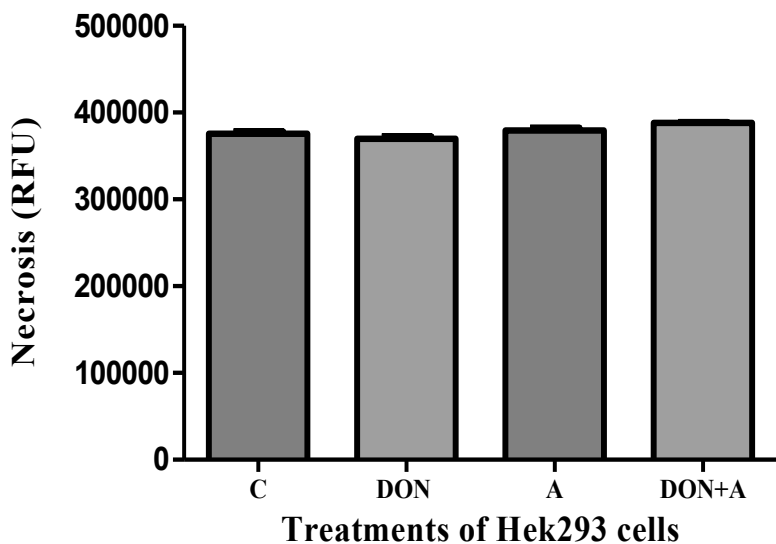


Figure 4.7.2: The levels of necrosis for all Hek293 treated cells were not significantly different from the control.

4.8 CASPASES

The activity of initiator caspases 9 and executioner caspase 3/7 was assessed using luminometry. Caspase activity was reduced in all treated Hek293 cells comparative to the control (Figure 4.8). Caspase 9 (Figure 4.8A) was depleted by 70% in DON ($p = 0.0705$) and 40% in allicin ($p = 0.1203$) treated Hek293 cells. The combined DON+A treatment resulted in further downregulation of caspase 9 compared to the individual DON ($p = 0.2832$) and allicin ($p = 0.0397$) treatment (Figure 4.8A). The individual DON treatment reduced caspase 3/7 by 40% ($p = 0.4431$), in a similar pattern to caspase 9 (Figure 4.8C). Allicin diminished caspase 3/7 activity by more than 45% ($p = 0.3950$), and the combination DON+A further downregulated caspase 3/7 activity ($p = 0.311$).

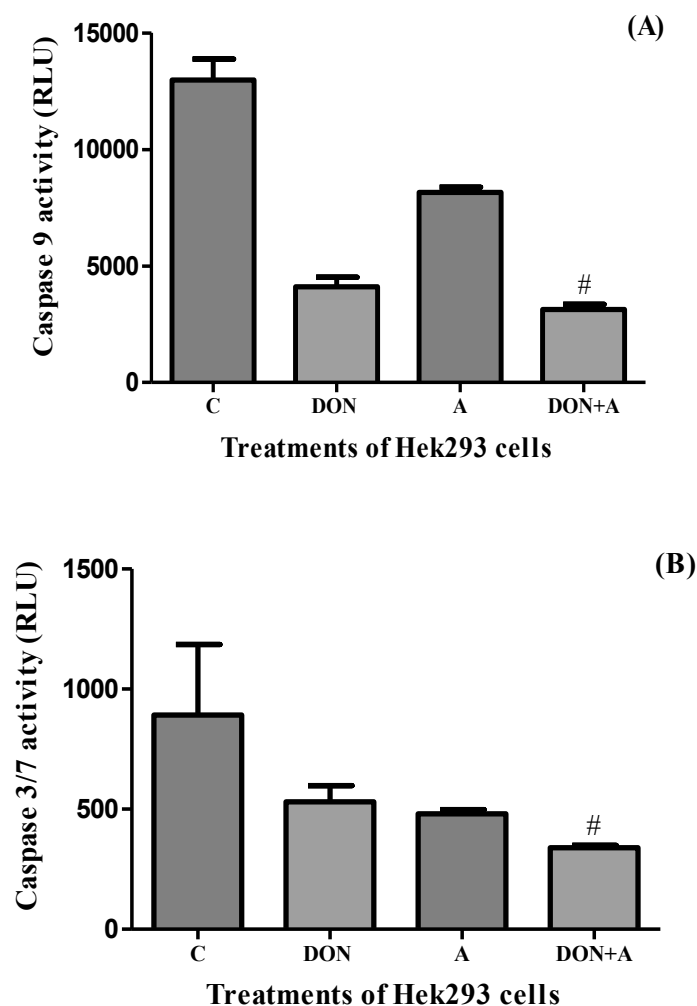


Figure 4.8: Caspase activity following Hek293 cell exposure to DON, allicin and DON+A treatments. Initiator caspase 9 (A), as well as executioner caspase 3/7 (B) were downregulated for all Hek293 cell treatments. The combined treatment for caspase 9 ($\#p = 0.0397$) and caspase 3/7 ($\#p = 0.0067$) were significantly different from the allicin-only treatment, Students t -test with Welch's correction.

4.9 LDH ASSAY

The LDH assay was used in measuring the release of LDH from cells as an indicator of cytotoxicity. All the treatments showed a reduction in cell membrane damage (Figure 4.9), especially in the DON treatment, with a 48% decrease in LDH ($p = 0.0342$). Allicin also displayed reduced levels of LDH and was similar to the combined treatment.

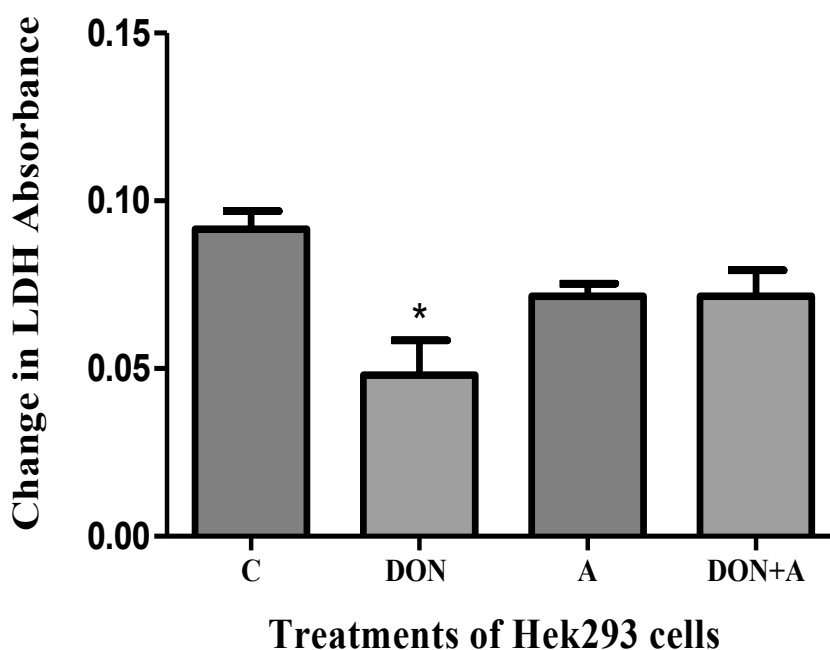


Figure 4.9: Reduced LDH levels in individual DON (* $p = 0.0342$) and allicin, and combined DON+A treated cells, Student t -test with Welch's correction.

4.10 APOPTOSIS PROTEINS

Apoptotic markers probed for were PARP-1, p53, and Bax (Figure 4.10). All treatments increased PARP expression (Figure 4.10A); DON induction of PARP-1 expression was similar to the control, while allicin significantly increased PARP-1 expression 59% ($p = 0.0048$) and the combined treatment ($p = 0.0004$). Similarly, the expression of p53 protein was elevated for all treatments (Figure 4.10B). A slight increase was noted following DON treatment ($p = 0.0008$), with a significantly greater increase in the allicin treatment ($p < 0.0001$). However, the combined allicin and DON treatment induced a synergistic 40% increase ($p < 0.0001$) in p53 protein expression. Bax (Figure 4.10C) was downregulated by 21% in the DON treatment ($p = 0.1071$) but was upregulated 64% in the Hek293 cells treated with allicin ($p < 0.0001$). Furthermore, allicin increased Bax expression in the DON+A treatment ($p = 0.0026$).

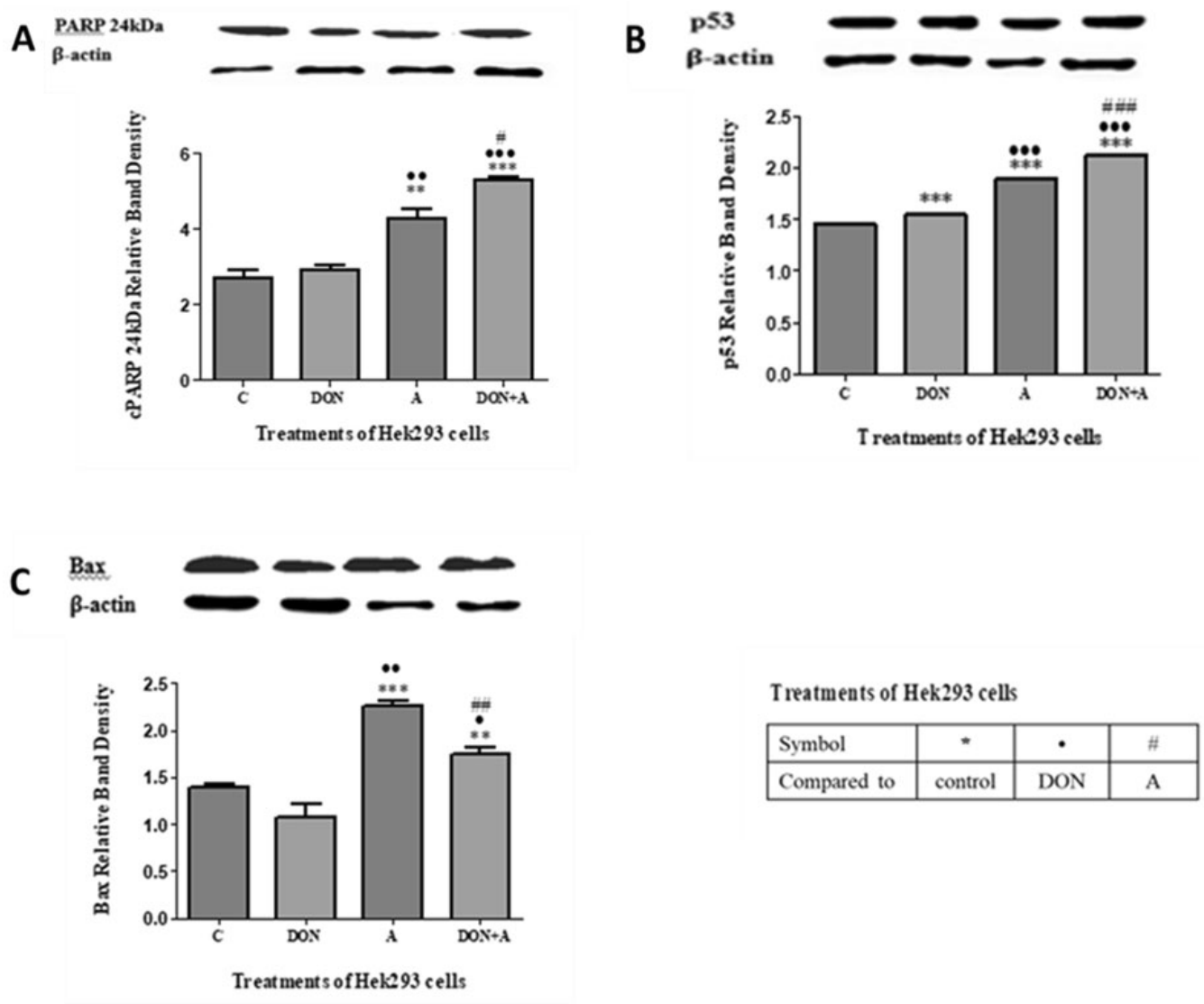


Figure 4.10: Expression of apoptosis-associated proteins in untreated and treated Hek293 cells. (A) PARP-1 was significantly upregulated by allicin ($***p = 0.0048$) and DON+A ($***p = 0.0004$) (B) p53 protein expression was upregulated by all treatments ($*** p < 0.0001$). (C) Bax was downregulated by DON ($p = 0.1071$); and upregulated by allicin ($p < 0.0001$) and in the DON+A treatment ($p = 0.0026$). Unpaired student *t*-test with Welch's correction.

4.11 DNA FRAGMENTATION

The DNA fragmentation pattern observed was similar for the control and allixin treatments (Figure 4.11). The streaking pattern corresponding to DNA fragmentation was detected in DON-treated Hek293 cells (Figure 4.11) and was subsequently reduced by co-treatment with allixin (Figure 4.11).

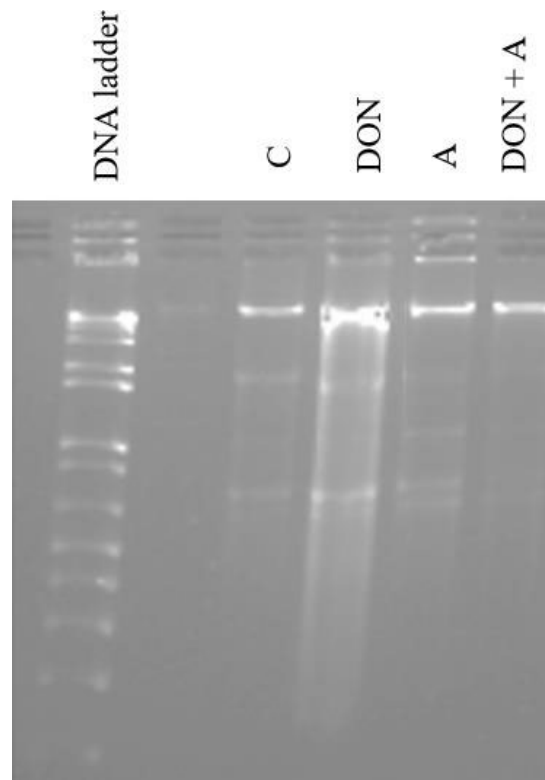


Figure 4.11: A 2% agarose gel electrophoresis depicting DNA fragmentation in DON-treated Hek293 cells.

CHAPTER 5 : DISCUSSION

The inevitable contamination of foods by mycotoxins presents a global challenge to human health and well-being (Chilaka *et al.*, 2017). Deoxynivalenol (DON) is a potent mycotoxin found throughout South Africa (Meyer *et al.*, 2019a). Consumed unintentionally through maize-derived products, DON is rapidly becoming a potential health risk to humans and animals as well as posing an economic threat to the local agricultural-associated industries (Misihairabgwi *et al.*, 2017). The pleiotropic effects of DON result in cellular and physiological effects that are evident at multiple levels of biological organization (Herrera *et al.*, 2019). DON effects are primarily instigated at the level of transcription through ribosome dysregulation, but this impacts protein production (Pestka, 2008, Amarasinghe *et al.*, 2019). In addition, the induction of oxidative stress by DON mediates oxidative damage to cellular macromolecules, including DNA fragmentation and lipid peroxidation that may lead to cell death (Carere *et al.*, 2018). In recent years, medicinal plants that are immensely popular in the treatment of various ailments have shown promise for their protective role against mycotoxicity (da Cruz Cabral *et al.*, 2013, Xue *et al.*, 2019). For example, extracts of *Allium sativum* that are renowned for their anti-cancer properties were shown to reduce ROS-induced macromolecule damage in Vero cells that were exposed to ZEN (Abid-Essefi *et al.*, 2012, Xue *et al.*, 2019). Allicin, a bioactive compound found in *Allium sativum*, is commonly used as an ayurvedic drug to treat diseases such as diabetes mellitus. Furthermore, it is known to possess anti-cancer properties, thus rendering allicin as a promising therapeutic agent against mycotoxicity. Therefore, this study aimed to determine the potential of allicin to alleviate DON-induced toxicity in Hek293 cells following acute exposure (24hrs).

Mitochondria sustain life by producing energy in the form of ATP. The ATP is produced in a series of steps that involve the transfer of electrons through specialized complexes embedded in the mitochondrial membrane to oxygen, reducing it to water. Electron transfer is coupled to the creation of a proton gradient; the energy derived from this proton gradient drives ATP synthesis by altering the conformation of ATP synthase and resulting in the phosphorylation of ADP to form ATP (Bhatti *et al.*, 2017). Mitochondrial integrity is crucial to the production of ATP that plays a role in maintaining cell function. Thus, the depletion of ATP is a sensitive and reliable marker for toxicity. In this study, DON induced a decrease in intracellular ATP (Figure 4.2) that corresponds to depleted ATP previously noted in DON-exposed Hek293 cells (Le *et al.*, 2018). The slight increase in ATP concentration in allicin-treated cells (Figure 4.2) demonstrates its ability to preserve ATP synthesis, as observed in other studies (Liu *et al.*, 2015, Zhang *et al.*, 2017b). However, in contrast to the protective effects observed for lipopolysaccharide-treated human umbilical vein endothelial (HUVEC) cells, co-administration with DON induced a further decrease in ATP

concentration (Figure 4.2) (Zhang *et al.*, 2017b). These findings are congruent with those observed by Dellafiora and Dall'Asta (2017) that suggested that the potential interactions between mycotoxins and beneficial plant phytochemicals may elicit synergistically or potentiating adverse effects, as noted by the interaction between DON and resveratrol in Caco-2 cells (Cano-Sancho *et al.*, 2015, Dellafiora and Dall'Asta, 2017).

The production of ATP is just one of several processes that occur in the mitochondrion. In the course of ATP synthesis, some molecules of oxygen are not completely reduced, leading to the formation of O_2^- (Bhatti *et al.*, 2017). The O_2^- generated is either dismutated to H_2O_2 by SOD2 or reacts with NO to form ONOO⁻, a potent RNS. The data produced in this study suggest that DON shifts O_2^- metabolism toward the formation of RNS. Exposure to DON was associated with reduced SOD2 protein expression (Figure 4.6A), implying a decreased capacity to simultaneously oxidize/reduce O_2^- to H_2O_2 and increased O_2^- availability, which in turn reacts with NO to form RNS (da Silva *et al.*, 2018). This finding is supported by the increased levels of RNS (Figure 4.3) and is entirely feasible as DON was shown to modulate NOS within Caco-2 cells (Graziani *et al.*, 2015). The ONOO⁻ is able to nitrate tyrosine residues within proteins resulting in the formation of nitrotyrosine. Nitrotyrosine may inhibit enzymatic activity and interfere with vital intracellular downstream signalling processes thereby impacting optimal cell functioning (Adesso *et al.*, 2017).

In addition, the downregulation of SOD2 decreases H_2O_2 levels. Consequently, fewer OH⁻ radicals, usually formed from H_2O_2 via the Fenton reaction and associated with lipid peroxidation, will be produced (Catapano *et al.*, 2019). This may explain the decreased lipid peroxidation (Figure 4.4), and LDH leakage (Figure 4.9) observed in this study. In addition, downregulation of CAT (Figure 4.6B) and depletion of GSH (Figure 4.5), both of which function in the detoxification of H_2O_2 to H_2O , occurred with DON exposure. Since the fate of H_2O_2 is determined by the relative abundance of CAT and GSH, the reverse should apply that decreased H_2O_2 would be associated with decreased antioxidant activity (Dinu *et al.*, 2011, Catapano *et al.*, 2019). However, GPx1 (Figure 4.6C) was increased. This may also account for decreased GSH (Figure 4.5) since GPx1 uses GSH in the detoxification of electrophilic species. Thus, lipid peroxidation induced by ROS would be reversed by GSH, accounting for the reduced MDA levels and contributing to GSH depletion. The GSH reaction is also important in the detoxification of xenobiotics; glutathione-S-transferase (GST) catalyzes the conjugation of GSH to electrophilic epoxides (Woelflingseder *et al.*, 2018). This reaction may be the main contributor to GSH depletion since DON contains an epoxide moiety at position C12-C13 (Woelflingseder *et al.*, 2018). The changes in antioxidant enzyme expression and depletion of GSH strongly indicates a state of oxidative stress. In previous studies

where DON was not associated with significant GSH depletion, a corresponding increase in Nrf2/ARE signalling was noted (Li *et al.*, 2014). However, in this study, ARE's were not activated by Nrf2 (Figure 4.6 D), and an important signalling pathway associated with transcription of antioxidant genes such as SOD2 and glutathione synthetase did not occur, resulting in the diminished generation and expression of these proteins (Jin *et al.*, 2014, Yu *et al.*, 2018). Thus, it can be deduced that the decreased expression of Nrf2 in DON-treated cells may serve as a justifiable reason that is responsible for the depletion of SOD2, GSH and catalase (Yu *et al.*, 2017b).

Although Nrf2 was not induced by allicin (Figure 4.6D), there is an associated increased expression of antioxidant enzymes by allicin (Tu *et al.*, 2016). Elevated SOD2 protein expression (Figure 4.6A) induced by allicin suggests increased O_2^- generation, some of which were converted to RNS (Figure 4.3). Allicin also increased the expression of catalase and GPx1 (Figures 4.6B and C), accounting for H_2O_2 detoxification, and decreased lipid peroxidation (Figure 4.4). The antioxidant properties of allicin have been identified previously (Chen *et al.*, 2014, Zhang *et al.*, 2017b). In particular, studies have successfully shown that allicin-induced depletion of GSH may arise through oxidation of GSH to GSSG or depletion of the GSH pool due to the formation of a mixed-disulfide. The result in this study (Figure 4.5) is consistent with a dose-dependent decrease of GSH observed in several cell lines, including human lung epithelium carcinoma (A549), mouse fibroblast (3T3), HUVEC, human colon carcinoma (HT29), and human breast cancer (MCF7) cells (Gruhlke *et al.*, 2016).

Allicin demonstrated protective effects against DON-induced cytotoxicity by restoring SOD2 protein expression within normal levels (Figure 4.6A), as shown in HUVECs (Chen *et al.*, 2014). Allicin also increased MDA towards homeostatic levels (Figure 4.4), possibly due to an increase in CAT and GPx1 (Figures 4.6B & C) that shunted H_2O_2 for detoxification or repair of oxidative damage through the utilization of GSH (Figure 4.5). These findings suggest that allicin has the ability to protect cells by impeding oxidative stress through upregulation of antioxidant activity, including scavenging of free radicals, inhibition of lipid peroxidation, and induction of cell membrane stabilization (Chen *et al.*, 2014). Therefore, the preservation of these endogenous antioxidant activities may ultimately protect cells against oxidative stress-induced cellular damage and increased susceptibility to cell death (Zhang *et al.*, 2017b).

DNA damage via oxidation that results in DNA strand breaks is a well-known consequence of ROS-mediated effects. In addition, RNS may induce both single and double-stranded DNA breaks or cause base modification through nitration, oxidation, and deamination (Ohshima *et al.*, 1999, Martin, 2008). Double strand DNA breaks are regarded as one of the most serious types of DNA damage-induced and can result

in cell death (Bohgaki *et al.*, 2010). A classic laddering pattern of inter-nucleosomal DNA fragmentation was observed in DON-treated cells (Figure 4.11) and is comparable with other studies where DON was shown to induce DNA damage; these studies implicate ROS in the *in vivo* and *in vitro* genotoxic effects of DON (Zhang *et al.*, 2009, Graziani *et al.*, 2015, Ren *et al.*, 2015, Payros *et al.*, 2017a, Ikwegbue *et al.*, 2017, Habrowska-Gorczyńska *et al.*, 2019). Hsp70 is known to protect cells from DNA fragmentation associated with ROS-mediated genotoxicity (Ikwegbue *et al.*, 2017). Failure of DON to upregulate Hsp70 (Figure 4.6E) was not surprising, as this was previously observed in HT29 cells (Bensassi *et al.*, 2009). Since Hsp70 was not upregulated in response to DON treatment, the presence of fragmented DNA (Figure 4.11) may not be attributed to increased ROS. However, the increased RNS and DNA adduct formation may result in strand breaks and the characteristic fragmentation pattern observed in Figure 4.11. Indeed, the chemical structure of DON facilitates adduct formation with cellular nucleophiles contained in DNA and protein, as reported in plants and HepG2 cells (Woelflingseder *et al.*, 2018). An alternate explanation is that the fragmentation could indicate the activation of apoptosis (Bohgaki *et al.*, 2010); however, apoptosis was not induced in DON-treated cells (Figure 4.7.1). In addition, cell death by necrosis was also not evident (Figure 4.7.2); these findings are in agreement with previous observations in chicken splenic lymphocytes (Ren *et al.*, 2015). Significantly less DNA fragmentation visualized with the allicin treatment (Figure 4.11) may be attributed to the upregulation of Hsp70 (Figure 4.6E) by the organosulfur compound; this benefit is conferred by Hsp70 to protect the cell from oxidative DNA damage as demonstrated in neuronal cells (Liu *et al.*, 2015). Alternatively, adduct formation in the presence of DON may have been inhibited in a manner similar to that exhibited for benzo-a-pyrene and N-nitroso compounds (Omar and Al-Wabel, 2010).

Single and double-stranded DNA breaks are known to activate p53, which in turn activates the transcription of DNA repair genes and translation of DNA repair proteins (Nelson and Kastan, 1994, Bohgaki *et al.*, 2010). In addition, PARP-1 functions in nuclear and base excision repair mechanisms that are required when either single- or double-stranded DNA breaks occur (Chaitanya *et al.*, 2010). It is interesting to note that neither p53 (Figure 4.10B) nor PARP-1 (Figure 4.10A) was activated by the presence of DNA damage in DON-treated cells (Figure 4.11), but this is entirely feasible given the effect of DON on translation (Amarasinghe *et al.*, 2019). This result also explains why apoptosis was not evident in DON-treated Hek293 cells via the intrinsic pathway. Under normal circumstances, when p53-directed DNA repair fails, p53 activates transcription of Puma and Noxa, which facilitate Bax-mediated pore formation and release of apoptotic proteins from the mitochondrial intermembrane space (Ren *et al.*, 2017). Cytochrome c released from mitochondria participates in apoptosome formation with the subsequent activation of caspase 9, caspase 3, and activation of cell death. DON did not induce Bax protein expression (Figure 4.10C), and

caspase 9 activity (Figure 4.8B) was decreased. In addition, caspase 8 activity was downregulated (Figure 4.8A), so apoptosis was unlikely initiated via the extrinsic route. Consequently, caspase 3 activity was inhibited (Figure 4.8C), phosphatidylserine was not externalized (Figure 4.7.1), and PARP-1 was not cleaved (Figure 4.10A). This observation has not yet been identified in Hek293 cells.

The reduced presence of DNA strand breaks in the allicin and combined treatments (Figure 4.11) demonstrates the protective effect of allicin. Allicin mediated the increase in p53 (Figure 4.10B) and PARP-1 (Figure 4.10A) to facilitate the repair of damaged DNA. However, Bax was upregulated in the allicin treatments (Figure 4.10C), while apoptosis was not initiated (Figure 4.8A, 4.8B) or executed (Figure 4.8C, Figure 4.7.1). These findings are supported in literature where allicin increased Bax levels in U87MG human glioblastoma cells (Cha *et al.*, 2012). In addition, allicin also reduced procaspase-3 cleavage in human umbilical vein endothelial cells so that subsequent cleavage of PARP-1 by caspase 3/7 did not occur and apoptosis was not induced (Chen *et al.*, 2014, Zhang *et al.*, 2017b). Allicin-induced upregulation of Hsp70 (Figure 4.6E) and its association with Apaf-1 may prevent Apaf-1 oligomerization with procaspase-9 (Figure 4.8B), consequently inhibiting the formation of the apoptosome, caspase 3/7 activation (Figure 4.8C) and ultimately leading to reduced cell death via the intrinsic pathway (Saleh *et al.*, 2000, Candé *et al.*, 2002). Previous studies have suggested that allicin-induced apoptosis is highly dependent on the cellular genotype, thus rendering cells more susceptible or more resistant to the effects of allicin. Changes that may take place regarding the expression of proteins that regulate apoptosis could ultimately cause the failure of allicin to induce apoptosis in certain cells (Oommen *et al.*, 2004). Similarly, allicin failed to induce apoptosis in the combined treatments, possibly due to DON effects on transcription and translation. However, the exact mechanism is currently unknown (Pestka, 2008, Kang *et al.*, 2019).

CHAPTER 6 : CONCLUSION AND FUTURE RECOMMENDATIONS

Recent studies have suggested that DON mediates its effects in kidney cells via oxidative stress and apoptosis. Phytochemicals such as allicin may limit mycotoxin-induced effects in cells. This study aimed to determine the cellular and molecular mechanisms of DON-induced cytotoxicity in Hek293 cells and the possible ameliorative effects of allicin.

The key findings (Figure 6.1) show that DON induced oxidative stress in Hek293 cells, but utilization of intracellular antioxidants minimized free radical damage to lipids. Depletion of GSH, which usually indicates oxidative stress, was possibly exacerbated by phase 2 removal of adducts and the failure to upregulate the Nrf2 system. Reactive nitrogen species that were increased as a result of SOD2 downregulation and adduct formation may be responsible for the observed DNA fragmentation. Despite the observed DNA damage, intrinsic apoptosis was not initiated by p53, and neither Bax nor caspase 9 was activated. In addition, apoptosis was not executed (caspase 3 was not activated, PARP was not cleaved, and phosphatidylserine was not externalized). Cell death by necrosis also did not occur. Figure 6.1 also shows that oxidative/nitrosative stress and not apoptosis may be the mechanism of allicin-induced effects in Hek293 cells. More importantly, allicin did not ameliorate the cytotoxic effects of DON in Hek293 cells (Figure 6.1). Indeed, although allicin is a beneficial plant phytochemical, it may elicit synergistically or potentiating adverse effects with DON.

Further investigation on the chronic effects of DON and allicin is recommended. The molecular mechanisms of DON and allicin should also be elucidated using an *in vivo* model. We believe that phytochemicals will prove valuable in the fight against mycotoxin-induced cell injury; therefore, other medicinal plants should be investigated in search of novel anticancer agents.

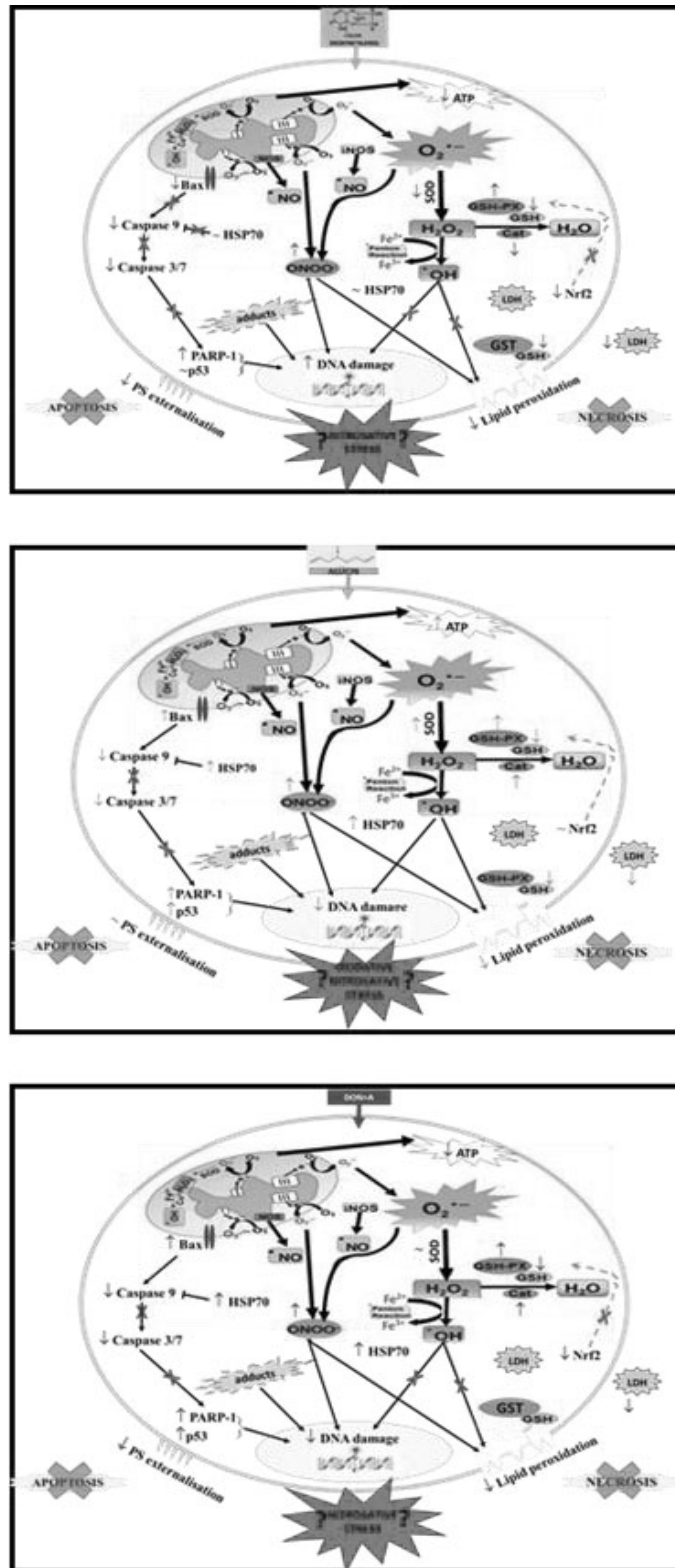


Figure 6.1: Schematic overview of the biochemical effects of DON, allicin and DON+A in human embryonic kidney (Hek293) cells (Prepared by author).

REFERENCESUncategorized References

- ABID-ESSEFI, S., BOUAZIZ, C., GOLLI-BENNOUR, E. E., OUANES, Z. & BACHA, H. 2009. Comparative study of toxic effects of zearalenone and its two major metabolites alpha-zearalenol and beta-zearalenol on cultured human Caco-2 cells. *J Biochem Mol Toxicol*, 23, 233-243.
- ABID-ESSEFI, S., ZAIED, C., BOUAZIZ, C., SALEM, I. B., KADERI, R. & BACHA, H. 2012. Protective effect of aqueous extract of *Allium sativum* against zearalenone toxicity mediated by oxidative stress. *Exp Toxicol Pathol*, 64, 689-695.
- ACHANTA, G. & HUANG, P. 2004. Role of p53 in sensing oxidative DNA damage in response to reactive oxygen species-generating agents. *Cancer Res*, 64, 6233– 6239.
- ADESSO, S., AUTORE, G., QUARONI, A., POPOLO, A., SEVERINO, L. & MARZOCCO, S. 2017. The Food Contaminants Nivalenol and Deoxynivalenol Induce Inflammation in Intestinal Epithelial Cells by Regulating Reactive Oxygen Species Release. *Nutrients*, 9, 1343.
- AL-JAAL, B. A., JAGANJAC, M., BARCARU, A., HORVATOVICH, P. & LATIFF, A. 2019. Aflatoxin, fumonisin, ochratoxin, zearalenone and deoxynivalenol biomarkers in human biological fluids: A systematic literature review, 2001–2018. *Food and Chemical Toxicology*, 129, 211-228.
- ALI-BOUCETTA, H., AL-JAMAL, K. T. & KOSTARELOS, K. 2011. Cytotoxic assessment of carbon nanotube interaction with cell cultures. *Methods Mol Biol*, 726, 299-312.
- ALI. 2019. *Genomic DNA Extraction – Principle, Steps and Functions of Reagents* [Online]. Available: www.HowBiotech.com [Accessed 18/11 2019].
- ALIZADEH, A., BRABER, S., AKBARI, P., KRANEVELD, A., GARSSSEN, J. & FINK-GREMMELS, J. 2016. Deoxynivalenol and Its Modified Forms: Are There Major Differences? *Toxins (Basel)*, 8.
- ALTOMARE, C., LOGRIECO, A., BOTTALICO, A., MULE, G., MORETTI, A. & EVIDENTE, A. 1995. Production of Type-a Trichothecenes and Enniatin-B by *Fusarium-Sambucinum* Fuckel Sensu-Lato. *Mycopathologia*, 129, 177-181.
- AMARASINGHE, C., SHARANOWSKI, B. & FERNANDO, W. G. D. 2019. Molecular Phylogenetic Relationships, Trichothecene Chemotype Diversity and Aggressiveness of Strains in a Global Collection of *Fusarium graminearum* Species. *Toxins (Basel)*, 11.
- AUPANUN, S., PHUEKTES, P., POAPOLATHEP, S., ALASSANE-KPEMBI, I., OSWALD, I. P. & POAPOLATHEP, A. 2019a. Individual and combined cytotoxicity of major trichothecenes type B, deoxynivalenol, nivalenol, and fusarenon-X on Jurkat human T cells. *Toxicon*, 160, 29-37.
- AUPANUN, S., POAPOLATHEP, S., PHUEKTES, P., GIORGI, M., ZHANG, Z., OSWALD, I. P. & POAPOLATHEP, A. 2019b. Individual and combined mycotoxins deoxynivalenol, nivalenol, and fusarenon-X induced apoptosis in lymphoid tissues of mice after oral exposure. *Toxicon*, 165, 83-94.
- AZCONA-OLIVERA, J. I., OUYANG, Y. L., WARNER, R. L., LINZ, J. E. & PESTKA, J. J. 1995. Effects of vomitoxin (deoxynivalenol) and cycloheximide on IL-2, 4, 5 and 6 secretion and mRNA levels in murine CD4+ cells. *Food Chem Toxicol*, 33, 433-441.
- BARREIRO, E. 2016. Role of Protein Carbonylation in Skeletal Muscle Mass Loss Associated with Chronic Conditions. *Proteomes*, 4, 18.
- BAT-CHEN, W., GOLAN, T., PERI, I., LUDMER, Z. & SCHWARTZ, B. 2010. Allicin purified from fresh garlic cloves induces apoptosis in colon cancer cells via Nrf2. *Nutrition and cancer*, 62, 947-957.
- BAYAN, L., KOULIVAND, P. H. & GORJI, A. 2014. Garlic: a review of potential therapeutic effects. *Avicenna journal of phytomedicine*, 4, 1-14.
- BEDA, N. & NEDOSPASOV, A. 2005. A spectrophotometric assay for nitrate in an excess of nitrite. *Nitric Oxide*, 13, 93-97.
- BENNETT, J. W. & KLICH, M. 2003. Mycotoxins. *Clin Microbiol Rev*, 16, 497-516.
- BENSASSI, F., EL GOLLI-BENNOUR, E., ABID-ESSEFI, S., BOUAZIZ, C., HAJLAOUI, M. R. & BACHA, H. 2009. Pathway of deoxynivalenol-induced apoptosis in human colon carcinoma cells. *Toxicology*, 264, 104-109.

- BENSASSI, F., GALLERNE, C., SHARAF EL DEIN, O., LEMAIRE, C., HAJLAOUI, M. R. & BACHA, H. 2012. Involvement of mitochondria-mediated apoptosis in deoxynivalenol cytotoxicity. *Food Chem Toxicol*, 50, 1680-1689.
- BEREK, L., PETRI, I. B., MESTERHAZY, A., TEREN, J. & MOLNAR, J. 2001. Effects of mycotoxins on human immune functions in vitro. *Toxicol Appl Pharmacol*, 15, 25–30.
- BERTERO, A., MORETTI, A., SPICER, L. J. & FRANCESCA, C. 2018. Fusarium Molds and Mycotoxins: Potential Species-Specific Effects. *Toxins (Basel)*.
- BEUKES, I., ROSE, L., SHEPHARD, G., FLETT, B. & VILJOEN, A. 2017. Mycotoxigenic Fusarium species associated with grain crops in South Africa – A Review. *South African Journal of Science*, Volume 113.
- BHANDARI, B. 2017. *Western Blot Technique: Principle, Procedures and Uses* [Online]. Available: <https://microbeonline.com/western-blot-technique-principle-procedures-advantages-and-disadvantages/> [Accessed 18/11 2019].
- BHAT, C. V., BEEDU, R., RAMAKRISHNA, Y. & MUNSHI, K. L. 1989. Outbreak of trichothecene toxicosis associated with consumption of mould dam aged wheat products in Kashmir Valley, India. *Lancet*
- BHATTI, J. S., BHATTI, G. K. & REDDY, P. H. 2017. Mitochondrial dysfunction and oxidative stress in metabolic disorders — A step towards mitochondria based therapeutic strategies. *Biochimica et Biophysica Acta (BBA) - Molecular Basis of Disease*, 1863, 1066 - 1077.
- BIO-TECHNE. 2014. *TBARS Parameter™ Kit for Measuring Oxidative Stress* [Online]. Available: <https://www.rndsystems.com/product-highlights/tbars-parameter-kit-measuring-oxidative-stress> [Accessed 18/11/2019 2019].
- BOHGAKI, T., BOHGAKI, M. & HAKEM, R. 2010. DNA double-strand break signaling and human disorders. *Genome Integr*, 1, 15.
- BORLINGHAUS, J., ALBRECHT, F., GRUHLKE, M. C., NWACHUKWU, I. D. & SLUSARENKO, A. J. 2014. Allicin: chemistry and biological properties. *Molecules*, 19, 12591-12618.
- BORUTOVA, R., FAIX, S., PLACHA, I., GRESAKOVA, L., COBANNOVA, K. & LENG, L. 2008. Effects of deoxynivalenol and zearalenone on oxidative stress and blood phagocytic activity in broilers. *Archives of Animal Nutrition*, 62, 303-312.
- BRACA, A., SORTINO, C., POLITI, M., MORELLI, I. & MENDEZ, J. 2002. Antioxidant activity of flavonoids from *Licania licaniaeflora*. *J Ethnopharmacol*, 79, 379-381.
- BRAICU, C., BERINDAN - NEAGOE, I., TUDORAN, O., BALACESCU, O., RUGINĂ, D., GHERMAN, C., SOCACIU, C. & IRIMIE, A. 2009. In vitro evaluation of the chemoprotective action of flavan-3-ols against deoxynivalenol related toxicity. *Arch Zootech*, 12, 45-55.
- BRETZ, M., BEYER, M., CRAMER, B. & HUMPF, H. U. 2006. Stable isotope dilution analysis of the Fusarium mycotoxins deoxynivalenol and 3-acetyldeoxynivalenol *Molecular Nutrition & Food research*, 50, 251-260.
- BRUNELLE, J. K. & ZHANG, B. 2010. Apoptosis assays for quantifying the bioactivity of anticancer drug products. *Drug Resistance Updates*, 13, 172-179.
- BRYAN, N. S. & GRISHAM, M. B. 2007. Methods to detect nitric oxide and its metabolites in biological samples. *Free Radic Biol Med*, 43, 645-657.
- CABRAL, L. D. C., PINTO, V. F. & PATRIARCA, A. 2013. Application of plant derived compounds to control fungal spoilage and mycotoxin production in foods. *International Journal of Food Microbiology*, 166, 1-14.
- CAMBAZA, E., KOSEKI, S. & KAWAMURA, S. 2019. Why RGB Imaging Should be Used to Analyze Fusarium Graminearum Growth and Estimate Deoxynivalenol Contamination. *Methods Protoc*, 2.
- CANDÉ, C., CECCONI, F., DESSEN, P. & KROEMER, G. 2002. Apoptosis-inducing factor (AIF): key to the conserved caspase-independent pathways of cell death? *Journal of Cell Science*, 115, 4727.
- CANO-SANCHO, G., GONZÁLEZ-ARIAS, C. A., RAMOS, A. J., SANCHIS, V. & FERNÁNDEZ-CRUZ, M. L. 2015. Cytotoxicity of the mycotoxins deoxynivalenol and ochratoxin A on Caco-2 cell line in presence of resveratrol. *Toxicol In Vitro*, 29, 1639-1646.

- CARERE, J., HASSAN, Y. I., LEPP, D. & ZHOU, T. 2018. The Identification of DepB: An Enzyme Responsible for the Final Detoxification Step in the Deoxynivalenol Epimerization Pathway in *Devosia mutans* 17-2-E-8. *Front Microbiol*, 9, 1573.
- CATAPANO, M. C., PROTTI, M., FONTANA, T., MANDRIOLI, R., MLADĚNKA, P. & MERCOLINI, L. 2019. An Original HPLC Method with Coulometric Detection to Monitor Hydroxyl Radical Generation via Fenton Chemistry. *Molecules*, 24.
- CHA, J. H., CHOI, Y. J., CHA, S. H., CHOI, C. H. & CHO, W. H. 2012. Allicin inhibits cell growth and induces apoptosis in U87MG human glioblastoma cells through an ERK-dependent pathway. *Oncol Rep*, 28, 41-48.
- CHAITANYA, G. V., STEVEN, A. J. & BABU, P. P. 2010. PARP-1 cleavage fragments: signatures of cell-death proteases in neurodegeneration. *Cell Commun Signal*, 8, 31.
- CHAN, F. K. M., MORIWAKI, K. & DE ROSA, M. J. 2013. Detection of necrosis by release of lactate dehydrogenase activity. *Immune Homeostasis: Methods and Protocols*, 65-70.
- CHANGWA, R., ABIA, W., MSAGATI, T., NYONI, H., NDLEVE, K. & NJOBEH, P. 2018. Multi-Mycotoxin Occurrence in Dairy Cattle Feeds from the Gauteng Province of South Africa: A Pilot Study Using UHPLC-QTOF-MS/MS. *Toxins (Basel)*, 10.
- CHEEKE, P. R. 1998. Natural toxicants in feeds, forages, and poisonous plants.
- CHEN, F., MA, Y., XUE, C., MA, J., XIE, Q., WANG, G., BI, Y. & CAO, Y., . 2008. The combination of deoxynivalenol and zearalenone at permitted feed concentrations causes serious physiological effects in young pigs. *J. Vet. Sci.*, 9, 39-44.
- CHEN, S., TANG, Y., QIAN, Y., CHEN, R., ZHANG, L., WO, L. & CHAI, H. 2014. Allicin prevents H₂O₂-induced apoptosis of HUVECs by inhibiting an oxidative stress pathway. *BMC complementary and alternative medicine*, 14, 321.
- CHEN, S. S., LI, Y. H. & LIN, M. F. 2017. Chronic Exposure to the Fusarium Mycotoxin Deoxynivalenol: Impact on Performance, Immune Organ, and Intestinal Integrity of Slow-Growing Chickens. *Toxins (Basel)*, 9.
- CHILAKA, C. A., DE BOEVRE, M., ATANDA, O. O. & DE SAEGER, S. 2017. The Status of Fusarium Mycotoxins in Sub-Saharan Africa: A Review of Emerging Trends and Post-Harvest Mitigation Strategies towards Food Control. *Toxins (Basel)*, 9.
- COSTA, S., SCHWAIGER, S., CERVELLATI, R., STUPPNER, H., SPERONI, E. & GUERRA, M. C. 2009. In vitro evaluation of the chemoprotective action mechanisms of leontopodic acid against aflatoxin B1 and deoxynivalenol-induced cell damage. *J Appl Toxicol*, 29, 7-14.
- COUSSENS, N. P., SITTAMPALAM, G. S., GUHA, R., BRIMACOMBE, K., GROSSMAN, A., CHUNG, T. D., WEIDNER, J. R., RISS, T., TRASK, O. J. & AULD, D. 2018. Assay guidance manual: quantitative biology and pharmacology in preclinical drug discovery. *Clinical and translational science*, 11, 461-470.
- DA CRUZ CABRAL, L., FERNANDEZ PINTO, V. & PATRIARCA, A. 2013. Application of plant derived compounds to control fungal spoilage and mycotoxin production in foods. *Int J Food Microbiol*, 166, 1-14.
- DA SILVA, E. O., BRACARENSE, A. P. F. L. & OSWALD, I. P. 2018. Mycotoxins and oxidative stress: where are we? *World Mycotoxin Journal*, 11, 113-134.
- DELLAFIORA, L. & DALL'ASTA, C. 2017. Forthcoming Challenges in Mycotoxins Toxicology Research for Safer Food—A Need for Multi-Omics Approach. *Toxins* 9.
- DENG, X. B., DIN, H. Z., HUANG, X. H., MA, Y. J., FAN, X. L., YAN, H. K., LU, P. C., LI, W. C. & ZENG, Z. L. 2015. Tissue distribution of deoxynivalenol in piglets following intravenous administration. *Journal of Integrative Agriculture*, 14, 2058-2064.
- DINU, D., BODEA, G. O., CEAPA, C. D., MUNTEANU, M. C., ROMING, F. I., SERBAN, A. I., HERMENEAN, A., COSTACHE, M., ZARNESCU, O. & DINISCHIOTU, A. 2011. Adapted response of the antioxidant defense system to oxidative stress induced by deoxynivalenol in Hek-293 cells. *Toxicol*, 57, 1023-1032.

- DIPAOLLO, J. A. & CARRUTHERS, C. 1960. The effect of allicin from garlic on tumor growth. *Cancer Res*, 20, 431-434.
- DROGE, W. 2002. Free radicals in the physiological control of cell function. *Physiol Rev*, 82, 47-95.
- DUTORDOIR, M. R. & BATES, D. A. A. 2016. Activation of apoptosis signalling pathways by reactive oxygen species. *Biochim Biophys Acta*, 1863, 2977-2992.
- EDMONDS, M. 2010. *What is apoptosis* [Online]. HowStuffWorks.com. Available: <https://science.howstuffworks.com/life/cellular-microscopic/apoptosis.htm> [Accessed 20 January 2020].
- EFSA 2013. Deoxynivalenol in food and feed: occurrence and exposure. *EFSA Journal*, 11.
- EL-SAWI, N., EL-WASSIMY, M. M. & YOUSSEF, O. 2001. Effect of verrucarin J toxin on liver and kidney tissue of male mice. *Texas Journal of Science*, 53, 375-384.
- ELMORE, S. 2007. Apoptosis: a review of programmed cell death. *Toxicologic pathology*, 35, 495-516.
- FERRIGO, D., RAIOLA, A. & CAUSIN, R. 2016. Fusarium Toxins in Cereals: Occurrence, Legislation, Factors Promoting the Appearance and Their Management. *Molecules*, 21.
- FIUME, L., MANERBA, M., VETTRAINO, M. & STEFANO, G. D. 2014. Inhibition of lactate dehydrogenase activity as an approach to cancer therapy. *Future medicinal chemistry*, 429-445.
- FOREST, V., FIGAROL, A., BOUDARD, D., COTTIER, M., GROSSEAU, P. & POURCHEZ, J. 2015. Adsorption of Lactate Dehydrogenase Enzyme on Carbon Nanotubes: How to Get Accurate Results for the Cytotoxicity of These Nanomaterials . . *Langmuir*. 31(12), 3635-3643.
- FOROUD, N. A., BAINES, D., GAGKAEVA, T. Y., THAKOR, N., BADEA, A., STEINER, B., BURSTMAYR, M. & BURSTMAYR, H. 2019. Trichothecenes in Cereal Grains - An Update. *Toxins (Basel)*, 11.
- FORSELL, J. H., WITT, J. M. F., TAIR.JENSEN, H. & PESTKA, J. J. 1986. Effects of 8-week exposure of the B6C3F1 mouse to dietary deoxynivalenol (vomitoxin) and zearalenone. *Food and Chemical Toxicology*, 24, 213 - 219.
- GARVEY, G. S., MCCORMICK, S. P. & RAYMENT, I. 2008. Structural and functional characterization of the TRI101 trichothecene 3-O-acetyltransferase from *Fusarium sporotrichioides* and *Fusarium graminearum*: kinetic insights to combating *Fusarium* head blight. *J Biol Chem*, 283, 1660-1669.
- GIMENO, A. 2004. Deoxynivalenol, a Risk Mycotoxin for Children. Analytical Methods. Deoxynivalenol Levels in Wheat-Based Food Products.
- GMBH, B. 2019. BioCat - Apoptosis Detection (Phosphatidylserin/Annexin based).
- GOTTSCHALK, C., BARTHEL, J., ENGELHARDT, G., MICHAEL, J. & KARSTEN MEYER, B. 2009. Simultaneous determination of type A, B, and D trichothecenes and their occurrence in cereals and cereal products. *Food Addit Contam*, 1273-1289.
- GRAZIANI, F., PINTON, P., OLLEIK, H., PUJOL, A., NICOLETTI, C., SICRE, M., QUINSON, N., AJANDOUZ, E. H., PERRIER, J., PASQUALE, E. D., OSWALD, I. P. & MARESCA, M. 2019. Deoxynivalenol inhibits the expression of trefoil factors (TFF) by intestinal human and porcine goblet cells. *Arch Toxicol*, 93, 1039-1049.
- GRAZIANI, F., PUJOL, A., NICOLETTI, C., PINTON, P., ARMAND, L., DI PASQUALE, E., OSWALD, I. P., PERRIER, J. & MARESCA, M. 2015. The food-associated ribotoxin deoxynivalenol modulates inducible NO synthase in human intestinal cell model. *Toxicological Sciences*, 145, 372-382.
- GRUHLKE, M. C., NICCO, C., BATTEUX, F. & SLUSARENKO, A. J. 2016. The Effects of Allicin, a Reactive Sulfur Species from Garlic, on a Selection of Mammalian Cell Lines. *Antioxidants (Basel)*, 6.
- GRUHLKE, M. C. & SLUSARENKO, A. J. 2012. The biology of reactive sulfur species (RSS). *Plant Physiol Biochem*, 59, 98-107.
- GU, X., GUO, W., ZHAO, Y., LIU, G., WU, J. & CHANG, C. 2019. Deoxynivalenol-Induced Cytotoxicity and Apoptosis in IPEC-J2 Cells Through the Activation of Autophagy by Inhibiting PI3K-AKT-mTOR Signaling Pathway. *ACS Omega*, 4, 18478-18486.

- GUERRERO-NETRO, H. M., ESTIENNE, A., CHORFI, Y. & PRICE, C. A. 2017. The mycotoxin metabolite deepoxy- deoxynivalenol increases apoptosis and decreases steroidogenesis in bovine ovarian theca cells. *Biol Reprod*, 97, 746-757.
- HABROWSKA-GORCZYNSKA, D. E., KOWALSKA, K., URBANEK, K. A., DOMINSKA, K., SAKOWICZ, A. & PIASTOWSKA-CIESIELSKA, A. W. 2019. Deoxynivalenol Modulates the Viability, ROS Production and Apoptosis in Prostate Cancer Cells. *Toxins (Basel)*, 11.
- HALLIWELL, B. & WHITEMAN, M. 2004. Measuring reactive species and oxidative damage in vivo and in cell culture: how should you do it and what do the results mean? *Br J Pharmacol*, 142, 231-255.
- HARRIS, J. C., COTTRELL, S. L., PLUMMER, S. & LLOYD, D. 2001. Antimicrobial properties of *Allium sativum* (garlic). *Appl Microbiol Biotechnol*, 57, 282-286.
- HASSAN, K. A., ELBOURNE, L. D., LI, L., GAMAGE, H., HASINIKA, K., LIU, Q., JACKSON, S. M., SHARPLES, D., KOLSTØ, A.-B. & HENDERSON, P. J. 2015. An ace up their sleeve: a transcriptomic approach exposes the AceI efflux protein of *Acinetobacter baumannii* and reveals the drug efflux potential hidden in many microbial pathogens. *Frontiers in microbiology*, 6, 333.
- HAYES, J. D. & STRANGE, R. C. 1995. Potential contribution of the glutathione S-transferase supergene family to resistance to oxidative stress. *Free Radic Res*, 22, 193-207.
- HAZEL, C. M., SCUDAMORE, K. A., PATEL, S. & SCRIVEN, F. 2009. Deoxynivalenol and other Fusarium mycotoxins in bread, cake, and biscuits produced from UK-grown wheat under commercial and pilot scale conditions. *Food Additives & Contaminants: Part A*, 26, 1191-1198.
- HE, K. & PESTKA, J. 2010. Deoxynivalenol-induced modulation of microRNA expression in RAW 264.7 macrophages-A potential novel mechanism for translational inhibition. *Toxicologist (Toxicol. Sci.)*, 114.
- HERRERA, M., BERVIS, N., CARRAMIÑANA, J. J., JUAN, T., HERRERA, A., ARIÑO, A. & LORÁN, S. 2019. Occurrence and Exposure Assessment of Aflatoxins and Deoxynivalenol in Cereal-Based Baby Foods for Infants. *Toxins (Basel)*, 11, 150.
- HIRSCH, K., DANILENKO, M., GIAT, J., MIRON, T., RABINKOV, A., WILCHEK, M., MIRELMAN, D., LEVY, J. & SHARONI, Y. 2000. Effect of purified allicin, the major ingredient of freshly crushed garlic, on cancer cell proliferation. *Nutrition and cancer*, 38, 245-254.
- HOOFT, J. M., FERREIRA, C., LUMSDEN, J. S., SULYOK, M., KRŠKA, R. & BUREAU, D. P. 2019. The effects of naturally occurring or purified deoxynivalenol (DON) on growth performance, nutrient utilization and histopathology of rainbow trout (*Oncorhynchus mykiss*). *Aquaculture*, 505, 319-332.
- HOU, Y. J., ZHAO, Y. Y., XIONG, B., CUI, X. S., KIM, N. H., XU, Y. X. & SUN, S. C. 2013a. Mycotoxin-containing diet causes oxidative stress in the mouse. *PLoS One*, 8, e60374.
- HOU, Y. J., ZHAO, Y. Y., XIONG, B., CUI, X. S., KIM, N. H., XU, Y. X. & SUN, S. C. 2013b. Mycotoxin-containing diet causes oxidative stress in the mouse.
- HUANG, Y., LIU, S., HOU, W., XIAO, P., CHEN, N. J., QIU, P., PENG, Z., LIAO, Y. X., WANG, L. L., LI, D., LIU, L. G. & YANG, W. 2019. High contamination levels of deoxynivalenol-induced erythrocyte damage in different models. *Trends in Food Science & Technology*, 86, 41-50.
- HUSSEIN, H. S. & BRASEL, J. M. 2001. Toxicity, metabolism, and impact of mycotoxins on humans and animals. *Toxicology*, 167, 101-134.
- IKWEGBUE, P. C., MASAMBA, P., OYINLOYE, B. E. & KAPPO, A. P. 2017. Roles of Heat Shock Proteins in Apoptosis, Oxidative Stress, Human Inflammatory Diseases, and Cancer. *Pharmaceuticals (Basel)*, 11.
- JACOB, C. & ANWAR, A. 2008. The chemistry behind redox regulation with a focus on sulphur redox systems. *Physiol Plant*, 133, 469-480.
- JI, G. E., PARK, S. Y., WONG, S. S. & PESTKA, J. J. 1998. Modulation of nitric oxide, hydrogen peroxide and cytokine production in a clonal macrophage model by the trichothecene vomitoxin (deoxynivalenol). *Toxicology*, 125, 203-214.

- JIN, J., XIONG, T., HOU, X., SUN, X., LIAO, J., HUANG, Z., HUANG, M. & ZHAO, Z. 2014. Role of Nrf2 activation and NF-kappaB inhibition in valproic acid induced hepatotoxicity and in diammonium glycyrrhizinate induced protection in mice. *Food Chem Toxicol*, 73, 95-104.
- KANG, R., LI, R., DAI, P., LI, Z., LI, Y. & LI, C. 2019. Deoxynivalenol induced apoptosis and inflammation of IPEC-J2 cells by promoting ROS production. *Environ Pollut*, 251, 689-698.
- KATIKA, M. R., HENDRIKSEN, P. J., SHAO, J., VAN LOVEREN, H. & PEIJNENBURG, A. 2012. Transcriptome analysis of the human T lymphocyte cell line Jurkat and human peripheral blood mononuclear cells exposed to deoxynivalenol (DON): New mechanistic insights. *Toxicol. Appl. Pharmacol*, 51-64.
- KAUSHAL, G. P., CHANDRASHEKAR, K. & JUNCOS, L. A. 2019. Molecular Interactions Between Reactive Oxygen Species and Autophagy in Kidney Disease. *Int J Mol Sci*, 20.
- KERR, J. F., WINTERFORD, C. M. & HARMON, B. V. 1994. Apoptosis. Its significance in cancer and cancer therapy. *Cancer*, 73, 2013-2026.
- KEW.ORG. 2016. *Allium sativum* (garlic).
- KNUTSEN, H. K., ALEXANDER, J., BARREGÅRD, L., BIGNAMI, M., BRÜSCHWEILER, B., CECCATELLI, S., COTTRILL, B., DINOVI, M., GRASL-KRAUPP, B., HOGSTRAND, C., HOOGENBOOM, L., NEBBIA, C. S., OSWALD, I. P., PETERSEN, A., ROSE, M., ROUDOT, A. C., SCHWERDTLE, T., VLEMINCKX, C., VOLLMER, G., WALLACE, H., DE SAEGER, S., ERIKSEN, G. S., FARMER, P., FREMY, J. M., GONG, Y. Y., MEYER, K., NAEGELI, H., PARENT-MASSIN, D., RIETJENS, I., VAN EGMOND, H., ALTIERI, A., ESKOLA, M., GERGELOVA, P., RAMOS BORDAJANDI, L., BENKOVA, B., DÖRR, B., GKRILLAS, A., GUSTAVSSON, N., VAN MANEN, M. & EDLER, L. 2017. Risks to human and animal health related to the presence of deoxynivalenol and its acetylated and modified forms in food and feed. *EFSA Journal*, 15.
- KOFF, J. L., RAMACHANDIRAN, S. & BERNAL-MIZRACHI, L. 2015. A Time to Kill: Targeting Apoptosis in Cancer. *International Journal of Molecular Sciences*, 16, 2942-2955.
- KOKKONEN, H., SODERSTROM, I., ROCKLOV, J., HALLMANS, G., LEJON, K. & RANTAPAA DAHLQVIST, S. 2010. Up-regulation of cytokines and chemokines predates the onset of rheumatoid arthritis. *Arthritis Rheum*, 62, 383-391.
- KOUTAKIS, P., ISMAEEL, A., FARMER, P., PURCELL, S., SMITH, R. S., EIDSON, J. L. & BOHANNON, W. T. 2018. Oxidative stress and antioxidant treatment in patients with peripheral artery disease. *Physiological Reports*, 6, e13650.
- KROKAN, H. E., STANDAL, R. & SLUPPHAUG, G. 1997. DNA glycosylases in the base excision repair of DNA. *Biochem. Journal*, 1-16.
- LE, T. H., ALASSANE-KPEMBI, I., OSWALD, I. P. & PINTON, P. 2018. Analysis of the interactions between environmental and food contaminants, cadmium and deoxynivalenol, in different target organs. *Sci Total Environ*, 622-623, 841-848.
- LEE, J. Y., LIM, W., PARK, S., KIM, J., YOU, S. & SONG, G. 2019. Deoxynivalenol induces apoptosis and disrupts cellular homeostasis through MAPK signaling pathways in bovine mammary epithelial cells. *Environ Pollut*, 252, 879-887.
- LI, D., YE, Y., LIN, S., DENG, L., FAN, X., ZHANG, Y., DENG, X., LI, Y., YAN, H. & MA, Y. 2014. Evaluation of deoxynivalenol-induced toxic effects on DF-1 cells in vitro: cell-cycle arrest, oxidative stress, and apoptosis. *Environ Toxicol Pharmacol*, 37, 141-149.
- LI, F. Q., LUO, X. Y. & YOSHIZAWA, T. 1999. Mycotoxins (trichothecenes, zearalenone and fumonisins) in cereals associated with human red-mold intoxications stored since 1989 and 1991 in China. *Natural Toxins*, 7, 93-97.
- LI, M. & PESTKA, J. J. 2008. Comparative induction of 28S ribosomal RNA cleavage by ricin and the trichothecenes deoxynivalenol and T-2 toxin in the macrophage. *Toxicol Sci*, 105, 67-78.
- LI, X. G., ZHU, M., CHEN, M. X., FAN, H. B., FU, H. L., ZHOU, J. Y., ZHAI, Z. Y., GAO, C. Q., YAN, H. C. & WANG, X. Q. 2019. Acute exposure to deoxynivalenol inhibits porcine enteroid activity via suppression of the Wnt/beta-catenin pathway. *Toxicol Lett*, 305, 19-31.

- LIANG, Z., REN, Z., GAO, S., CHEN, Y., YANG, Y., YANG, D., DENG, J., ZUO, Z., WANG, Y. & SHEN, L. 2015. Individual and combined effects of deoxynivalenol and zearalenone on mouse kidney. *Environ Toxicol Pharmacol*, 40, 686-691.
- LIGUORI, I., RUSSO, G., CURCIO, F., BULLI, G., ARAN, L., DELLA-MORTE, D., GARGIULO, G., TESTA, G., CACCIATORE, F., BONADUCE, D. & ABETE, P. 2018. Oxidative stress, aging, and diseases. *Clinical Interventions in Aging*, 13.
- LIMA, R. R. M. P. A. N. 2010. Toxicology of mycotoxins. *Molecular, Clinical and Environmental Toxicology*, 2.
- LIU, S. G., REN, P. Y., WANG, G. Y., YAO, S. X. & HE, X. J. 2015. Allicin protects spinal cord neurons from glutamate-induced oxidative stress through regulating the heat shock protein 70/inducible nitric oxide synthase pathway. *Food & Function*, 6, 321-330.
- LIU, Z., ZHANG, G., ZHANG, Y., JIN, Q., ZHAO, J. & LI, J. 2016. Factors controlling mycotoxin contamination in maize and food in the Hebei province, China. *Agronomy for Sustainable Development*, 36, 39.
- MARESCA, M. 2013. From the gut to the brain: journey and pathophysiological effects of the food-associated trichothecene mycotoxin deoxynivalenol. *Toxins (Basel)*, 5, 784-820.
- MARQUEZ, R., TSAO, W.-C., FAUST, N. & XU, L. 2013. Drug Resistance and Molecular Cancer Therapy: Apoptosis Versus Autophagy.
- MARTIN, L. J. 2008. DNA damage and repair: relevance to mechanisms of neurodegeneration. *J Neuropathol Exp Neurol*, 67, 377-387.
- MCCORMICK, S. P., STANLEY, A. M., STOVER, N. A. & ALEXANDER, N. J. 2011. Trichothecenes: from simple to complex mycotoxins. *Toxins (Basel)*, 3, 802-814.
- MCILWAIN, D. R., BERGER, T. & MAK, T. W. 2013. Caspase functions in cell death and disease. *Cold Spring Harbor perspectives in biology*, 5(4).
- MEYER, H., SKHOSANA, Z. D., MOTLANTHE, M., LOUW, W. & ROHWER, E. 2019a. Long Term Monitoring (2014-2018) of Multi-Mycotoxins in South African Commercial Maize and Wheat with a Locally Developed and Validated LC-MS/MS Method. *Toxins (Basel)*, 11.
- MEYER, H., SKHOSANA, Z. D., MOTLANTHE, M., LOUW, W. & ROHWER, E. 2019b. Long Term Monitoring (2014-2018) of Multi-Mycotoxins in South African Commercial Maize and Wheat with a Locally Developed and Validated LC-MS/MS Method. *Toxins*, 11, 271.
- MILICEVIC, D., NESIC, K. & JAKSIC, S. 2015. Mycotoxin Contamination of the Food Supply Chain - Implications for One Health Programme. *Procedia Food Science*, 5, 187-190.
- MIRON, T., RABINKOV, A., MIRELMAN, D., WILCHEK, M. & WEINER, L. 2000. The mode of action of allicin: its ready permeability through phospholipid membranes may contribute to its biological activity. *Biochimica et Biophysica Acta (BBA) - Biomembranes*, 1463, 20-30.
- MISHRA, S., DWIVEDI, P. D., PANDEY, H. P. & DAS, M. 2014. Role of oxidative stress in Deoxynivalenol induced toxicity. *Food Chem Toxicol*, 72, 20-29.
- MISIHAIABGWI, J., EZEKIEL, C., SULYOK, M., SHEPHARD, G. & KRKA, R. 2017. Mycotoxin contamination of foods in Southern Africa: A 10-year review (2007-2016). *Critical reviews in food science and nutrition*, 59.
- MOGHADAMNIA, Y., MOUSAVI KANI, S. N., GHASEMI-KASMAN, M., KAZEMI KANI, M. T. & KAZEMI, S. 2019. The Anti-cancer Effects of Capparis spinosa Hydroalcoholic Extract. *Avicenna J Med Biotechnol*, 11, 43-47.
- MOON, Y. & PESTKA, J. J. 2002. Vomitoxin-induced cyclooxygenase-2 gene expression in macrophages mediated by activation of ERK and p38 but not JNK mitogen-activated protein kinases. *Toxicol Sci*, 69, 373-382.
- MUKHOPADHYAY, S., PANDA, P. K., SINHA, N., DAS D. N. & BHUTIA, S. K. 2014. Autophagy and apoptosis: where do they meet? *Apoptosis*, 19, 555-566.
- NELSON, W. G. & KASTAN, M. B. 1994. DNA strand breaks: the DNA template alterations that trigger p53-dependent DNA damage response pathways. *Molecular and cellular biology*, 14, 1815-1823.

- NJOBEH, P. B., DUTTON, M. F., ABERG, A. T. & HAGGBLOM, P. 2012. Estimation of multi-mycotoxin contamination in South African compound feeds. *Toxins (Basel)*, 4, 836-848.
- NUNNARI, J. R. F. A. J. 2014. Mitochondrial form and function. *NIH Public Access*, 335–343.
- O'BRIEN, E. & DIETRICH, D. 2005. Mycotoxins Affecting the Kidney. *First publ. in: Toxicology of Kidney 2005, chapter 21, pp. 895-936.*
- OHSHIMA, H., YERMILOV, V., YOSHIE, Y. & RUBIO, J. 1999. DNA Damage Induced by Reactive Nitrogen Species. In: Dizdaroglu M., Karakaya A.E. . In: DIZDAROGLU, M. & KARAKAYA, A. E. (eds.) *Advances in DNA Damage and Repair. NATO ASI Series (Series A: Life Sciences)*. Boston, MA.: Springer.
- OMAR, S. H. & AL-WABEL, N. A. 2010. Organosulfur compounds and possible mechanism of garlic in cancer. *Saudi Pharm J*, 18, 51-58.
- OOMMEN, S., ANTO, R. J., SRINIVAS, G. & KARUNAGARAN, D. 2004. Allicin (from garlic) induces caspase-mediated apoptosis in cancer cells. *Eur J Pharmacol*, 485, 97-103.
- OOSTHUIZEN, C. B., REID, A.-M. & LALL, N. 2018. Garlic (*Allium sativum*) and Its Associated Molecules, as Medicine. *Medicinal Plants for Holistic Health and Well-Being*.
- PARK, S. Y., CHO, S. J., KWON, H. C., LEE, K. R., RHEE, D. K. & PYO, S. 2005. Caspase-independent cell death by allicin in human epithelial carcinoma cells: involvement of PKA. *Cancer Lett*, 224, 123-132.
- PAYROS, D., ALASSANE-KPEMBI, I., PIERRON, A., LOISEAU, N., PINTON, P. & OSWALD, I. P. 2016. Toxicology of deoxynivalenol and its acetylated and modified forms. *Arch Toxicol*, 2931–2957.
- PAYROS, D., DOBRINDT, U., MARTIN, P., SECHER, T., BRACARENSE, A. P., BOURY, M., LAFFITTE, J., PINTON, P., OSWALD, E. & OSWALD, I. P. 2017a. The Food Contaminant Deoxynivalenol Exacerbates the Genotoxicity of Gut Microbiota. *MBio*, 8.
- PAYROS, D., DOBRINDT, U., MARTIN, P., SECHER, T., BRACARENSE, A. P. F. L., BOURY, M., LAFFITTE, J., PINTON, P., OSWALD, E. & OSWALD, I. P. 2017b. The Food Contaminant Deoxynivalenol Exacerbates the Genotoxicity of Gut Microbiota. *MBio*, 8, e00007-00017.
- PERAICA, M., RADIC, B., LUCIC, A. & PAVLOVIC, M. 1999. Toxic effects of mycotoxins in humans. *Bull World Health Organ*, 77, 754-766.
- PESTKA, J. J. 2003. Deoxynivalenol-induced IgA production and IgA nephropathy-aberrant mucosal immune response with systemic repercussions. *Toxicol Lett*, 140-141, 287-295.
- PESTKA, J. J. 2008. Mechanisms of deoxynivalenol-induced gene expression and apoptosis. *Food Addit Contam Part A Chem Anal Control Expo Risk Assess*, 25, 1128-1140.
- PESTKA, J. J. 2010a. Deoxynivalenol-induced proinflammatory gene expression: mechanisms and pathological sequelae. *Toxins (Basel)*, 2, 1300-1317.
- PESTKA, J. J. 2010b. Deoxynivalenol: mechanisms of action, human exposure, and toxicological relevance. *Arch Toxicol*, 84, 663-679.
- PESTKA, J. J. 2010c. Toxicological mechanisms and potential health effects of deoxynivalenol and nivalenol. *World Mycotoxin Journal*, v. 3, pp. 323-347-2010 v.2013 no.2014.
- PESTKA, J. J., ISLAM, Z. & AMUZIE, C. J. 2008. Immunochemical assessment of deoxynivalenol tissue distribution following oral exposure in the mouse. *Toxicol Lett*, 178, 83-87.
- PESTKA, J. J. & SMOLINSKI, A. T. 2005. Deoxynivalenol: toxicology and potential effects on humans. *J Toxicol Environ Health B Crit Rev*, 8, 39-69.
- PICKETT, C. B. & LU, A. Y. 1989. Glutathione S-transferases: gene structure, regulation, and biological function. *Annu Rev Biochem*, 58, 743-764.
- PINTON, P. & OSWALD, I. P. 2014. Effect of deoxynivalenol and other Type B trichothecenes on the intestine: a review. *Toxins (Basel)*, 6, 1615-1643.
- PRAGER-KHOUTORSKY, M., GONCHAROV, I., RABINKOV, A., MIRELMAN, D., GEIGER, B. & BERSHADSKY, A. D. 2007. Allicin inhibits cell polarization, migration and division via its direct effect on microtubules. *Cell motility and the cytoskeleton*, 64, 321-337.
- PROMEGA caspase-glo-3-7-assay-protocol.pdf.

- RABINKOV, A., MIRON, T., MIRELMAN, D., WILCHEK, M., GLOZMAN, S., YAVIN, E. & WEINER, L. 2000. S-Allylmercaptogluthione: the reaction product of allicin with glutathione possesses SH-modifying and antioxidant properties. *Biochim Biophys Acta*, 1499, 144-153.
- REDDY, K. E., LEE, W., JEONG, J. Y., LEE, Y., LEE, H. J., KIM, M. S., KIM, D. W., YU, D., CHO, A., OH, Y. K. & LEE, S. D. 2018. Effects of deoxynivalenol- and zearalenone-contaminated feed on the gene expression profiles in the kidneys of piglets. *Asian-Australas J Anim Sci*, 31, 138-148.
- REN, Z., DENG, H., DENG, Y., LIANG, Z., DENG, J., ZUO, Z., HU, Y., SHEN, L., YU, S. & CAO, S. 2017. Combined effects of deoxynivalenol and zearalenone on oxidative injury and apoptosis in porcine splenic lymphocytes in vitro. *Exp Toxicol Pathol*, 69, 612-617.
- REN, Z., WANG, Y., DENG, H., DENG, Y., DENG, J., ZUO, Z., WANG, Y., PENG, X., CUI, H. & SHEN, L. 2015. Deoxynivalenol induces apoptosis in chicken splenic lymphocytes via the reactive oxygen species-mediated mitochondrial pathway. *Environ Toxicol Pharmacol*, 39, 339-346.
- RICHARD, J. L. 2007. Some major mycotoxins and their mycotoxicoses--an overview. *Int J Food Microbiol*, 119, 3-10.
- RISS, T. L., MORAVEC, R. A. & NILES, A. L. 2011. Cytotoxicity testing: measuring viable cells, dead cells, and detecting mechanism of cell death. *Mammalian Cell Viability*. Springer.
- ROBYN 2019. Buy The Real Thing ALLI-Biotic Caps Vegicaps Online at Faithful to Nature.
- ROTTER, B. A., PRELUSKY, D. B. & PESTKA, J. J. 1996. Toxicology of deoxynivalenol (vomitoxin). *J Toxicol Environ Health*, 48, 1-34.
- SAHU, S. C., GARTHOFF, L. H., ROBL, M. G., CHIRTEL, S. J., RUGGLES, D. I., FLYNN, T. J. & SOBOTKA, T. J. 2008. Rat liver clone-9 cells in culture as a model for screening hepatotoxic potential of food-related products: hepatotoxicity of deoxynivalenol. *J Appl Toxicol*, 28, 765-772.
- SALEH, A., SRINIVASULA, S. M., BALKIR, L., ROBBINS, P. D. & ALNEMRI, E. S. 2000. Negative regulation of the Apaf-1 apoptosome by Hsp70. *Nat Cell Biol*, 2, 476-483.
- SALEHIA, B., ZUCCAB, P., ORHANC, I. E., AZZINID, E., ADETUNJIE, C. O., MOHAMMEDF, S. A., BANERJEEF, S. K., SHAROPOVG, F., RIGANO, D., SHARIFI-RADI, J., ARMSTRONGJ, L., MARTORELLK, M., SUREDAL, A., MARTINSM, N., SELAMOĞLUO, Z. & AHMAD, Z. 2019. Allicin and Health: A comprehensive review. *Trends in Food Science & Technology*, 86, 502-516.
- SAVARD, C., PINILLA, V., PROVOST, C., GAGNON, C. A. & CHORFI, Y. 2014. In vivo effect of deoxynivalenol (DON) naturally contaminated feed on porcine reproductive and respiratory syndrome virus (PRRSV) infection. *Vet Microbiol*, 174, 419-426.
- SCF, S. C. O. F. 2002. Opinion of the Scientific Committee on Food on the risks to human health of Polycyclic Aromatic Hydrocarbons in food.
- SCHOTHORST, R. C., JEKEL, A. A., VAN EGMOND, H. P., DE MUL, A., BOON, P. E. & VAN KLAVEREN, J. D. 2005. Determination of trichothecenes in duplicate diets of young children by capillary gas chromatography with mass spectrometric detection. *Food Additives & Contaminants*, 22, 48-55.
- SCIENTIFIC COMMITTEE ON FOOD 1999. Opinion on Fusarium toxins. Part 1: Deoxynivalenol (DON).
- SEFATER, G., NTAKADZENI EDWIN, M., SARAH DE, S., MARTHE DE, B., IFEOLUWA, A., OLUWAFEMI AYODEJI, A. & PATRICK BERKA, N. 2019. The Socio-Economic Impact of Mycotoxin Contamination in Africa.
- SHIFRIN, V. I. & ANDERSON, P. 1999. Trichothecene mycotoxins trigger a ribotoxic stress response that activates c-Jun N-terminal kinase and p38 mitogen-activated protein kinase and induces apoptosis. *J Biol Chem*, 274, 13985-13992.
- SIEGERS, C. P., STEFFEN, B., RÖBKE, A. & PENTZ, R. 1999. The effects of garlic preparations against human tumor cell proliferation. *Phytomedicine : international journal of phytotherapy and phytopharmacology*, 6, 7-11.
- SIMMONS, H. 2019. HEK293-Cells-Applications-and-Advantages.

- SINGH, S., BANERJEE, S., CHATTOPADHYAY, P., BORTHAKUR, S. K. & VEER, V. 2015. Deoxynivalenol induces cytotoxicity and genotoxicity in animal primary cell culture. *Toxicol Mech Methods*, 25, 184-191.
- SOBROVA, P., ADAM, V., VASATKOVA, A., BEKLOVA, M., ZEMAN, L. & KIZEK, R. 2010. Deoxynivalenol and its toxicity. *Interdiscip Toxicol*, 3, 94-99.
- SOUTH AFRICA FOODSTUFFS, C. A. D. A. 2016. Regulations Governing Tolerances for fungus-produced toxins in Foodstuffs: Amendment. In Government Gazette; No 40250, Government Notice number 987: .
- SPANIC, V., ZDUNIC, Z., DREZNER, G. & SARKANJ, B. 2019. The Pressure of Fusarium Disease and Its Relation with Mycotoxins in The Wheat Grain and Malt. *Toxins (Basel)*, 11.
- STANCIU, O., JUAN, C., BERRADA, H., MIERE, D., LOGHIN, F. & MANES, J. 2019. Study on Trichothecene and Zearalenone Presence in Romanian Wheat Relative to Weather Conditions. *Toxins (Basel)*, 11.
- STEPIĆ, S., HACKENBERGER, B. K., HACKENBERGER, D. K., VELKI, M. & LONČARIĆ, Ž. 2012. Impact of Oxidative Stress Indicated by Thiobarbituric Acid Reactive Substances (TBARS) and Protein Carbonyl Levels (PC) on Ethoxyresorufin-O-deethylase (EROD) Induction in Common Carp (*Cyprinus carpio*). *Water, Air, & Soil Pollution*, 223, 4785-4793.
- STREIT, E., SCHWAB, C., SULYOK, M., NAEHRER, K., KRŠKA, R. & SCHATZMAYR, G. 2013. Multi-mycotoxin screening reveals the occurrence of 139 different secondary metabolites in feed and feed ingredients. *Toxins (Basel)*, 5, 504-523.
- SUN, L.-H., LEI, M.-Y., ZHANG, N.-Y., ZHAO, L., KRUMM, C. S. & QI, D.-S. 2014. Hepatotoxic effects of mycotoxin combinations in mice. *Food and Chemical Toxicology*, 74, 289-293.
- SUN, L. H., LEI, M. Y., ZHANG, N. Y., GAO, X., LI, C., KRUMM, C. S. & QI, D. S. 2015. Individual and combined cytotoxic effects of aflatoxin B1, zearalenone, deoxynivalenol and fumonisin B1 on BRL 3A rat liver cells. *Toxicol*, 95, 6-12.
- SUN, X. M., BRATTON, S. B., BUTTERWORTH, M., MACFARLANE, M. & COHEN, G. M. 2002. Bcl-2 and Bcl-xL inhibit CD95-mediated apoptosis by preventing mitochondrial release of Smac/DIABLO and subsequent inactivation of X-linked inhibitor-of-apoptosis protein. *J Biol Chem*, 277, 11345-11351.
- SUNDSTOL ERIKSEN, G. & PETTERSSON, H. 2003. Lack of de-epoxidation of type B trichothecenes in incubates with human faeces. *Food Addit Contam*, 20, 579-582.
- TU, G., ZHANG, Y. F., WEI, W., LI, L. G., ZHANG, Y. M., YANG, J. & XING, Y. Q. 2016. Allicin attenuates H2O2-induced cytotoxicity in retinal pigmented epithelial cells by regulating the levels of reactive oxygen species. *Molecular Medicine Reports*, 13, 2320-2326.
- UENO, Y. 1984. Toxicological features of T-2 toxin and related trichothecenes. *Fundamental and Applied Toxicology*, 4, S124-S132.
- VALENTA, H. 2004. Handbook of Secondary Fungal Metabolites, 3 Volume Set. *Animal Feed Science and Technology*, 114, 309-310.
- VALKO, M., LEIBFRITZ, D., MONCOL, J., CRONIN, M. T., MAZUR, M. & TELSER, J. 2007. Free radicals and antioxidants in normal physiological functions and human disease. *Int J Biochem Cell Biol*, 39, 44-84.
- VANDER, A., SHERMAN, J. & LUCIANO, D. 2001. The Mechanism of Body Function. *Human Physiology*, 554-587.
- VILJOEN, A., FLETT, C. F., SHEPHARD, G. S., ROSE, L. J. & BEUKES, I. 2017. Mycotoxigenic Fusarium species associated with grain crops in South Africa – A review. *South African Journal of Science*, Volume 113.
- WALLOCK-RICHARDS, D., DOHERTY, C. J., DOHERTY, L., CLARKE, D. J., PLACE, M., GOVAN, J. R. & CAMPOPIANO, D. J. 2014. Garlic revisited: antimicrobial activity of allicin-containing garlic extracts against *Burkholderia cepacia* complex. *PLoS One*, 9, e112726.

- WANNEMACHER, R. & WIENER, S. L. 2000. Trichothecenes mycotoxins In. *Medical aspects of chemical and biological warfare*, 656–676.
- WARTH, B., SULYOK, M., BERTHILLER, F., SCHUHMACHER, R. & KRŠKA, R. 2013. New insights into the human metabolism of the Fusarium mycotoxins deoxynivalenol and zearalenone. *Toxicol Lett*, 220, 88-94.
- WIJNANDS, L. M. & VAN LEUSDEN, F. M. 2000. An overview of adverse health effects caused by mycotoxins and bioassays for their detection.
- WILD, C. P. & GONG, Y. Y. 2010. Mycotoxins and human disease: a largely ignored global health issue. *Carcinogenesis*, 31, 71-82.
- WOELFLINGSIEDER, L., DEL FAVERO, G., BLAZEVIĆ, T., HEISS, E. H., HAIDER, M., WARTH, B., ADAM, G. & MARKO, D. 2018. Impact of glutathione modulation on the toxicity of the Fusarium mycotoxins deoxynivalenol (DON), NX-3 and butenolide in human liver cells. *Toxicol Lett*, 299, 104-117.
- XUE, R., DONGXIAO, S.-W., DAN, W., YANG, J., FENG, L., YILUN, C., SHANCANG, Z. & DAPENG, L. 2019. The Significance of Regulatory MicroRNAs: Their Roles in Toxicodynamics of Mycotoxins and in the Protection Offered by Dietary Therapeutics Against Mycotoxin-Induced Toxicity. *Comprehensive Reviews in Food Science and Food Safety*, 18.
- Y, U. 1977. Mode of action of trichothecenes.
- YANG, G. H., JARVIS, B. B., CHUNG, Y. J. & PESTKA, J. J. 2000. Apoptosis induction by the satratoxins and other trichothecene mycotoxins: relationship to ERK, p38 MAPK, and SAPK/JNK activation. *Toxicol Appl Pharmacol*, 164, 149-160.
- YANG, W., YU, M., FU, J., BAO, W., WANG, D., HAO, L., YAO, P., NUSSLER, A. K., YAN, H. & LIU, L. 2014. Deoxynivalenol induced oxidative stress and genotoxicity in human peripheral blood lymphocytes. *Food Chem Toxicol*, 64, 383-396.
- YIANNIKOURIS, A. & JOUANY, J. 2002. Mycotoxins in feeds and their fate in animals: a review. *Anim. Res.*, 51, 81-99.
- YOUNG, I. S. & WOODSIDE, J. V. 2001. Antioxidants in health and disease. *J Clin Pathol*, 54, 176-186.
- YU, M., CHEN, L., PENG, Z., NUSSLER, A. K., WU, Q., LIU, L. & YANG, W. 2017a. Mechanism of deoxynivalenol effects on the reproductive system and fetus malformation: Current status and future challenges. *Toxicol In Vitro*, 41, 150-158.
- YU, M., CHEN, L., PENG, Z., WANG, D., SONG, Y., WANG, H., YAO, P., YAN, H., NÜSSLER, A. K., LIU, L. & YANG, W. 2017b. Embryotoxicity Caused by DON-Induced Oxidative Stress Mediated by Nrf2/HO-1 Pathway. *Toxins*, 9, 188.
- YU, M., WEI, Z. Y., XU, Z. H., PAN, J. Q. & CHEN, J. H. 2018. Oxidative Damage and Nrf2 Translocation Induced by Toxicities of Deoxynivalenol on the Placental and Embryo on Gestation Day 12.5 d and 18.5 d. *Toxins (Basel)*, 10.
- YUAN, J. & KROEMER, G. 2010. Alternative cell death mechanisms in development and beyond. *Genes Dev*, 24, 2592-2602.
- ZAIN, M. E. 2011. Impact of mycotoxins on humans and animals. *Journal of Saudi Chemical Society*, 15, 129-144.
- ZHANG, L., YAN, J., LIU, Y., ZHAO, Q., DI, C., CHAO, S., JIE, L., LIU, Y. & ZHANG, H. 2017a. Contribution of caspase-independent pathway to apoptosis in malignant glioma induced by carbon ion beams. *Oncol Rep*, 37, 2994-3000.
- ZHANG, M., PAN, H., YINJIE, X., WANG, X., ZHAOHUI, Q. & JIANG, L. 2017b. Allicin Decreases Lipopolysaccharide-Induced Oxidative Stress and Inflammation in Human Umbilical Vein Endothelial Cells through Suppression of Mitochondrial Dysfunction and Activation of Nrf2. *Cell Physiol Biochem*.
- ZHANG, W., ZHANG, S., ZHANG, M., YANG, L., CHENG, B., LI, J. & SHAN, A. 2018. Individual and combined effects of Fusarium toxins on apoptosis in PK15 cells and the protective role of N-acetylcysteine. *Food Chem Toxicol*, 111, 27-43.

- ZHANG, X., JIANG, L., GENG, C., CAO, J. & ZHONG, L. 2009. The role of oxidative stress in deoxynivalenol-induced DNA damage in HepG2 cells. *Toxicol*, 54, 513-518.
- ZHOU, H. R., ISLAM, Z. & PESTKA, J. J. 2003. Rapid, sequential activation of mitogen-activated protein kinases and transcription factors precedes proinflammatory cytokine mRNA expression in spleens of mice exposed to the trichothecene vomitoxin. *Toxicol Sci*, 72, 130-142.
- ZINEDINE, A., SORIANO, J. M., MOLTO, J. C. & MANES, J. 2007. Review on the toxicity, occurrence, metabolism, detoxification, regulations and intake of zearalenone: an oestrogenic mycotoxin. *Food Chem Toxicol*, 45, 1-18.

APPENDICES

Appendix



Miss Yandisa Zintle Mamane (219095889)
School Of Lab Med & Medical Sc
Westville

Dear Miss Yandisa Zintle Mamane,

Protocol reference number: 00007886

Project title: The ameliorative effects of allicin on deoxynivalenol-induced cytotoxicity in human embryonic kidney (Hek293) cells

Exemption from Ethics Review

In response to your application received on [redacted], your school has indicated that the protocol has been granted **EXEMPTION FROM ETHICS REVIEW**.

Any alteration/s to the exempted research protocol, e.g., Title of the Project, Location of the Study, Research Approach and Methods must be reviewed and approved through an amendment/modification prior to its implementation. The original exemption number must be cited.

For any changes that could result in potential risk, an ethics application including the proposed amendments must be submitted to the relevant UKZN Research Ethics Committee. The original exemption number must be cited.

In case you have further queries, please quote the above reference number.

PLEASE NOTE:

Research data should be securely stored in the discipline/department for a period of 5 years.

I take this opportunity of wishing you everything of the best with your study.

Yours sincerely,



Dr Brenda Zola De Gama
Academic Leader Research
School Of Lab Med & Medical Sc

UKZN Research Ethics Office
Westville Campus, Govan Mbeki Building
Postal Address: Private Bag X54001, Durban 4000
Website: <http://research.ukzn.ac.za/Research-Ethics/>

Founding Campuses: ■ Edgewood ■ Howard College ■ Medical School ■ Pietermaritzburg ■ Westville

INSPIRING GREATNESS

Appendix B : Turnitin report

Yandisa 2			
ORIGINALITY REPORT			
14%	8%	13%	0%
SIMILARITY INDEX	INTERNET SOURCES	PUBLICATIONS	STUDENT PAPERS
PRIMARY SOURCES			
1	Thobeka Madide, Anou M. Somboro, Daniel G. Amoako, Hezekiel M. Khumalo, Rene B. Khan. "Di-2-picolyamine triggers caspase-independent apoptosis by inducing oxidative stress in human liver hepatocellular carcinoma cells", Biotechnology and Applied Biochemistry, 2020 Publication	2%	
2	docplayer.net Internet Source	2%	
3	www.mdpi.com Internet Source	1%	
4	Zhen Liang, Zhihua Ren, Shuang Gao, Yun Chen, Yanyi Yang, Dan Yang, Junliang Deng, Zhicai Zuo, Ya Wang, Lihong Shen. "Individual and combined effects of deoxynivalenol and zearalenone on mouse kidney", Environmental Toxicology and Pharmacology, 2015 Publication	1%	
5	Thobeka Madide, Anou M. Somboro, Daniel G. Amoako, Hezekiel M. Khumalo, Rene B. Khan.	1%	

"Di-2-picoylamine triggers caspase-independent apoptosis by inducing oxidative stress in human liver hepatocellular carcinoma cells",
Biotechnology and Applied Biochemistry, 2020
Publication

-
- | | | |
|-----------|--|-----------|
| 6 | Sakshi Mishra, Premendra D. Dwivedi, Haushila P. Pandey, Mukul Das. "Role of oxidative stress in Deoxynivalenol induced toxicity", Food and Chemical Toxicology, 2014
Publication | 1% |
| 7 | www.wageningenacademic.com
Internet Source | 1% |
| 8 | 146.230.128.141
Internet Source | 1% |
| 9 | res.mdpi.com
Internet Source | 1% |
| 10 | James J. Pestka, Alexa T. Smolinski. "Deoxynivalenol: Toxicology and Potential Effects on Humans", Journal of Toxicology and Environmental Health, Part B, 2005
Publication | 1% |
| 11 | Thanh-Huong Le, Imourana Alassane-Kpembi, Isabelle P. Oswald, Philippe Pinton. "Analysis of the interactions between environmental and food contaminants, cadmium and deoxynivalenol, in different target organs", | 1% |

Science of The Total Environment, 2018

Publication

12	Carel B. Oosthuizen, Anna-Mari Reid, Namrita Lall. "Garlic (<i>Allium sativum</i>) and Its Associated Molecules, as Medicine", Elsevier BV, 2018 Publication	1%
13	link.springer.com Internet Source	1%
14	Sharon Maphala Mokubedi, Judith Zanele Phoku, Rumbidzai Naledi Changwa, Sefater Gbashi, Patrick Berka Njobeh. "Analysis of Mycotoxins Contamination in Poultry Feeds Manufactured in Selected Provinces of South Africa Using UHPLC-MS/MS", Toxins, 2019 Publication	1%
15	Mohamed E. Zain. "Impact of mycotoxins on humans and animals", Journal of Saudi Chemical Society, 2011 Publication	1%

Exclude quotes On

Exclude matches < 1%

Exclude bibliography On

Appendix C : Allicin cell viability data

Hek293 cells were treated with a range of allicin concentrations (0–150mM) over a 24hr period. Allicin induced a non- inconsistent decrease in cell viability. An EC₅₀ of 1.7mM was determined (Appendix Table 1).

Table 1: The determination of the EC₅₀ using the cell viability (MTT) assay.

Allicin concentration (mM)	log [allicin]	Average Absorbance	Average cell viability (%/)
0		0.91	100
10	1.00	1.10	121
15	1.18	1.18	129
20	1.30	1.20	131
25	1.40	1.21	133
30	1.48	1.18	129
40	1.60	1.24	135
50	1.70	1.28	139
75	1.88	1.42	155
100	2.00	1.46	159
125	2.10	1.35	147
150	2.18	1.24	135

Appendix D : Nitrates standard curve

Table 1: The determination of the nitrates and nitrites standard reference curve

Nitrite Standard Concentrations (μM)	OD1	OD2	Average OD
0	0.008	0.008	0.008
12.5	0.022	0.015	0.0185
25	0.034	0.029	0.0315
50	0.052	0.053	0.0525
100	0.075	0.072	0.0735
200	0.096	0.099	0.0975

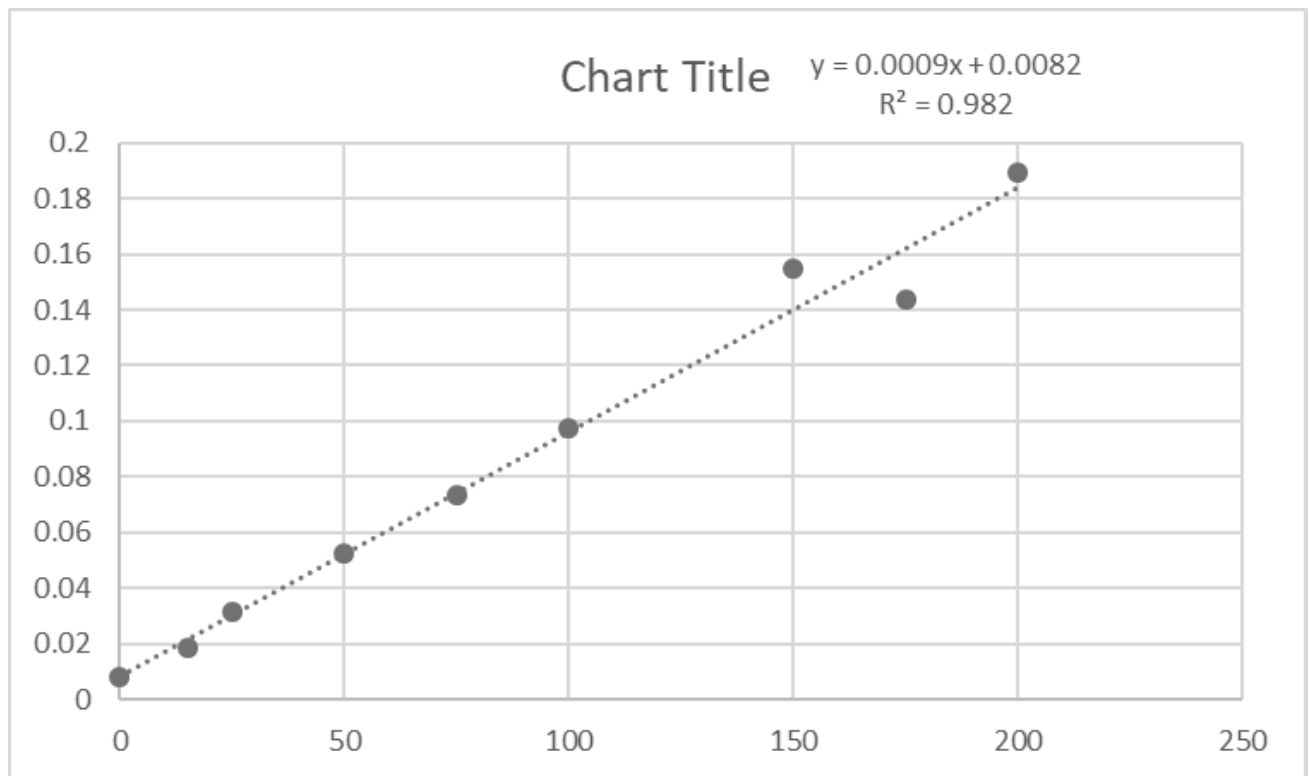


Figure 1: Nitrates and nitrites standard reference curve used to determine nitrates and nitrites concentration in samples.

Appendix E : Protein standard curve

Table 1: Protein quantification and standardization using Bovine Serum Albumin (BSA).

Protein Standard (mg/ml)	OD1	OD2	Average OD
0	0.111	0.111	0.1
0.2	0.22	0.225	0.2
0.4	0.369	0.366	0.4
0.6	0.458	0.455	0.5
0.8	0.571	0.579	0.6
1	0.76	0.671	0.7

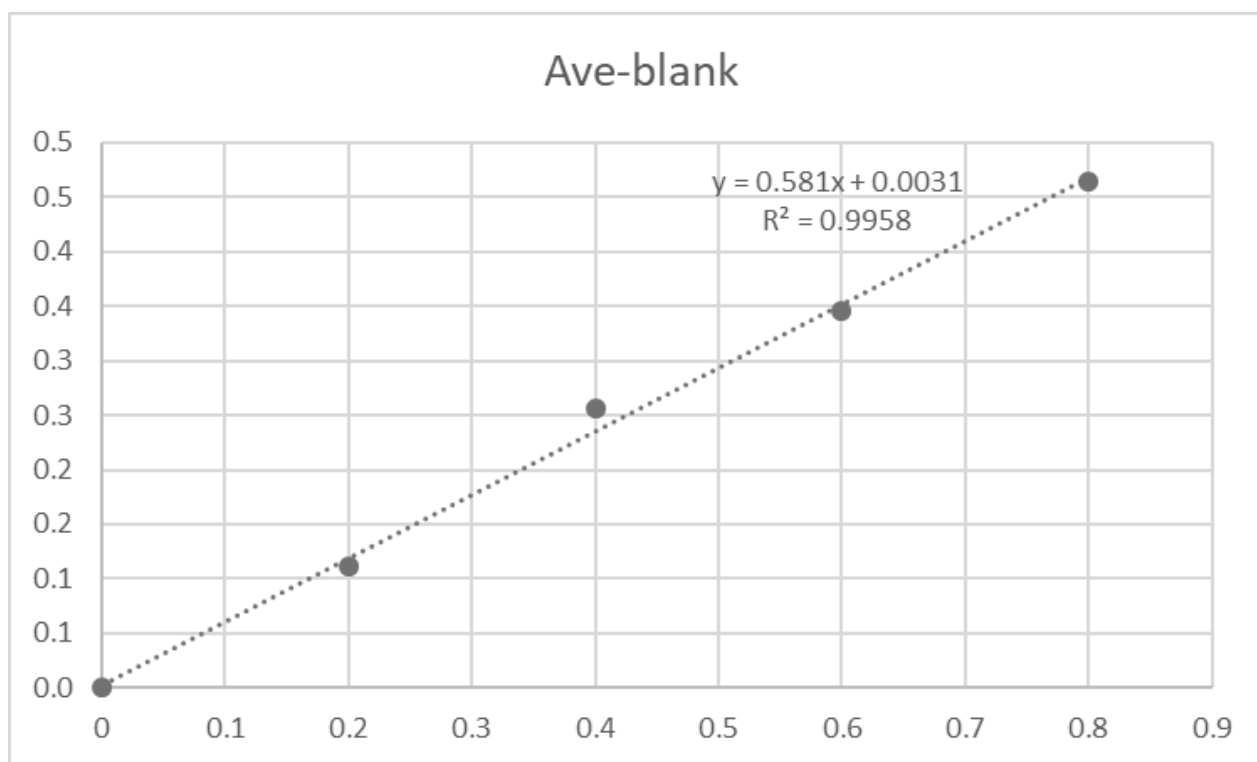


Figure 1: Standard calibration curve using a range of known bovine serum albumin concentrations for determination of sample protein concentrations using the bicinchoninic acid assay.